MONOPROPELLANT ENGINE INVESTIGATION FOR SPACE SHUTTLE REACTION CONTROL SYSTEM

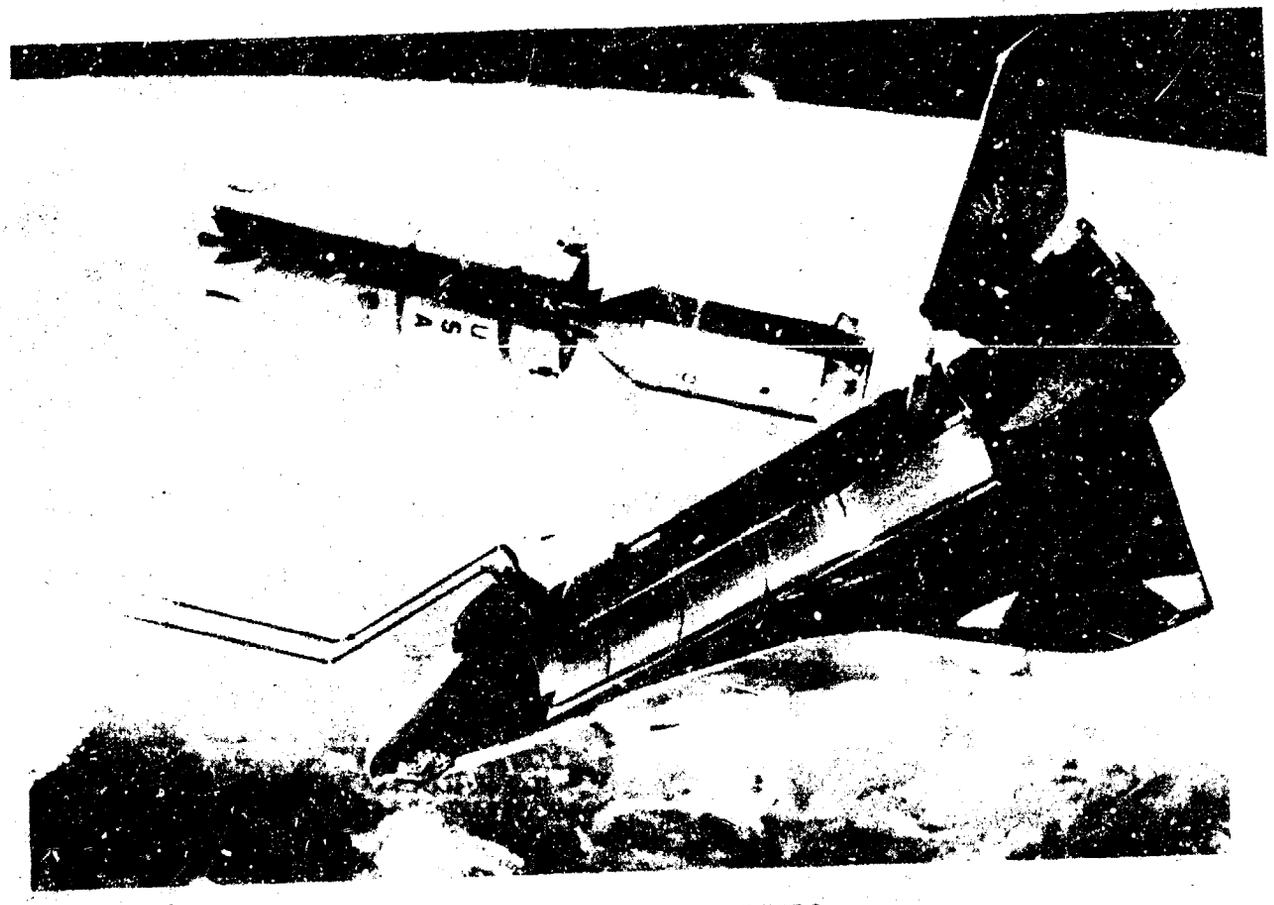

CONTRACT NAS 8-2-8950
NASA/JSC

FINAL REPORT
75-R-460
Volume II

Design, Fabrication, and Demonstration Test of a Catalytic Gas Generator for the Space Shuttle APU

Rocket Research Corporation
Redmond, Washington

TABLE OF CONTENTS

LIST OF FIGURES

LIST OF FIGURES (Concluded)

LIST OF TABLES

FOREWORD

This document is Volume II of the final report (Contract NAS 8-28950), which presents the results of Task IV-A entitled, *Design, Fabrication, Demonstration Test, and Delivery of a Catalytic Gas Generator for the Space Shuttle APU*. The program encompassed design studies, subscale testing, and three separate full-scale life demonstration tests.

The project manager for the program was Dr. Don L. Emmons. Mr. Douglas D. Huxtable was responsible for technical direction of the analytical and experimental efforts. Major contributors to the program included K. W. Arasim, M. Archer, C. Cunningham, J. Daly, Dr. J. D. Rockenfeller, Dr. E. W. Schmidt, I. Stewart, and many manufacturing personnel responsible for fabricating the hardware. The NASA technical monitor for the program was Mr. D. R. Blevins.

1.0 INTRODUCTION

1.1 GENERAL

Monopropellant hydrazine offers many attractive advantages as a working fluid for turbine-powered devices. The use of hydrazine for such applications, however, has not been fully exploited primarily because of an insufficient technology base. With the advent of the Space Shuttle Program, with its unique mission requirements, it became clear that the hydrazine APU system was the optimum approach. The primary question was whether life requirements of a catalytic gas generator could be achieved. Consequently, a technology program (Task IV-A of Contract NAS-8-2895) was undertaken by RRC to establish the capability of a catalytic gas gnerator to meet the requirement specified for the Space Shuttle APU (Reference 1-1). The specified requirements for the gas generator were as follows:

a. Gas horsepower – 40 to 400 GHP (pressure modulation)
b. Hot gas temperature – 1,600°F (pressure modulation); 1,700°F (pulse modulation)
c. Inlet pressure – 1,200 psig (pressure modulation); 1,000 psig (pulse modulation)
d. External temperature – 600°F maximum
e. Design life of 500 hours (structural elements)
f. Operating life of 100 missions at 90 minutes per mission
g. Shelf life of 10 years
h. High performance throughout the throttle range, especially at low power levels
i. Minimum cost
j. Ease of maintenance and checkout
k. Minimum pressure drop
l. Repeatable performance
m. Fast response to changes in power demand
n. Insensitivity to duty cycle
o. Unlimited restart capability under all expected operating conditions without use of gas purge
p. Simplicity and reliability
q. Clean exhaust products – not detrimental to long life turbine components
r. Steady-state and pulse-mode capability.

1.2 SCOPE OF THE PROGRAM

In order to meet the above requirements, detailed analytical and experimental studies were conducted to form the basis for selection of the optimum catalyst bed configuration for the gas

generator. On the basis of the analytical and experimental studies, a full-scale gas generator, designed to operate at a chamber pressure of 750 psia and a flow rate of 0.36 lbm/sec, was fabricated and subjected to three separate life test series.

An additional task (Task VI) undertaken during the program was an investigation of the nickel foam metal used for catalyst retention. Inspection of the foam metal following the first life tests revealed significant degradation. Consequently an investigation was conducted to determine the mechanism of degradation and to provide an improved foam metal.

2.0 SUMMARY OF RESULTS

2.1 GAS GENERATOR DESIGN

A drawing of the full-scale gas generator assembly is presented in Figure 2-1. The unit is a radial outflow design consisting of an injector body, outer and inner bed cylinders, bed closure plates, catalyst spacers, chamber closure, and an outer pressure chamber. A summary of the gas generator design point operating characteristics is presented in Table 2-1.

Table 2-1
GAS GENERATOR DESIGN SUMMARY

Design gas horsepower	= 400 ghp
Design flow rate	= 0.36 lbm/sec (pressure modulated)
	= 0.23 lbm/sec (pulse modulated)
Outlet gas temperature	= 1,700°F (maximum)
Feed pressure	= 1,200 psia
Chamber pressure	= 750 psia
Catalyst bed pressure drop	= 11.4 psid
Injector pressure drop	= 30 psid

The injector body contained four injection elements (Rigimesh) for distributing propellant to the catalyst bed. The catalyst bed consisted of an inner and outer bed separated by an inner bed cylinder. No screens were used for catalyst retention. The inner catalyst bed incorporated a metallic (nickel) open-cell foam, throughout which the catalyst was uniformly distributed. The inner bed, although initially designed for 25- to 30-mesh Shell 405 catalyst, was also tested using 14- to 18-mesh Shell 405. The outer bed catalyst was 14- to 18-mesh Shell 405 for all tests.

2.2 DEMONSTRATION TEST PROGRAM

Following completion of the detailed design effort and fabrication of the gas generator, a series of tests were conducted to demonstrate the gas generator performance and operational characteristics during simulated Space Shuttle mission firings.

Two modes of operation were under consideration by NASA for varying the output power of the APU, namely pulse modulation and pressure modulation. Of major concern was the life capability of the gas generator in the two modes of operation. It was, therefore, the goal of the test program to obtain life data for both modes of operation during simulated mission firings. This was accomplished by first conducting 20 simulated missions in the pressure-modulated mode of operation, refurbishing the unit, and then conducting 20 simulated missions in pulse mode. Upon completion of the pulse-modulated missions, the gas generator was again refurbished and delivered to NASA-JSC where an additional 20 missions (pulse-modulated) were conducted.

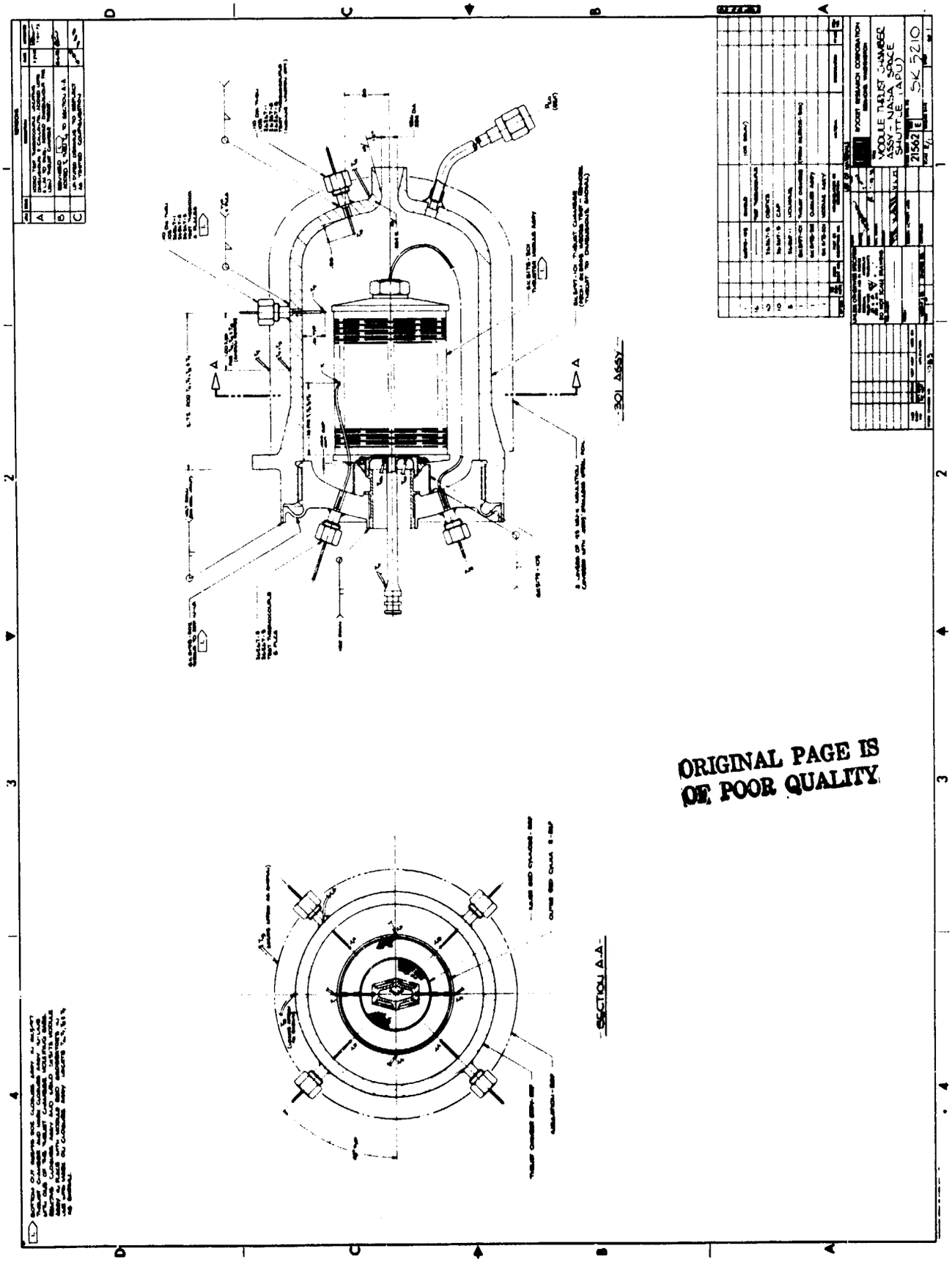

ORIGINAL PAGE IS
OF POOR QUALITY

Figure 2-1

For the NASA tests, the gas generator was refurbished by use of 14- to 18-mesh Shell 405 catalyst for both inner and outer beds, whereas 25- to 30-mesh catalyst was used in the inner bed for the previous tests. Prior to delivery of the reactor to NASA, a series of tests was conducted to demonstrate attitude insensitivity and the hot restart capability of the gas generator under various thermal conditions.

A summary of the accomplishments achieved during the three life test series is presented in Table 2-2. A comparison of the test results revealed no significant difference in the mission capability for the gas generator operating in pulse-mode or steady-state.

Table 2-2
SUMMARY OF LIFE TEST ACCOMPLISHMENTS

	Pressure-Modulated Tests	Pulse-Modulated Tests	NASA-JSC Tests
Number of missions	21	20	20
Number of pulses	1,196	342,500	347,000
Number of starts*	57	48	56
Total on-time, hours	30	9.3	9.4
Total propellant consumed, lbm	12,500	9,600	8,700
Catalyst loss, %			
Inner bed	2.25	3.3	7.1
Outer bed	(1.71)**	(0.23)**	(1.6)**

*All starts were with an initial bed temperature of 200°F

**Gain in weight

The effect of replacing the inner bed 25- to 30-mesh catalyst with 14- to 18-mesh catalyst was to increase gas temperature by 80°F with a small increase in chamber pressure roughness. Contrary to initial predictions, attrition of the coarser mesh catalyst was somewhat more than that encountered with the 25- to 30-mesh catalyst. It was postulated that the relatively low packing density of the coarse-mesh catalyst in the foam metal may have been a factor in the higher attrition rate.

Tests conducted with the gas generator in various orientations revealed no discernible effect of attitude on performance or operating characteristics. Tests were conducted with the gas generator in the vertical down and various horizontal attitudes. Hot restart tests were successfully conducted with the gas generator initially at temperatures ranging from 200 to 1,200°F. A potential problem was found to exist under bootstrap startup conditions when the bed temperature exceeded 600°F. The problem involved coupling between the reactor and feed system during the bootstrap start transient.

Foam metal, used for retention of the catalyst, showed evidence of degradation during the tests. Studies were undertaken to improve the nickel foam durability, which resulted in a rhodium-coated nickel foam. Unfortunately, no life test data of the improved foam was obtained. Results of the foam improvement investigation are presented in Volume III of this final report.

The Hastelloy B material used for fabrication of the major components showed very little degradation with the exception of the bedplates which showed evidence of nitriding attack. The chamber had an accumulated exposure time of 120 hours while the injector had 90 hours. The same injector was used throughout the test program with a total propellant throughput of 30,800 lbm.

Based on the results of the program, it was concluded that a catalytic gas generator could be designed to meet the requirements of the Space Shuttle APU. It was recommended that vibration testing be conducted with the gas generator firing to identify any potential problems associated with Space Shuttle launch conditions.

3.0 GAS GENERATOR DESIGN STUDIES

3.1 DESIGN APPROACH

The design approach for the gas generator evolved as a result of subscale RCS testing conducted during Tasks I and II of the RCS program (Reference 3-1). The flow rate for the subscale engines was approximately one-half that required for the Space Shuttle gas generator. A design approach subsequently evolved which consisted basically of two subscale engines arranged in a radial configuration (Figure 3-1). A combination of several of these "modules" within a single chamber to form a modular RCS engine was considered during the RCS phase of the program.

Based on successful in-house development of the use of foam metal in catalyst beds, a pure nickel foam metal was considered for use in the inner bed of the gas generator. Shell 405 catalyst was selected for both inner and outer beds, since the quantity of catalyst involved was not a significant cost factor. One of the goals of the design studies was to experimentally evaluate, using subscale hardware, the life capability of two subscale reactors – one with foam metal and the other without. The results of the evaluation are presented in the following section. Details of the final gas generator design are presented in paragraph 3.3. The results of the analytical studies are presented in subsequent sections.

3.2 SUBSCALE TESTING

In order to evaluate the life improvement capability of the composite bed in a cost effective manner, two subscale reactors (38 percent full size) were fabricated and tested. The subscale reactors, shown in Figure 3-2, were designed to provide bed loading equal to or slightly greater than the full-scale gas generator while operating at the design chamber pressure of 750 psia. Table 3-1 compares the operational and design parameters of the subscale reactors to the full-scale gas generator. The objective of the subscale test program was to compare the life capability of two catalyst bed design concepts – one with foam metal and the other without. The following paragraphs discuss each reactor and test program in detail.

3.2.1 Reactor No. 1

Subscale Reactor No. 1 was assembled in the scalloped bed retention configuration using the conventional catalyst bed configuration (no foam). The planned demonstration was to conduct 30 hours of firing time while throttling the reactor from 100 percent design flow to 10 percent design flow during a series of simulated mission firings. The subscale reactor was tested for 6,820 seconds prior to a premature shutdown due to a thermal perk in the injector during tailoff. The unit was refurbished and testing reinitiated, but the reoccurrence of a thermal perk in the injector caused a second premature shutdown. In both cases the tailoff perk resulted in increased chamber pressure roughness (from 1.5 to 10 percent) during subsequent firings. Although no major hardware damage was involved (limited to bowing of the Rigimesh), it was decided that the injector end-closure should either be water-cooled or excessive metal should be removed from the area around the

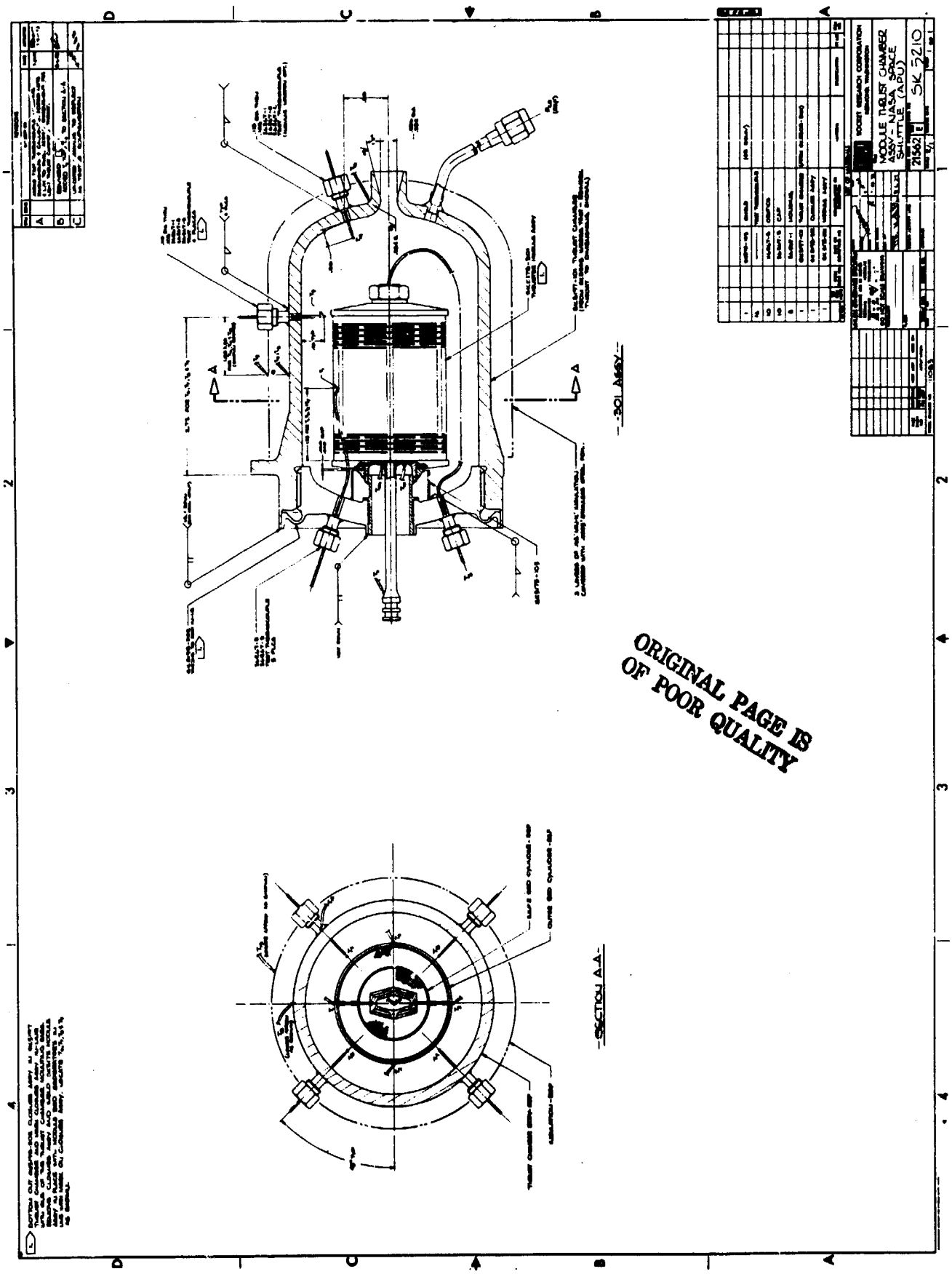

ORIGINAL PAGE IS
OF POOR QUALITY

Figure 3-1

SUBSCALE ENGINE SCALLOPED WEDGE

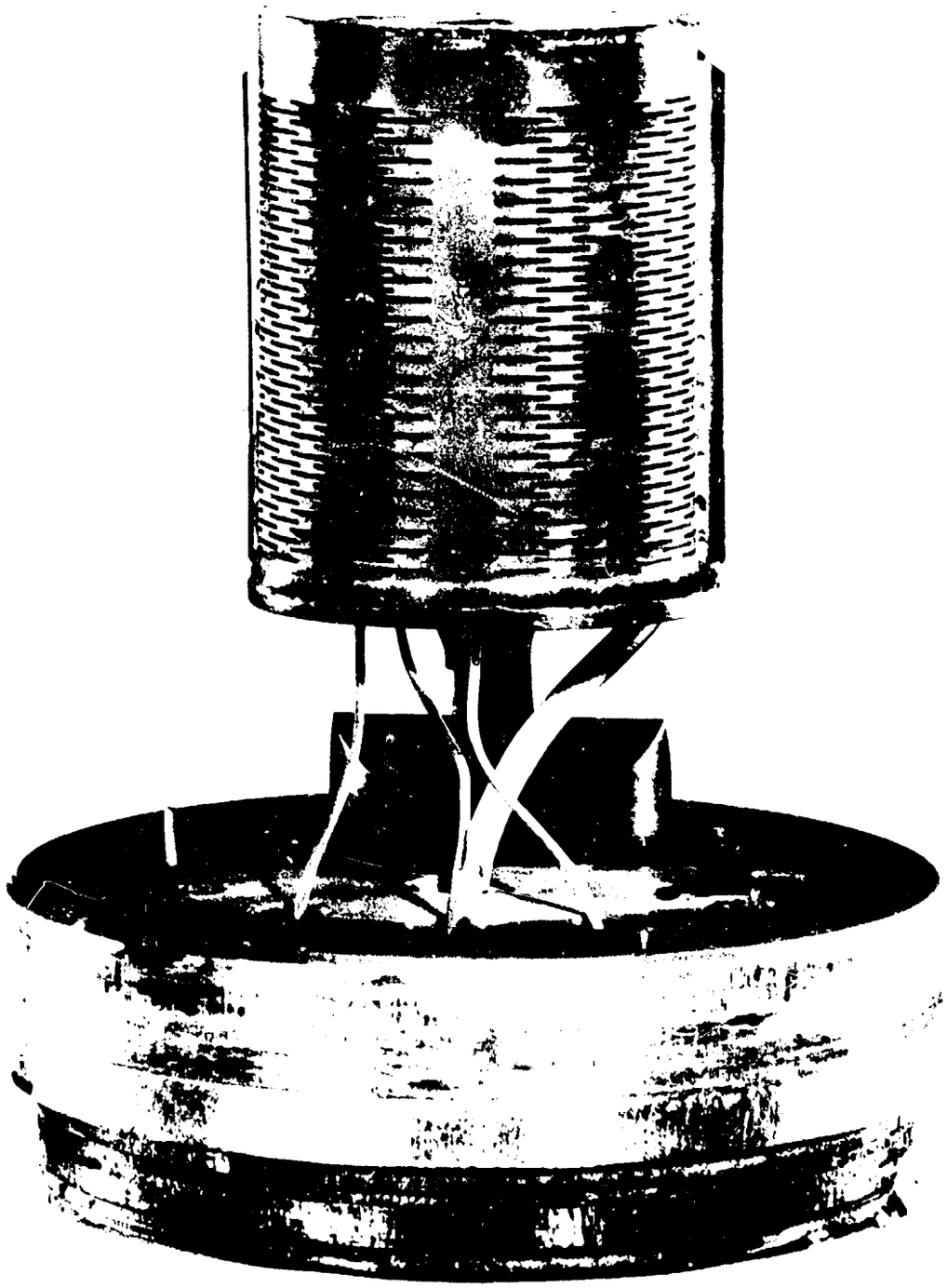

Table 3-1

COMPARISON OF OPERATIONAL/DESIGN PARAMETERS OF SUBSCALE REACTOR AND FULL SCALE REACTOR

	NASA FULL SCALE REACTOR	SUBSCALE REACTOR
BED LOADING* – lbm/in^2 sec	0.0075	0.01
MAXIMUM PROPELLANT BED LOADING** – lbm/in^2 sec	0.033	0.038
WEIGHT OF CATALYST BED – lbm	0.33	0.11
TOTAL SURFACE AREA OF INJECTOR ELEMENTS – in^2	2.4	0.9
NUMBER OF INJECTOR ELEMENTS	4	2
MAXIMUM CHAMBER PRESSURE – psia	750	750
MAXIMUM FLOW RATE – lbm/sec	0.36	0.135

*Based on 15% GHP flow rate for a typical mission and inner bedplate area

**Based on maximum flow rate for a typical mission and inner bedplate area

V01759

injector inlet tube. As can be seen in Figure 3-2, the end closure is a large heat sink which supplies a large flow of heat to the propellant stagnated in the injector following shutdown. For the second subscale reactor, it was decided to water-cool the injector and end-closure. It should be noted that water cooling was necessary only because of the massive end-closure design used for the subscale hardware. As can be seen in Figure 3-1, the end-closure used for the full-scale gas generator was designed to avoid the thermal soakback problem and was not water cooled.

3.2.2 Reactor No. 2

Subscale Reactor No. 2 was identical to the first unit except that the inner bed utilized a nickel foam for compartmentation of the inner bed. The goal of the test was to obtain 30 hours of demonstrated life with 28 starts at 200°F, and substantiate the predicted performance for the full-scale gas generator. All testing was conducted at sea-level conditions. The duty cycle used during this 30-hour demonstration is shown in Table 3-2.

Sequences 1 and 2 were incorporated to measure performance of the reactor at power levels of 15, 30, 50, and 100 percent. Performance characteristics at the four different flow rates were as predicted.

Life capability was demonstrated by conducting sequences 3 through 28. Steady-state burn times varied from 2,520 seconds (0.7 hours) to 8,400 seconds (2.33 hours) at a flow rate of 0.040 lbm/sec (15 percent GHP simulation). Tests were also conducted at a flow rate of 0.060 lbm/sec (30 percent GPH) for 60 seconds at accumulated burn time of 10, 20, and 30 hours.

Table 3-3 lists the performance data obtained from sequences 1, 2, and 3. The gas temperatures recorded are the average of two thermocouples monitoring temperature of the gas exiting the outer bedplate of the reactor.

The average gas temperatures are within 20°F of the predicted values for each power level. Maximum deviation between the two measured temperatures was 25°F.

Reactor performance was excellent throughout the 30-hour test at all power levels. A discussion of the measured performance characteristics is presented below.

Ignition Delay – Figure 3-3 shows the effect of accumulated burn time on reactor ignition delay (defined as valve signal to 10 percent P_C). Beginning with sequence 3 (7 minutes' accumulated burn time), the ignition delay was 139 milliseconds for the 0.040 lbm/sec flow rate. Pressure rise was very smooth with no indication of ignition perks or spikes. The smooth pressure rise, characteristic on ignition, occurred on all 28 sequences. At the conclusion of 30 hours' burning time the ignition delay values increased by less than 40 milliseconds. The ability of the catalyst bed, after 30 hours' accumulated burn time, to respond at nearly the same rate as the initial sequence indicates negligible activity loss. The absolute value of ignition delay for this reactor is substantially higher than the flight designed unit due to a slow acting valve and large liquid hold-up time (90 milliseconds at 0.04 lbm/sec flow rate).

Table 3-2
APU SUBSCALE REACTOR DUTY CYCLE

Sequence	Flow Rate (lbm/sec)	Power Level %	On Time (Seconds)	Cumulative On-Time (Hours)
1	0.040	15	40	
	0.060	30	20	
	Cool to 200°F			
2	0.085	50	180	
	0.135	100	180	
	Cool to 200°F			
3	0.040	15	4,200	1.28
	Cool to 200°F			
4	↑	15	↑	2.45
5		15		3.62
6		15		4.78
7		15		5.95
8		15		7.12
9	0.040	15	4,200	8.28
	Cool to 200°F			
10	0.040	15	2,460	
	0.060	30	60	8.98
	Cool to 200°F			
11	0.040	15	4,200	10.15
	Cool to 200°F			
12	↑	15	↑	11.32
13		15		12.48
14		15		13.65
15		15		14.82
16		15	4,200	15.98
17	0.040	15	8,400	18.32
	Cool to 200°F			
18	0.040	15	2,460	
	0.060	30	60	
	Cool to 200°F			
19	0.040	15	4,500	20.27
	Cool to 200°F			
20	↑	15	↑	21.52
21		15		22.77
22		15		24.02
23		15		25.17
24		15		26.52
25		15	4,500	27.77
26		15	2,806	28.55
27	0.040	15	2,714	29.30
	Cool to 200°F			
28	0.040	15	2,460	
	0.060	30	60	30.00

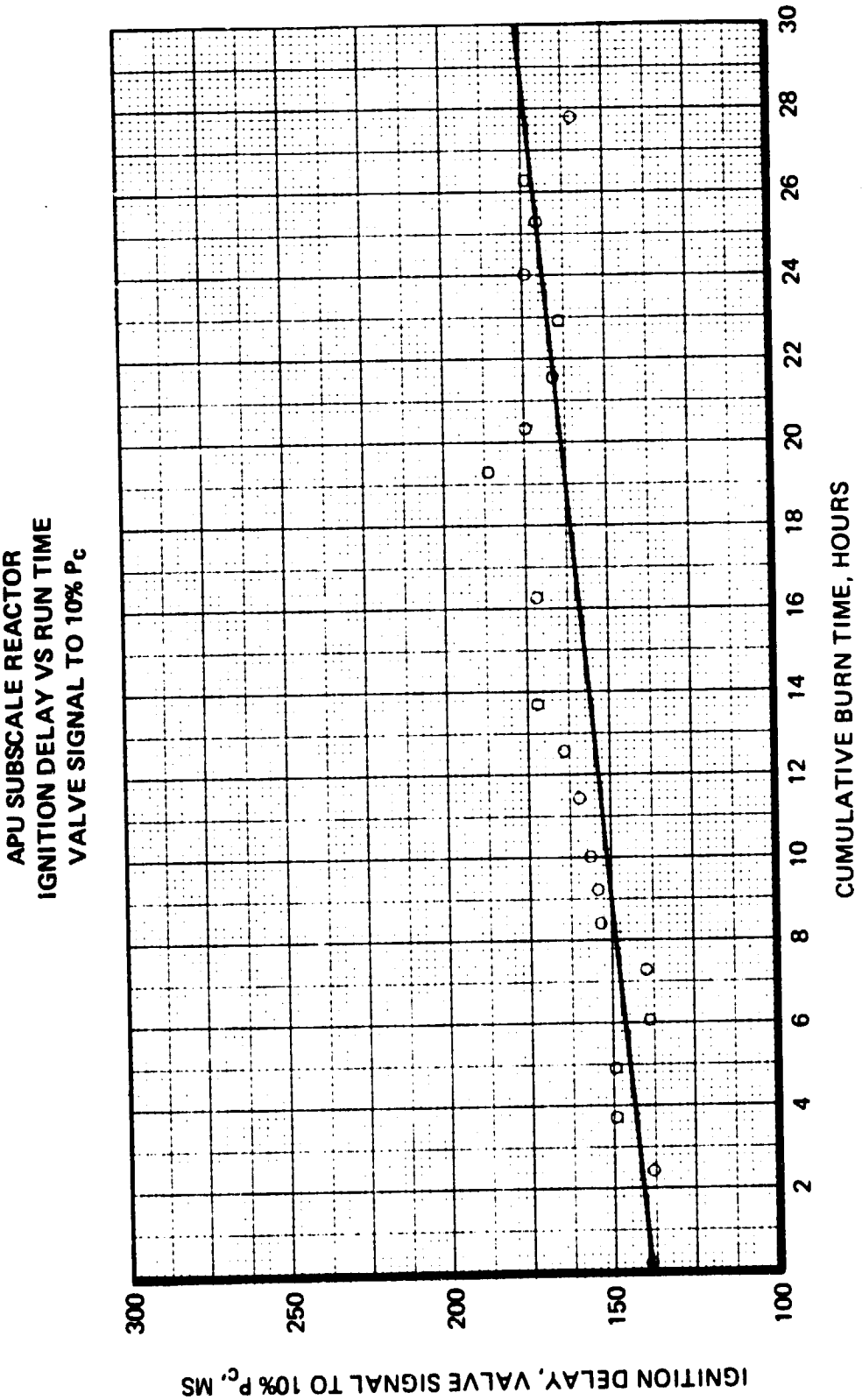
APU SUBSCALE REACTOR
IGNITION DELAY VS RUN TIME
VALVE SIGNAL TO 10% P_c
IGNITION DELAY, VALVE SIGNAL TO 10% P_c, MS
300
250
200
150
100
2
4
6
8
10
12
14
16
18
20
22
24
26
28
30
CUMULATIVE BURN TIME, HOURS

Figure 3-3

Table 3-3
COMPARISON OF PREDICTED AND MEASURED GAS TEMPERATURES

Percent Power	Predicted Gas Temperature	Actual Gas Temperature
15	1,525°F	1,510°F
30	1,570°F	1,550°F
50	1,615°F	1,595°F
100	1,690°F	1,675°F

Gas Temperature – Figure 3-4 shows the effect of accumulated burn time on the measured gas temperature. Gas temperature increased from approximately 1,510°F for sequence 3 to 1,590°F for sequence 28 at a flow rate of 0.04 lbm/sec. As can be seen two gas temperatures are shown in Figure 3-4, the lower temperature taken at 2,000 seconds into the firing, and the higher temperature taken at the conclusion of the firing. It was noted during testing that the gas temperature at the conclusion of the low flow rate sequences began to change markedly after an accumulated firing time of 22 hours. Prior to this there was very little observed difference in gas temperature at 2,000 seconds into the firing and at the conclusion of the sequence. Based on the earlier experience with injector boiling it was postulated that the combination of higher gas temperature and catalyst attrition had again led to boiling in the injector. This hypothesis was later partially substantiated when disassembly of the engine revealed the downstream portion of the injection elements to be discolored. It was concluded that water-cooling of the massive end-closure was inadequate for the low flow rate condition. As noted in Section 4.0, this problem was not encountered with the full-scale gas generator.

Pressure Roughness – Figure 3-5 shows chamber pressure roughness versus accumulated burn time. After 10 hours, a maximum average roughness (average value of seven specific peak to nominal chamber pressure values divided by nominal chamber pressure) of ±9 percent occurs. No further increase was noted for the remaining 20 hours.

After completing the planned test sequence to accumulate 30 hours of burn time, teardown of the engine for post-test analysis was initiated. The bed closure plate and outer bedplate appeared to be in an "as-built" condition with no yielding or detrimental nitriding or hydrogen embrittlement. The inner bedplate showed evidence of nitriding. Both catalyst beds appeared to be in nearly the same condition as when assembled.

All catalyst originally loaded into the reactor was recovered. A total of 5.6 percent of the inner bed catalyst, however, had migrated to the outer bed. Seventy-five percent of the inner bed catalyst remained within 25- to 30-mesh, and 98 percent of the outer bed was 14- to 18-mesh. The catalyst loss rate in the inner bed was nominally 0.2 percent per hour.

Table 3-4 lists the pertinent data of the inner and outer catalyst bed. Hydrogen chemisorption measures the active metal surface area which is an indirect measurement of activity. Both catalysts

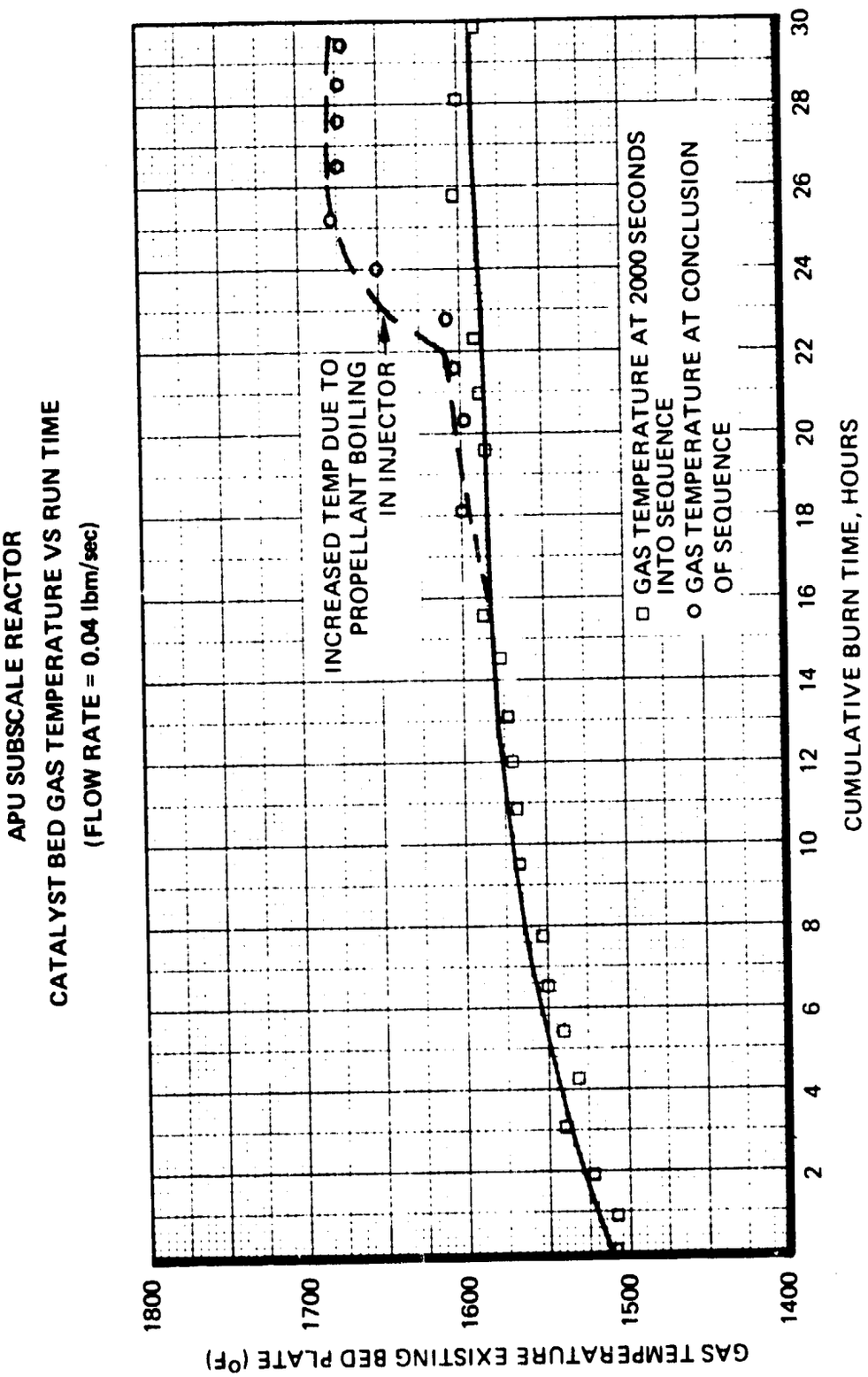

11072-32

Figure 3-4

APU SUBSCALE REACTOR NO. 2 AVERAGE ROUGHNESS VS RUN TIME

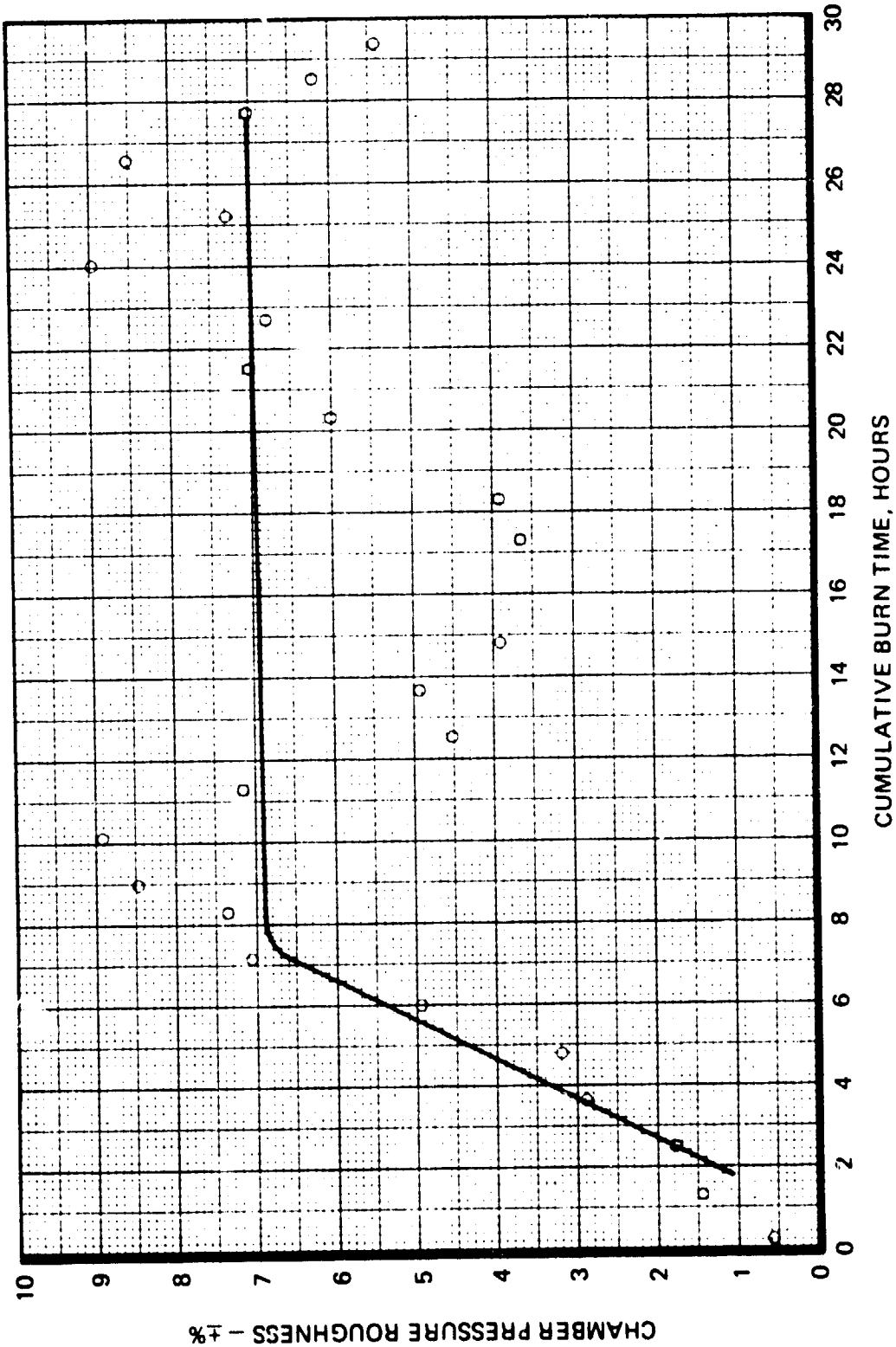

11072-33

Figure 3-5

Table 3-4
SPACE SHUTTLE APU 30-HOUR SUBSCALE REACTOR CATALYST DATA

Inner Bed, Shell 405 Catalyst, 25–30 Mesh

	Loaded	Recovered
Total weight, grams	16.86	15.93
25–30 mesh, gm	16.86	12.66
30–35 mesh, gm		1.22
>35 mesh, gm		2.05
Percent loss	--	5.5
Hydrogen chemisorption μ moles/gram	156	127
Iron contamination, ppm	*40	950

Outer Bed, Shell 405 Catalyst, 14–18 Mesh

Total weight, grams	34.41	35.75
14–18 mesh, gm	34.41	33.62
>18 mesh, gm		2.13
Percent loss (gain)		(3.9)
Hydrogen chemisorption μ moles/gram	152	139
Iron contamination	*40	355

*40 ppm iron is a nominal value

show negligible change in metal surface area. A spot plate test of catalyst activity also showed excellent activity. Examination of the catalyst surface was conducted using microprobe analysis techniques. No change in the basic iridium/alumina structure was noted, however a build-up of iron and nickel contaminants did occur. To confirm the microprobe analysis, atomic adsorption was conducted to determine total metal build-up; concentrations of 950 ppm iron and 500 ppm nickel were observed.

3.3 GAS GENERATOR DESIGN

A sketch of the full-scale gas generator assembly is presented in Figure 3-1. The unit is a radial outflow design consisting of an injector body, outer and inner bed cylinders, bed closure plates, catalyst spacers, chamber closure, and an outer pressure chamber. Photographs of the fabricated unit in various stages of assembly are presented in Figure 4-1. A summary of the gas generator design point operating characteristics is presented in Table 3-5.

The injector body contains four injection elements (rigimesh) for distributing propellant to the catalyst bed. Each of the elements is 2 inches long and 0.3 inch wide. Propellant enters the injector body through the propellant supply tube. At the head end of the injector the propellant flow is diverted to four circular passages to transfer the propellant to manifolding behind the rigimesh elements. Propellant then flows axially along the manifold and radially outward into the catalyst bed.

Table 3-5
GAS GENERATOR DESIGN SUMMARY

Design gas horsepower	= 400 ghp
Design flow rate	= 0.36 lbm/sec (pressure modulated) 0.23 lbm/sec (pulse modulated)
Outlet gas temperature	= 1,700°F (maximum)
Feed pressure	= 1,200 psia
Chamber pressure	= 750 psia
Catalyst bed pressure drop	= 11.4 psid
Injector pressure drop	= 30 psid

The catalyst bed consists of an inner and outer bed separated by an inner bed cylinder. Longitudinal spacers (Figure 3-1) were incorporated in the first series of life tests to provide compartmentation of the bed. Based on data from the first test series, it was decided to remove the spacers for subsequent tests. The inner catalyst bed incorporates a metallic (nickel) open-cell foam, throughout which the catalyst is uniformly distributed. The inner bed, although initially designed for 25- to 30-mesh Shell 405 catalyst, was also tested with 14- to 18-mesh Shell 405. The outer bed catalyst was 14- to 18-mesh Shell 405 for all tests.

The gas generator assembly is designed for refurbishment through use of a threaded end closure at the injectory body/outer chamber joint. A machinable weld is used to provide a pressure seal. The catalyst bed downstream end closure is retained with a threaded nut and washer to permit easy access to the catalyst. Disassembly of the unit is accomplished by first machining off the weld at the chamber joint, followed by removal of the injector body/catalyst bed assembly. The bed end-closure nut is then removed to permit removal of the end-closure and access to the catlayst.

Hastelloy B was selected as the material for all components with the exception of the injection elements, which were fabricated from Haynes 25.

A modified E-Systems valve supplied by NASA-JSC was used during the pressure modulated tests. A Marotta MV-130 valve was used for on/off control for the pressure modulated tests as well as the primary control valve for the pulse modulated tests.

The gas generator assembly was insulated with three layers of 0.125-inch "Min-K" insulation covered with 0.0005-inch stainless steel foil

The gas generator was designed to restart under all conditions without the use of an injector purge. No purge was used to prevent catalyst oxidation.

3.4 THERMAL ANALYSIS

This section includes significant aspects of the thermal design approach, methods of solution, preliminary results, and experimental correlation of sea-level test data. It is noted that much of the

thermal design analysis were conducted for a flightweight gas generator design which incorporated a spherical chamber. Because of schedule problems, the gas generator fabricated for test incorporated a non-flightweight cylindrical chamber.

3.4.1 Thermal Design Objectives and Approach

The thermal design objectives and operational requirements employed for the analysis were as follows:

a. Predict gas generator thermal characteristics as functions of duty cycle and flow rate.

b. Maximize performance by minimizing heat loss to the surroundings and turbomachinery.

c. Minimize valve and injector soakback heating during operational and post-firing periods.

d. Minimize heater power required to maintain catalyst bed above 200 to 225°F and propellant valves above 45°F.

e. Maintain the gas generator outer surface temperature below 600°F during operation with bulk insulation.

f. Minimize heat soak to surrounding vehicle and adjacent turbomachinery.

The worst-case combinations of environmental and vehicular conditions used in the study are shown in Table 3-6.

Table 3-6

LIMITING ENVIRONMENTAL VARIATIONS FOR APU GAS GENERATOR OPERATION

Operational Cold Bias Conditions:

1. Vehicle conductive interface is an infinite capacity heat sink at -100°F
2. Vehicle radiative interface is a perfectly absorbing heat sink at -100°F
3. Gas generator is conductively attached to turbomachinery at -100°F
4. Minimum active heater voltage supplied at 24 volts
5. Minimum propellant temperature, 50°F

Operational Hot Bias Conditions:

1. Vehicle conductive interface is an infinite capacity heat sink at +200°F
2. Vehicle radiative interface is a perfectly absorbing heat sink at +200°F with short excursions to +350°F during re-entry
3. Gas generator is conductively attached to turbomachinery at 1,130°F
4. Maximum active heater voltage supplied at 24 volts
5. Maximum propellant temperature, 150°F

3.4.2 Summary of Analytical Results

Table 3-7 summarizes the basic thermal design goals and analytical results. A firm mechanical interface definition is required to further optimize the proposed thermal design. The preliminary boundary conditions and assumed conductive coupling heat path to the turbomachinery necessitate

Table 3-7
APU GAS GENERATOR THERMAL DESIGN GOALS AND ANALYTICAL RESULTS

Design Parameter	Goal	Intent of Goal	Limits	Predicted Values and Comments	
Catalyst bed minimum temperature	>200- 225°F	Provide smooth start, eliminate catalyst damage by self-induced NH_3 deactivation, ensure catalyst bed life.	150°F	205°F	Cold bias environment, reactor heater at 40 watts. Turbomachinery at -100°F.
Propellant valve minimum temperature	>45°F	Prevent propellant freezing	35.6°F	45°F	Cold bias environment, valve heater at 6.9 watts.
Propellant valve maximum temperature	<250°F	Avoid valve overheat and prevent excessive propellant preheat	300°F	285°F	Hot bias environment, valve heater at 6.9 watts.
Maximum gas generator surface temperature	<600°F	Specified requirement	600°F	500°F	Hot bias environment.
Active heater power consumption	Minimize	Energy conservation	TBD	46.9 watts	Cold bias environment -100°F; turbomachinery at -100°F.
Propellant feed tube O-ring	<350°F continuous operation	EPT rubber O-ring service temperature	400°F	125°F (operational) 385°F (soak)	Hot bias environment with 6.9-watt valve heater. Short-term soak period.
Minimum flow rate pressure modulation	0.062 lbm/sec	Specified requirement	0.062	0.042 lbm/sec	Analytical value based upon assumed temperature limits.

a 40-watt gas generator heater to maintain the catalyst bed at 225°F when subjected to the -100°F environment. This heater wattage can be reduced if the turbomachinery sink temperature estimate is greater than the assumed -100°F.

Both pressure and pulse modulated operational conditions are thermally acceptable by the gas generator configuration. A minimum recommended flow rate of 0.042 lbm/sec. based on a conservative analytical model. is well below the design goal of 0.062 lbm/sec. The minimum recommended duty cycle is 0.8 percent.

3.4.3 Thermal Design Approach

The thermal design approach for the gas generator is described in Table 3-8. The analytical model used in the analysis relates the simultaneous interaction of conduction, convection, and radiation heat transfer. The conduction network is given in Figure 3-6 with identification of lumped mass nodes noted. Conduction resistances were calculated from the following relation:

$$R = \frac{L}{kA}\left(\frac{hr\ ^{o}F}{Btu}\right)$$

where temperature variance of thermal conductivity was considered. For instance, the following relation is typical:

$$k = (0.00343)\,T + 5.69 \text{ (Hastelloy B)}$$

where T is temperature in degrees Fahrenheit and k is in Btu/hr-ft-°F. Dimensions used for calculations of L/A were taken from engineering design drawings.

The convection network is given in Figure 3-7. Convection resistances were calculated from the following relation:

$$R = \frac{L}{hA}\left(\frac{hr\ ^{o}F}{Btu}\right)$$

where h is the value of the unit surface conductance in units of Btu/hr-ft^2-°F, and A is surface area in square feet.

Convection coefficients, h, between the hot gas and the containing pressure vessel walls were based upon applicable empirical data obtained from tests on similar rocket engine and gas generator systems. A detailed injector boiling method is followed in calculating forced convective heat transfer coefficients between the fuel and injector passage walls. The basic result of this method is a calculation of bulk propellant temperature flowing out of a specific section of the injector. The injector was broken into 12 sections. The feed tube was one section (node 4), the two feed tube transition sections (nodes 5 and 6), the branch passage interior (node 7), four injector passage interior surfaces (nodes 8 to 11), and the four Rigimesh screen sections (nodes 12 to 15).

Three basic heat transfer regimes are considered: turbulent, nucleate, and film boiling.

Table 3-8
APU GAS GENERATOR THERMAL DESIGN APPROACH

Component	Approach	Comments
Thermal standoffs	Conductively isolate reactor from valve with thin wall Hastelloy B tubes	Limits valve heat soak, and conserves heat energy to improve performance and reduce active heating requirements.
Valve and catalyst bed heaters	Active heating provisions to maintain components at operational temperatures.	Cold bias environment considered for power level requirements.
Injector feed tube	Control length and wall thickness to conductively isolate stem inlet.	Reduce heat soak to feed tube O-rings.
Injector passages	Size for proper velocity and pressure drop with minimum thermal mass.	Eliminate bulk two-phase flow and limit post firing heat soak to tailoff propellant.
Insulation	Johns-Manville Min-K 2000 insulation blanket covering reactor and injector, retained with stainless steel jacket.	Maintains outer surface temperature below 300°F with 1-1/2" blanket thickness and below 500°F with 1/2-inch blanket thickness.
Black paint	Sicon-Black 7 x 983 or equivalent low gloss paint applied to insulation jacket exterior.	Promote heat loss during hot bias environment firing periods.

SPACE SHUTTLE APU GAS GENERATOR CONDUCTION NETWORK

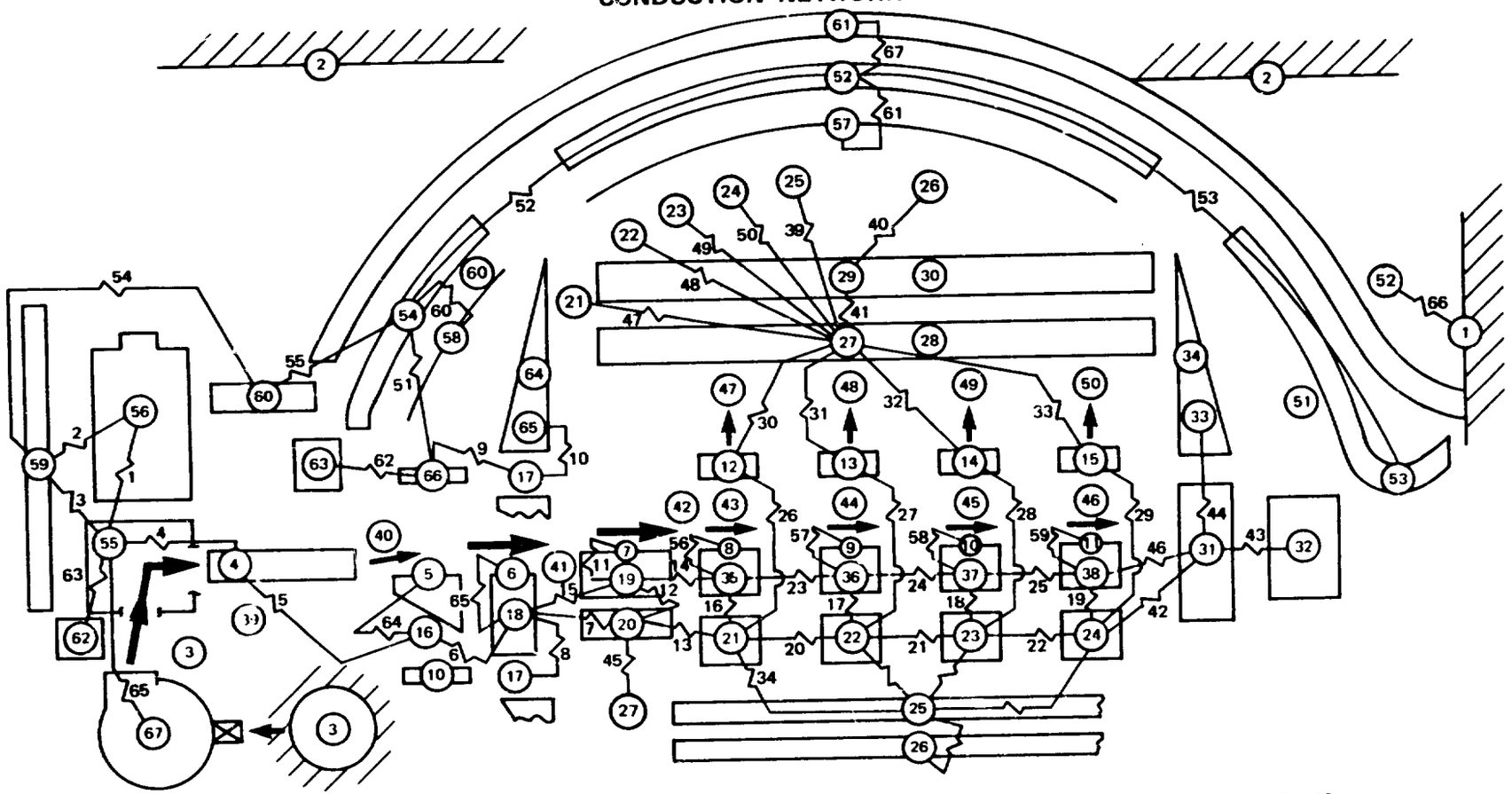

1 TURBOMACHINERY
2. RADIATIVE HEAT SINK
3. PROPELLANT SUPPLY
4. FEED TUBE O-RING FLANGE
5. & 6. INSIDE FEED TUBE TRANSITION SECTIONS
7. INSIDE INJ BRANCHES
8. – 11. INSIDE INJ PASSAGES
12. – 15. RIGIMESH
16. OUTSIDE FEED TUBE
17. SUPPORT RING JUNCTION
18. SUPPORT RING FLANGE
19. BRANCH TUBE BOSS
20. OUTSIDE BRANCH TUBES
21. – 24. INJECTOR WEBBS
25. INNER BED SEPARATOR
26. OUTER BED SEPARATOR
27. INNER CATALYST BED MAX
28. INNER CATALYST BED MIN
29. OUTER CATALYST BED MAX
30. OUTER CATALYST BED MIN
31. INJECTOR PASSAGE BOSS
32. RETAINER SECTION
33. LOWER CLOSURE MAX
34. LOWER CLOSURE MIN
35. – 38. OUTSIDE OF PASSAGES
39. – 50. TRAPPED PROPELLANT DURING SOAKBACK OR FLOWING PROPELLANT DURING FIRING
51. HOT GAS OUTFLOW
52. CHAMBER WALL
53. NOZZLE TRANSITION
54. CHAMBER FORWARD CLOSURE TRANSITION
55. VALVE FILTER
56. VALVE MOTOR HOUSING
57. & 58. CONVECTIVE HEAT SHIELDS
59. VALVE MOUNT PLATE
60. THERMAL STANDOFFS
61. CHAMBER INSULATION
62. VALVE HEATER
63. CATALYST BED HEATER
64. FWD BED CLOSURE MIN
65. FWD BED CLOSURE MAX
66. SUPPORT TUBE
67. PROPELLANT PUMP & SHUTOFF VALVE

Figure 3-6

11071-43

SPACE SHUTTLE APU GAS GENERATOR CONVECTION NETWORK

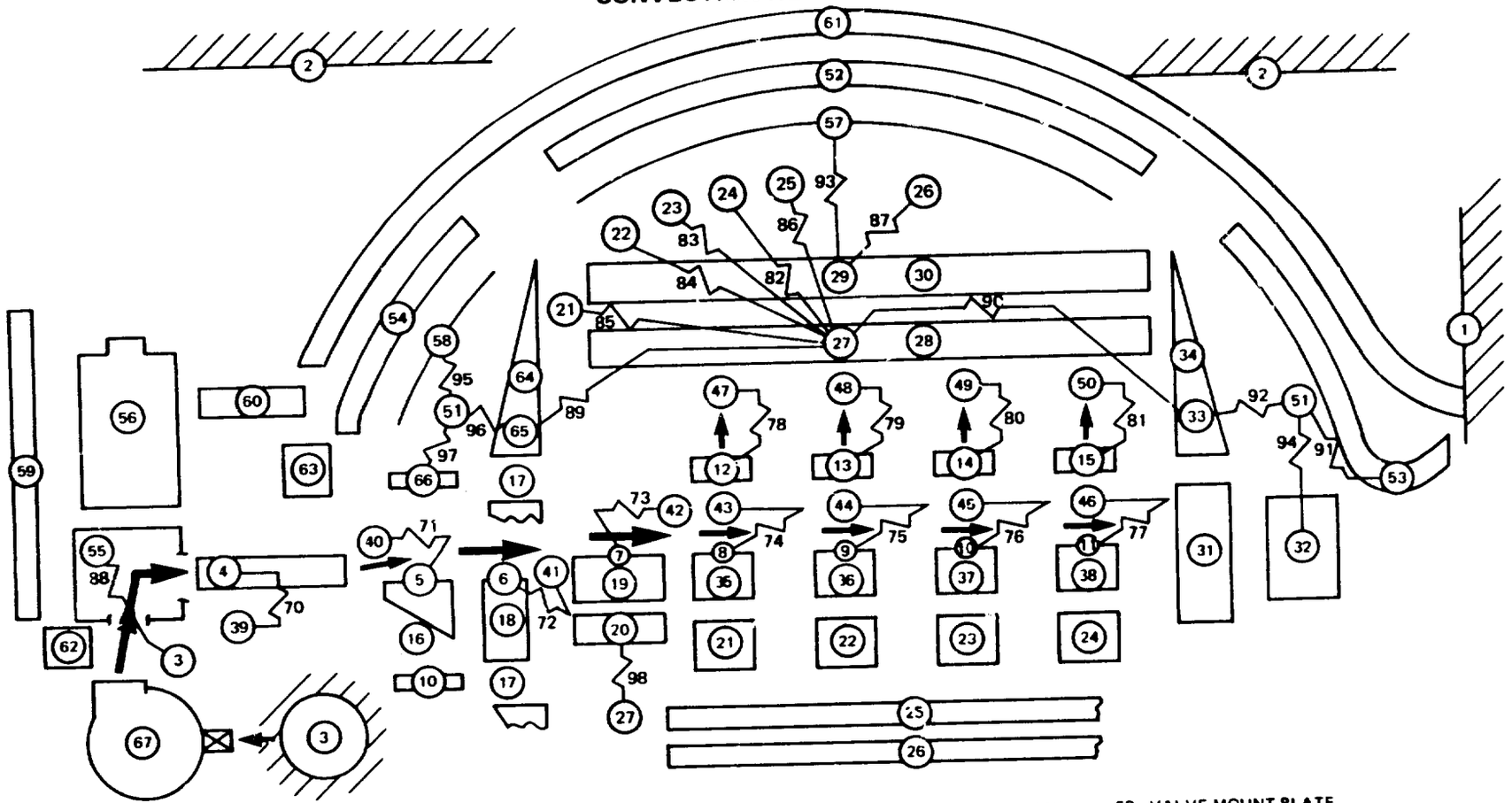

1 TURBOMACHINERY
2. RADIATIVE HEAT SINK
3 PROPELLANT SUPPLY
4. FEED TUBE O-RING FLANGE
5. & 6. INSIDE FEED TUBE TRANSITION SECTIONS
7. INSIDE INJ BRANCHES
8. – 11. INSIDE INJ PASSAGES
12. – 15. RIGIMESH
16. OUTSIDE FEED TUBE
17. SUPPORT RING JUNCTION
18 SUPPORT RING FLANGE
19. BRANCH TUBE BOSS
20. OUTSIDE BRANCH TUBES
21. – 24. INJECTOR WEBBS
25. INNER BED SEPARATOR
26. OUTER BED SEPARATOR
27. INNER CATALYST BED MAX
28. INNER CATALYST BED MIN
29. OUTER CATALYST BED MAX
30. OUTER CATALYST BED MIN
31. INJECTOR PASSAGE BOSS
32. RETAINER SECTION
33. LOWER CLOSURE MAX
34. LOWER CLOSURE MIN
35. – 38. OUTSIDE OF PASSAGES
39. – 50. TRAPPED PROPELLANT DURING SOAKBACK OR FLOWING PROPELLANT DURING FIRING
51. HOT GAS OUTFLOW
52. CHAMBER WALL
53. NOZZLE TRANSITION
54. CHAMBER FORWARD CLOSURE TRANSITION
55. VALVE FILTER
56. VALVE MOTOR HOUSING
57. & 58. CONVECTIVE HEAT SHIELDS
59. VALVE MOUNT PLATE
60. THERMAL STANDOFFS
61. CHAMBER INSULATION
62. VALVE HEATER
63. CATALYST BED HEATER
64. FWD BED CLOSURE MIN
65. FWD BED CLOSURE MAX
66. SUPPORT TUBE
67. PROPELLANT PUMP & SHUTOFF VALVE

Figure 3-7

Peak nucleate boiling heat flux may occur anywhere between 10 and 90°F above saturation, and minimum film boiling occurs very near 100°F above saturation. Thus, in calculating the bulk propellant temperature in separate sections of the injector, forced convection equations were used for wall temperatures below saturation plus 10°F. Nucleate boiling was used for wall temperatures between 10 and 100°F above saturation and film boiling equations were used for wall temperatures in excess of saturation plus 100°F.

The above approach is felt to be conservative since heat flux falls rapidly around the peak nucleate value; however it is felt to be a safe approach for design due to the unreliability of predicting the ΔT for peak nucleate boiling.

The gas generator radiation network is shown in Figure 3-8. All surfaces were assumed diffuse and grey, and the Oppenheim network method was employed for this preliminary analysis. Values of nodal capacitance were calculated from:

$$C = \rho c V$$

where ρ is material density (lbm/ft^3), V is the lumped nodal volume (ft^3), and c is material specific heat (Btu/lbm°F). Boundary nodes can be thought of as having infinite capacitance. Interface nodes have no physical significance and are used just to facilitate the mathematics. However, temperatures are calculated for these and represent the average of surrounding nodes. Zero capacitance is assigned to interface nodes.

3.4.4 Analytical Results

3.4.4.1 Heater Power Requirements

Considering the specified cold-bias environment listed in Table 3-6, catalyst bed and propellant valve and propellant valve temperature variations were calculated as dependent functions of heater power, Figure 3-9, using the previously described analysis methods and thermal model network. Individual active heaters are required to maintain both the bed and valve temperatures above the minimum threshold levels of 200 to 225 and 45°F, respectively. These threshold temperatures ensure smooth, reliable initial start characteristics that are necessary for long mission life when subjected to vehicle and turbomachinery temperatures as low as -100°F. Figure 3-5 shows that a 40-watt heater will maintain the catalyst bed at 205°F while the valve requires 6.9 watts to maintain its temperature level at 45°F.

If the REA heaters are turned off for prolonged periods, the units must be activated with sufficient time allowed for a transient warming period prior to operation. Figure 3-10 shows the transient warming period to be 4.0 hours if the initial component temperatures are at 40°F, when the ambient and turbomachinery temperatures are -100°F. A more detailed account of the flight environment and turbomachinery temperature profiles is desirable for optimization of the heater power requirements.

SPACE SHUTTLE APU GAS GENERATOR RADIATION NETWORK

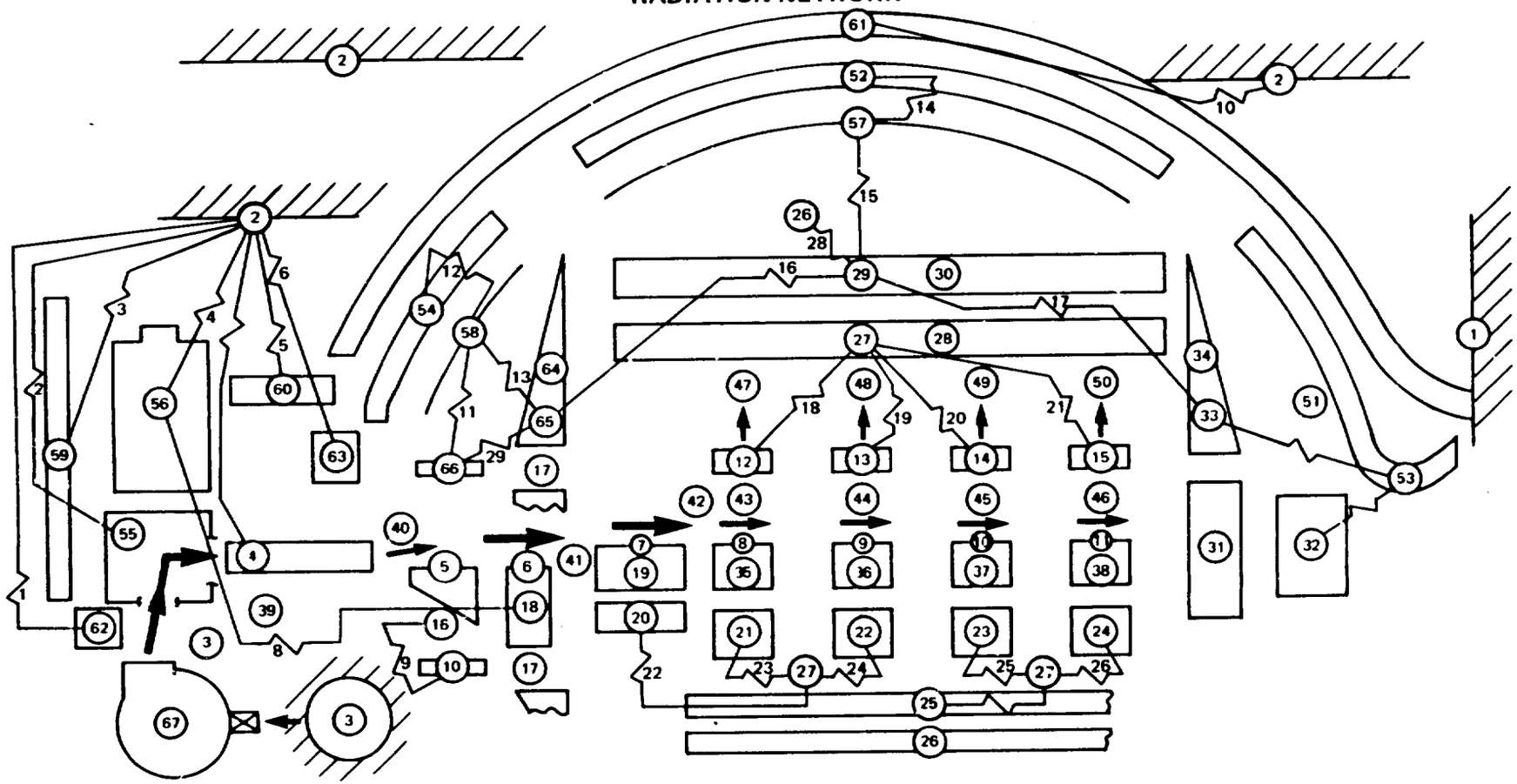

1. TURBOMACHINERY
2. RADIATIVE HEAT SINK
3. PROPELLANT SUPPLY
4. FEED TUBE O-RING FLANGE
5. & 6. INSIDE FEED TUBE TRANSITION SECTIONS
7. INSIDE INJ BRANCHES
8. – 11. INSIDE INJ PASSAGES
12. – 15. RIGIMESH
16. OUTSIDE FEED TUBE
17. SUPPORT RING JUNCTION
18. SUPPORT RING FLANGE
19. BRANCH TUBE BOSS
20. OUTSIDE BRANCH TUBES
21. – 24. INJECTOR WEBBS
25. INNER BED SEPARATOR
26. OUTER BED SEPARATOR
27. INNER CATALYST BED MAX
28. INNER CATALYST BED MIN
29. OUTER CATALYST BED MAX
30. OUTER CATALYST BED MIN
31. INJECTOR PASSAGE BOSS
32. RETAINER SECTION
33. LOWER CLOSURE MAX
34. LOWER CLOSURE MIN
35. – 38. OUTSIDE OF PASSAGES
39. – 50. TRAPPED PROPELLANT DURING SOAKBACK OR FLOWING PROPELLANT DURING FIRING
51. HOT GAS OUTFLOW
52. CHAMBER WALL
53. NOZZLE TRANSITION
54. CHAMBER FORWARD CLOSURE TRANSITION
55. VALVE FILTER
56. VALVE MOTOR HOUSING
57. & 58. CONVECTIVE HEAT SHIELDS
59. VALVE MOUNT PLATE
60. THERMAL STANDOFFS
61. CHAMBER INSULATION
62. VALVE HEATER
63. CATALYST BED HEATER
64. FWD BED CLOSURE MIN
65. FWD BED CLOSURE MAX
66. SUPPORT TUBE
67. PROPELLANT PUMP & SHUTOFF VALVE

Figure 3-8

11071-45

SHUTTLE APU GAS GENERATOR HEATER POWER SUMMARY (COLD ENVIRONMENTAL CONDITIONS)

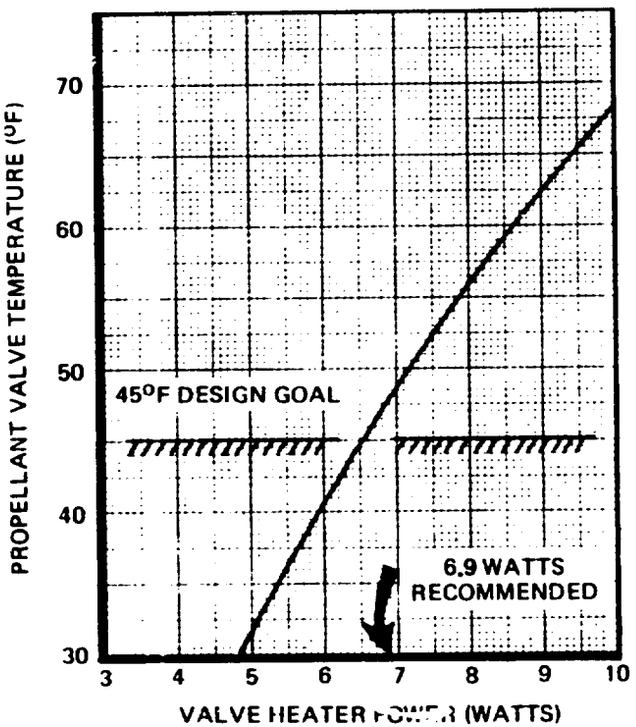

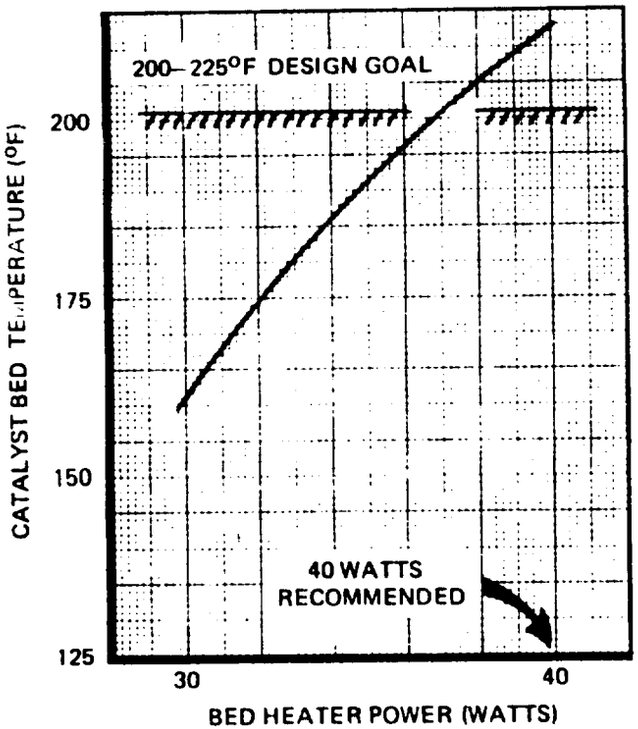

3-21

Figure 3-9

HEATER TRANSIENT RESPONSE

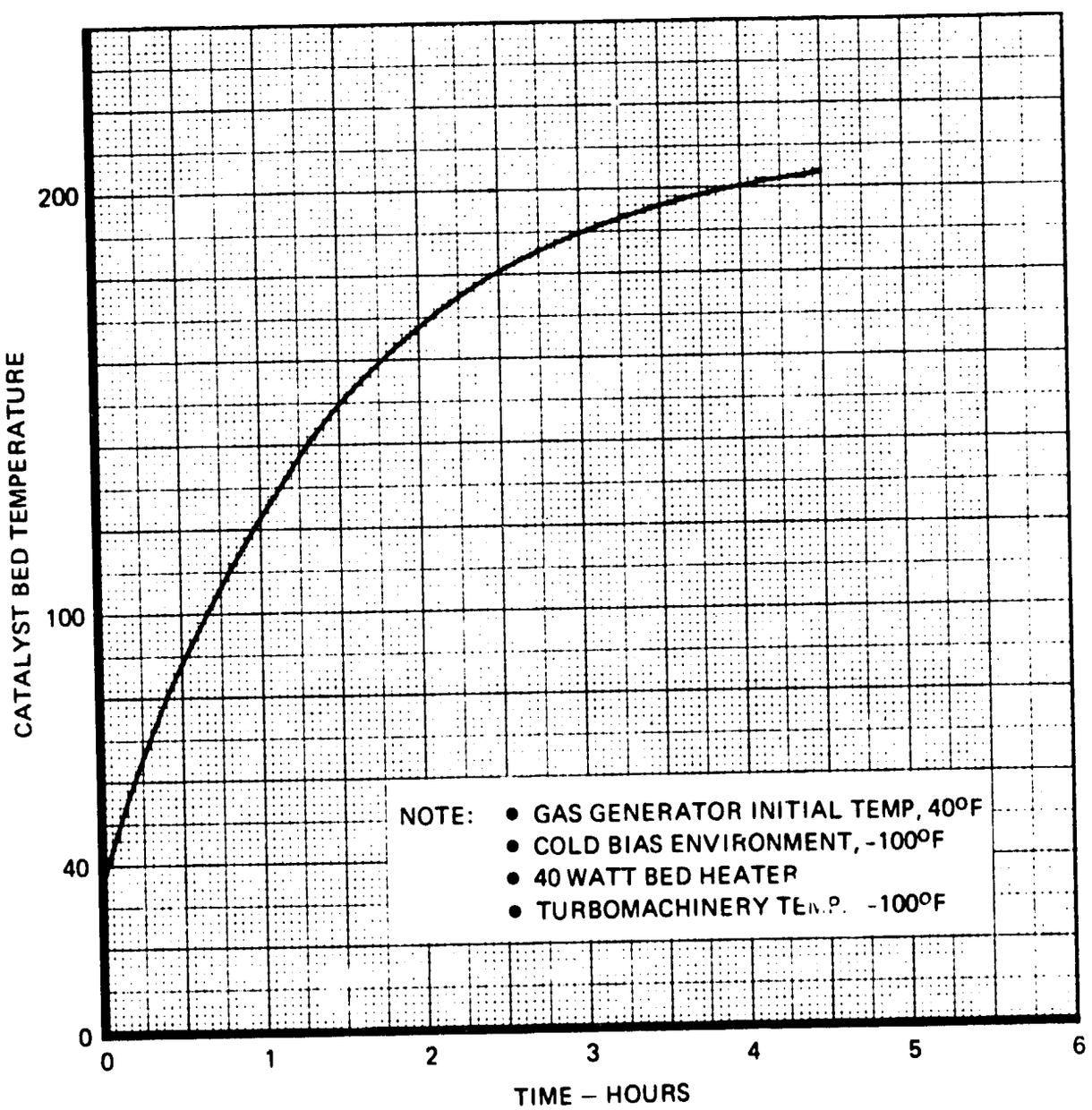

11071-46

Figure 3-10

3.4.4.2 Insulation Requirements

Application of a blanket of Johns-Manville Min-K-2000 insulation will limit the gas generator surface temperature. The insulation blanket is contained in a vented jacket of stainless steel foil in a manner similar to that employed on the RRC flight qualified Transtage engine. Figure 3-11 shows the variation of surface temperature with respect to insulation thickness. Note that the outer surface of the foil jacket must be painted black to reduce the surface temperature. The recommended black coating is Sicon-Black 7X983 or equivalent low gloss, high temperature black paint. This product has also been flight qualified at RRC on the P-95 REM-Mono Program.

As shown in Figure 3-11, the gas generator surface temperature can be limited to 500°F with an insulation thickness of approximately 0.5 inch.

3.4.4.3 Maximum Component Temperatures

Temperatures of the valve, injector, and gas generator were evaluated for operational and post-firing soakback conditions. The hot environment of Table 3-6 was assumed with both bed and valve heaters active during and after firing periods. Convective cooling effects of the incoming propellant keeps the valve (node 55) at a temperature level of 154°F. As the propellant flows through the injector liquid circuit, its temperature increases to the maximum value of 157°F as it flows through the Rigimesh screen.

During the soak period the propellant valve reaches a maximum of 283°F approximately 12 minutes after shutdown. The feed tube O-ring reaches a peak temperature of 345°F in 12 minutes after shutdown from maximum flow rate. Although the O-ring temperature exceeds the design goal, it is within specification limits of the manufacturer. Maximum temperature for continuous service is specified to be 350°F.

3.4.4.4 Pulse Modulated Duty Cycle Limits

Figure 3-12 presents the results of analyses to determine duty cycle limits for pulse modulated operation. The data of Figure 3-12 are based upon equilibrium pulsing in a hot environment with 40-millisecond pulse widths at a feed pressure that would deliver a 0.23 lbm/sec flow rate at steady state.

It is assumed that the limiting condition corresponds to when the injector surface temperature upstream of the Rigimesh covered passages exceeds a value in excess of 450°F.

For the gas generator, two regions of the injector were considered as critical – the feed tube exit and the feed-to-branch tube transition area. For this application the feed tube exit was considered most critical. A critical temperature limit of 450°F was also established which was not to be exceeded in soakback between pulses at any duty cycle. Figure 3-12 shows the temperatures of various areas as a function of duty cycle. Based on the foregoing assumptions, a duty cycle of 0.8 percent was established as the minimum allowable. It is recommended that testing be conducted to more accurately define the limiting conditions.

SHUTTLE APU GAS GENERATOR INSULATION REQUIREMENTS
(HOT ENVIRONMENTAL CONDITIONS)

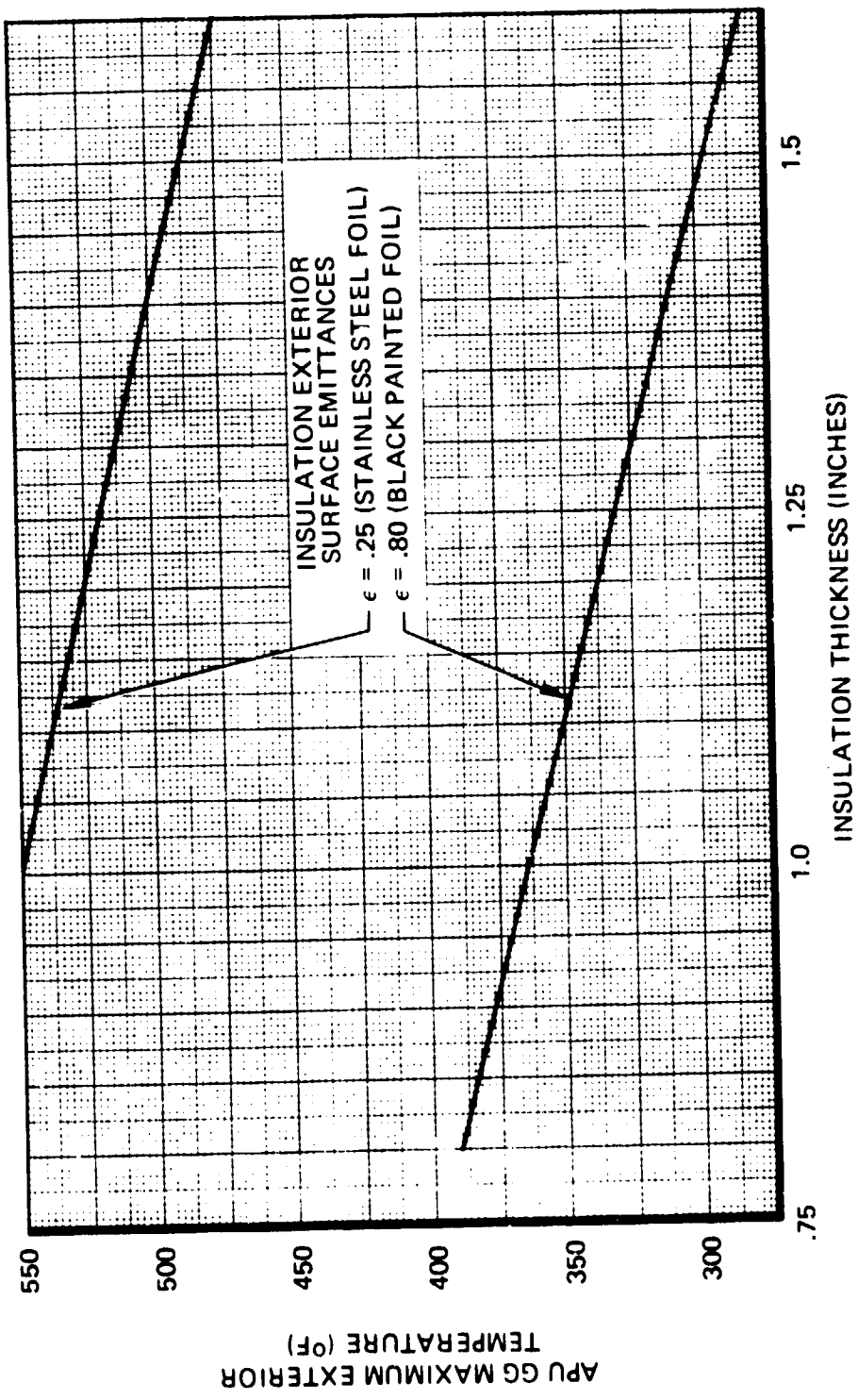

11071-47

Figure 3-11

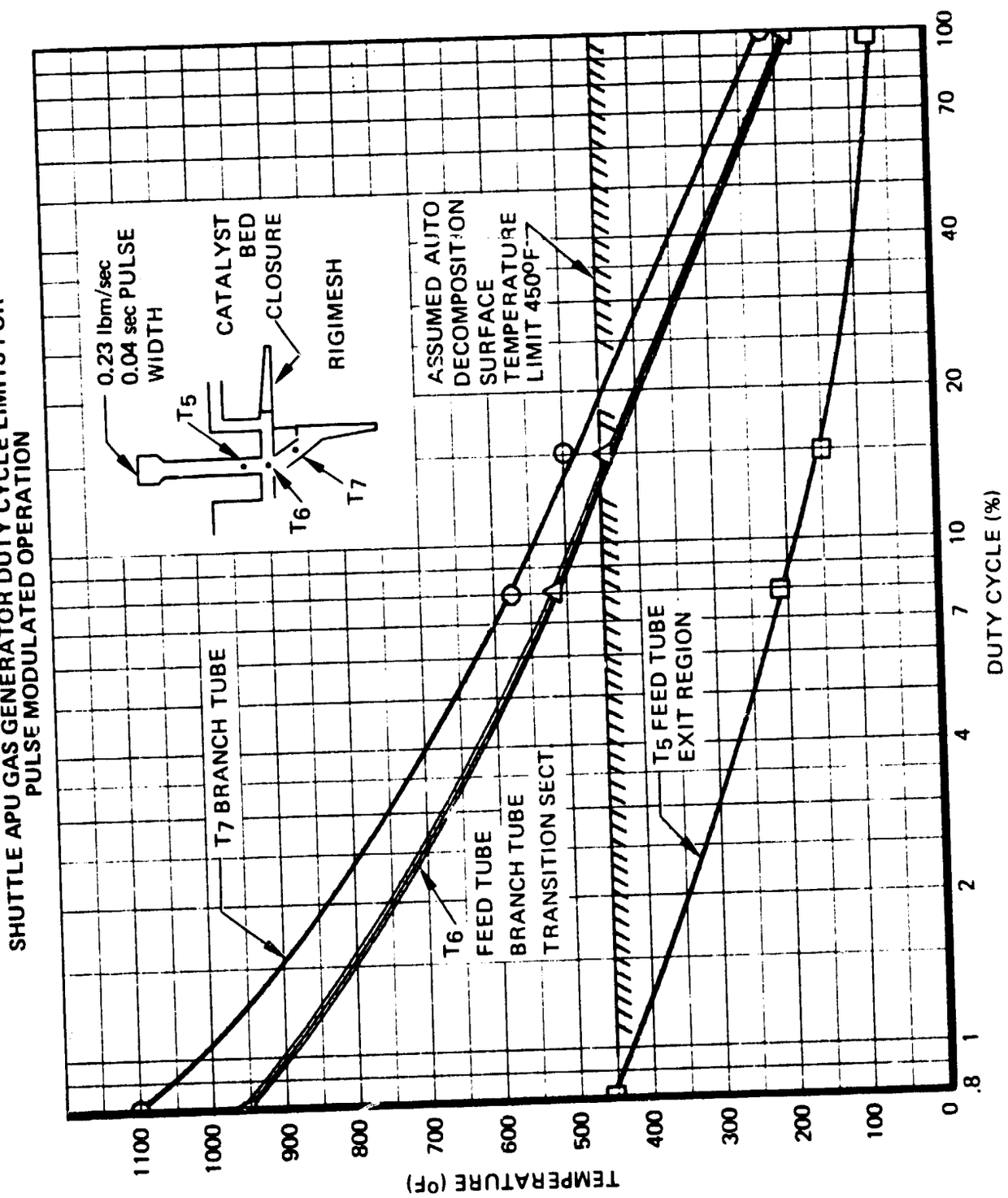
SHUTTLE APU GAS GENERATOR DUTY CYCLE LIMITS FOR PULSE MODULATED OPERATION
TEMPERATURE (°F)
DUTY CYCLE (%)
1100
1000
900
800
700
600
500
400
300
200
100
0
.8
1
2
4
7
10
20
40
70
100
T7 BRANCH TUBE
T6 FEED TUBE BRANCH TUBE TRANSITION SECT
T5 FEED TUBE EXIT REGION
ASSUMED AUTO DECOMPOSITION SURFACE TEMPERATURE LIMIT 450°F
0.23 lbm/sec
0.04 sec PULSE WIDTH
CATALYST BED CLOSURE
RIGIMESH
T5
T6
T7

Figure 3-12

3.4.4.5 Pressure Modulated Flow Rate Limits

The minimum flow rate allowable during steady-state operation was calculated based upon the following assumptions:

- Heat transfer rates based on turbulent flow
- Hot orbit propellant entering the injector
- Minimum flow rate allowable established when a local injector surface temperature adjacent to liquid propellant exceeds the local propellant saturation temperature or the 450°F arbitrarily established decomposition temperature.

As the operating feed pressure decreases, the propellant flow rate and convective cooling capability within the injector passages decrease proportionately. The general outcome is an increase in local passage wall temperature as well as a decrease in the propellant saturation temperature. Eventually the hydrazine saturation temperature falls below the local wall temperature, whereupon nucleate boiling and two-phase flow could possibly occur.

For the APU gas generator the critical local injector surface temperature was found to be in the downstream part of the Rigimesh element. Here, surface temperature increased at the greatest rate as the flow rate dropped. Figure 3-13 is a plot of lower Rigimesh temperature versus local propellant saturation temperature. This plot established 0.042 lbm/sec as the recommended minimum flow rate limit.

3.4.5 Experimental Results

3.4.5.1 Injector Temperatures

Figure 3-14 shows correlation of measured injector temperature with the thermal model. The correlation shows that the thermal model is conservative. This is significant because the duty cycle and minimum flow rate limits recommended in Figures 3-12 and 3-13 are based on the injector temperature calculations.

3.4.5.2 Bedplate Temperatures

Only outer bedplate temperatures were measured; however, from correlation of these data a satisfactory confidence level can be established for the inner bedplates. The predicted maximum and minimum outer bedplate temperatures were 1,930 and 1,680°F, respectively. At the corresponding flow rate, experimental bedplate temperatures ranged from 1,900 to 1,700°F.

The combinations of maximum temperature, maximum temperature gradient, and maximum bedplate pressure differential all contribute to the structural design. As discussed above, the predicted maximum temperature and thermal gradient are 1,930 and 250°F compared with measured values of 1,900 and 200°F. From these results it can be concluded that a bedplate structural design based on such information is conservative.

APU GAS GENERATOR MINIMUM FLOW RATE LIMITS FOR PRESSURE MODULATED OPERATIONS

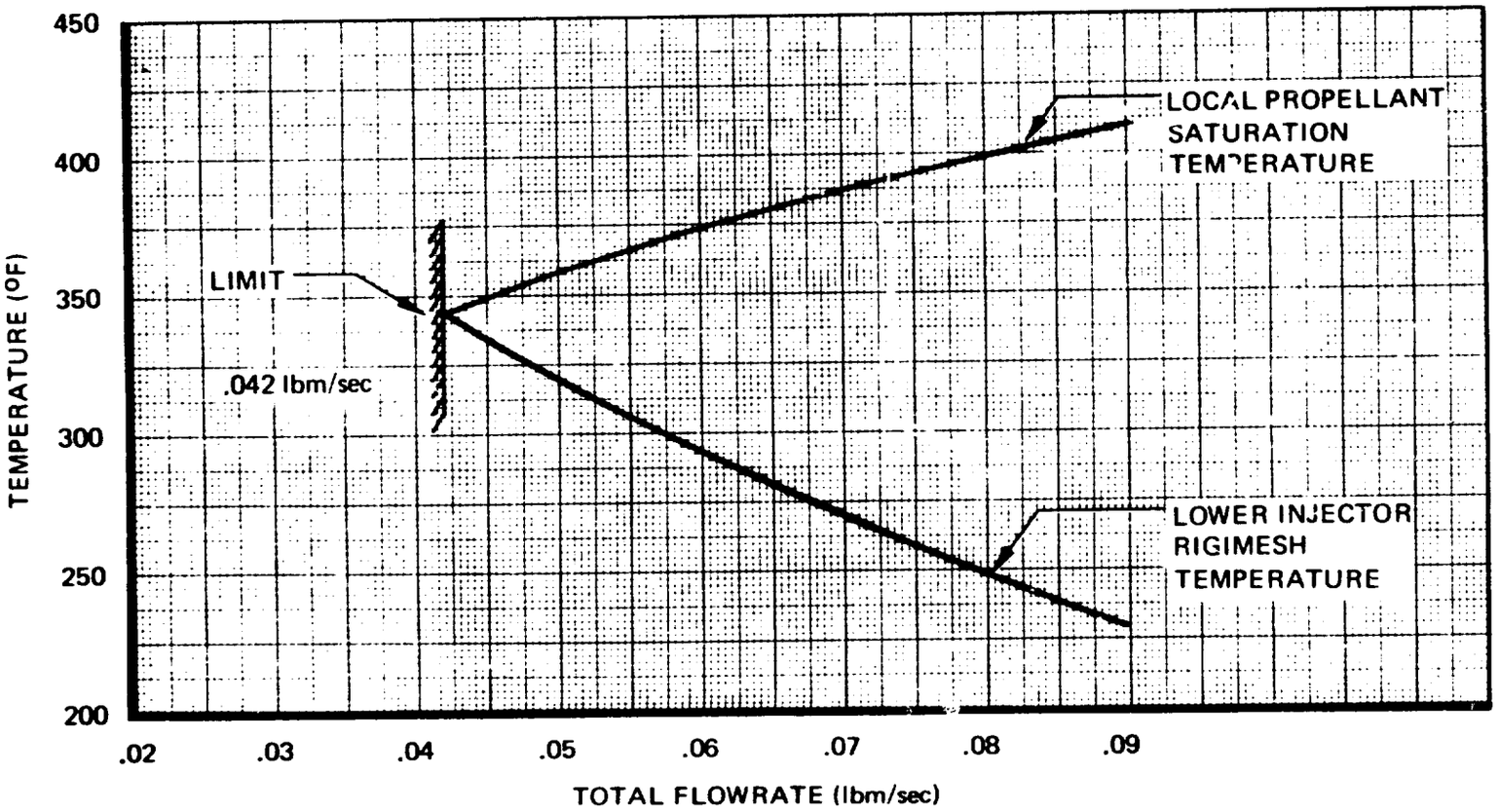

Figure 3-13

SPACE SHUTTLE APU GAS GENERATOR
THERMAL MODEL CORRELATION DATA

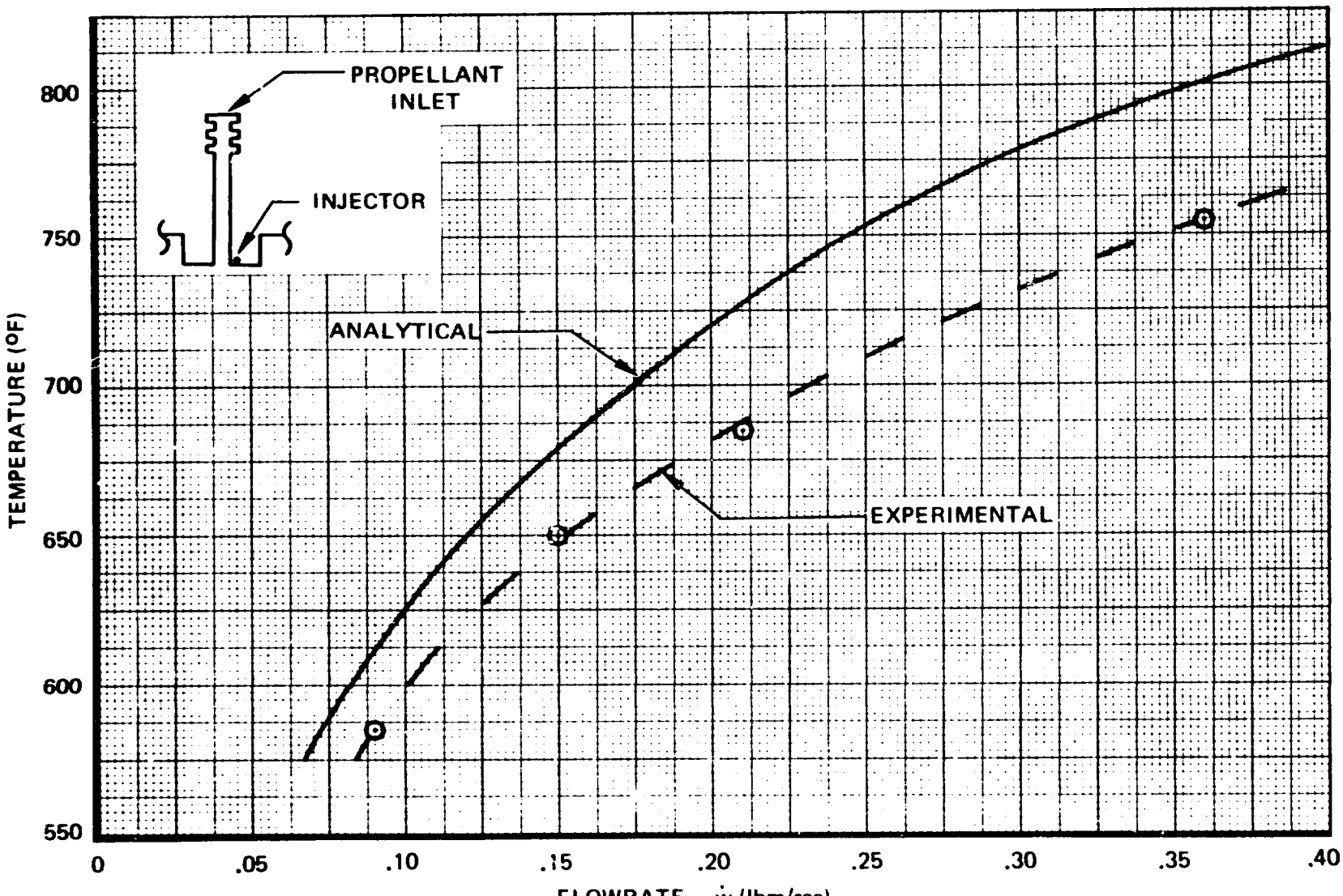

Figure 3-14

3.5 STRESS AND DYNAMICS ANALYSIS

3.5.1 Static Stress Analysis

A stress analysis has been made using the design criteria presented in Table 3-9. Short-term yield and burst, long-term distortion, and creep rupture have been considered as static failure modes. Results of the analysis are presented in Table 3-10.

3.5.2 Dynamic Analysis

An analysis of dynamic stresses was conducted based on a dynamic input random vibration of 1.6 g^2/Hz maximum level. Critical stresses occur in the standoffs during hot vibrating conditions. For the assumed conditions, the analysis indicates a positive margin on yield and ultimate. Results are presented in Table 3-11.

Table 3-9
STRUCTURAL DESIGN CRITERIA

Temperatures	1,700°F maximum peak chamber temperature 1,650°F maximum operating chamber temperature 1,750°F maximum outer bed temperature 1,800°F maximum inner bed temperature		
Pressure Schedule			
Chamber	750 psi	180 sec/mission	17 hours life
	375 psi	150 sec/mission	14 hours life
	225 psi	630 sec/mission	60 hours life
	140 psi	4,320 sec/mission	408 hours life
			499 hours life
Bed Drop	12 psid average over life 50 psid burst pressure		
Life Structural Components	500 hours total exposure 100 hours at maximum life average chamber pressure 200 startup cycles operational life, internal components 1,000 startup cycles, total life pressure chamber and external structural components		
Safety factors	2.0 on burst 1.5 on yield 1.0 on creep		
Allowables			
Stress -- Hastelloy B			
Short term yield	f_{ty}	29.1 ksi at 1,700°F	23.0 ksi at 1,800°F
Short term ultimate	f_{tu}	29.7 ksi at 1,700°F	23.0 ksi at 1,800°F
Creep rupture	f_r at 1,650°F, 100 hours		14 ksi
0.5% uniaxial creep	f_d at 1,650°F, 100 hours		5.5 ksi

Table 3-10
SUMMARY OF MINIMUM MARGINS OF SAFETY

$$MS = \left(\frac{Sa}{SD \times SF}\right) - 1$$

CHAMBER

FOREWARD CLOSURE: $MS_{YIELD} = \left(\frac{29.1}{10.7 \times 1.5} - 1\right) = +0.813$

FOREWARD CLOSURE: $MS_{ULT} = \left(\frac{29.7}{7.13 \times 2.0} - 1\right) = +1.08$

CHAMBER THREAD: $MS_{ULT} = \left(\frac{29.7}{7.5 \times 2.0} - 1\right) = +0.98$

CREEP – DEFORMATION OR RUPTURE

DEFORMATION – INCREASE IN RADIUS = +0.015 IN.

CREEP RUPTURE (20 HOURS AT 1,700°F AND 750 psia):

CHAMBER BODY: $MS = \left(\frac{11.0}{5.8} - 1\right) = +0.896$

CHAMBER THREAD: $MS = \left(\frac{11.0}{7.5} - 1\right) = +0.467$

BED ASSEMBLY

MS ON RUPTURE, RETAINING NUT, AND THREAD

ASSUME 1,800°F, 500 psi SHORT-TERM ULTIMATE PRESSURE DIFFERENTIAL

$MS = \left(\frac{23.0}{19.5} - 1\right) = +0.178$

Table 3-11
DYNAMICS ANALYSIS RESULTS

- INPUT RANDOM VIBRATION 28.2 g rms OVERALL

LEVEL	RATE	RANGE
0.1 g^2/Hz	FLAT	20 TO 90 Hz
–	+12 db/OCTAVE	90 TO 180 Hz
1.6 g^2/Hz	FLAT	180 TO 350 Hz
–	-6 db/OCTAVE	350 TO 2,000 Hz

- FUNDAMENTAL FREQUENCY OF MODULE: 585 Hz
- FUNDAMENTAL FREQUENCY OF FEED TUBE: 863 Hz
- THREE-SIGMA SUPPORT TUBE STRESS: 34.7 ksi
- THREE-SIGMA FEED TUBE STRESS: 19.6 ksi
- THREE-SIGMA DISPLACEMENT AT AFT END OF INJECTOR: 0.010 INCH
- THREE-SIGMA DISPLACEMENT AT FEED TUBE FORWARD END: 0.012 INCH
- g rms OVERALL AT AFT END OF INJECTOR: 120 g rms
- g rms OVERALL AT FORWARD END OF INJECTOR: 34 g rms

4.0 HARDWARE FABRICATION, TEST, AND EVALUATION

4.1 GAS GENERATOR ASSEMBLY

A drawing of the gas generator assembly was presented in Figure 3-1. Photographs of the unit in various stages of assembly are shown in Figure 4-1. The gas generator is a radial outflow design consisting of an injector body, inner and outer bed cylinders, bed closure plates, bed spacers, chamber closure, and an outer pressure chamber.

The injector, shown in the upper left-hand photo of Figure 4-1, incorporated four Rigimesh injection elements EB-welded to the injector body. The downstream end of the injector was threaded to permit easy removal of the catalyst bed end closure.

The bedplate cylinders contained slots designed to permit passage of the decomposition gases while retaining the catalyst particles. No screen wires were used for catalyst retention. The slots were EDM machined after finish machinging the bed cylinders.

The nickel foam used in the inner bed was fabricated at RRC (see Volume III).

Thermocouples were attached to the outer bed cylinder (4 locations) as shown in Figure 4-1. Four thermocouples were also installed in the annular area between the outer chamber wall and catalyst bed to monitor outlet gas temperature (Figure 3-1).

Hastelloy B was the material selected for fabrication of all components with the exception of the Rigimesh injection elements, which were fabricated from Haynes 25.

4.2 TEST PROGRAM

Following completion of the detailed design effort and fabrication of the gas generator, a series of tests was conducted to demonstrate the gas generator performance and operational characteristics during simulated Space Shuttle mission firings. Two modes of operation were under consideration by NASA for varying the output power of the APU, namely pulse modulation and pressure modulation. In the former, output power was varied by operating the gas generator at different pulse widths and duty cycles, whereas, in pressure modulation, output power variations were achieved by throttling flow rate during steady-state operation.

Of major concern was the life capability of the gas generator in the two modes of operation. It was, therefore, the goal of the test program to obtain life data for both modes of operation during simulated mission firings. This was accomplished by first conducting 20 simulated missions in the pressure-modulated mode of operation, refurbishing the unit, and then conducting 20 simulated missions in pulse mode. Upon completion of the pulse-modulated mission, the gas generator was again refurbished and delivered to NASA-JSC where an additional 20 missions (pulse-modulated) were conducted.

GAS GENERATOR ASSEMBLY

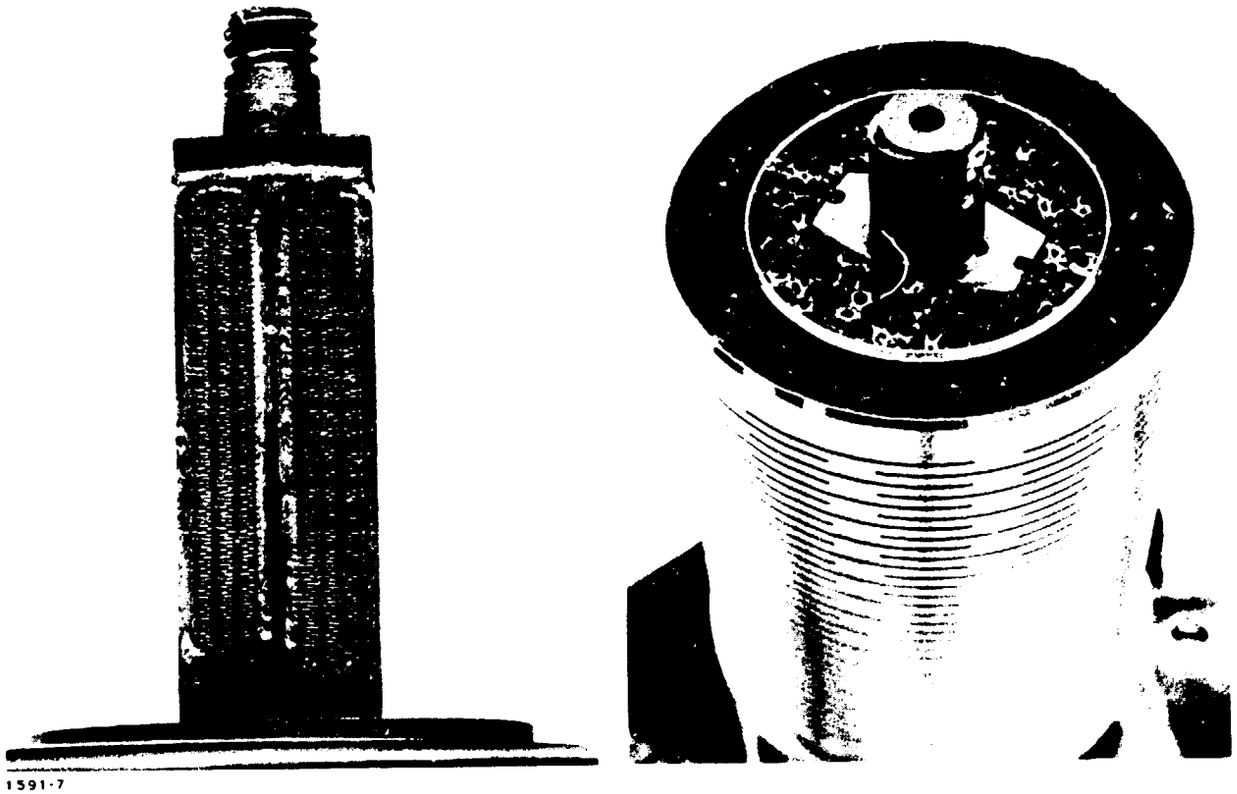

1591-7

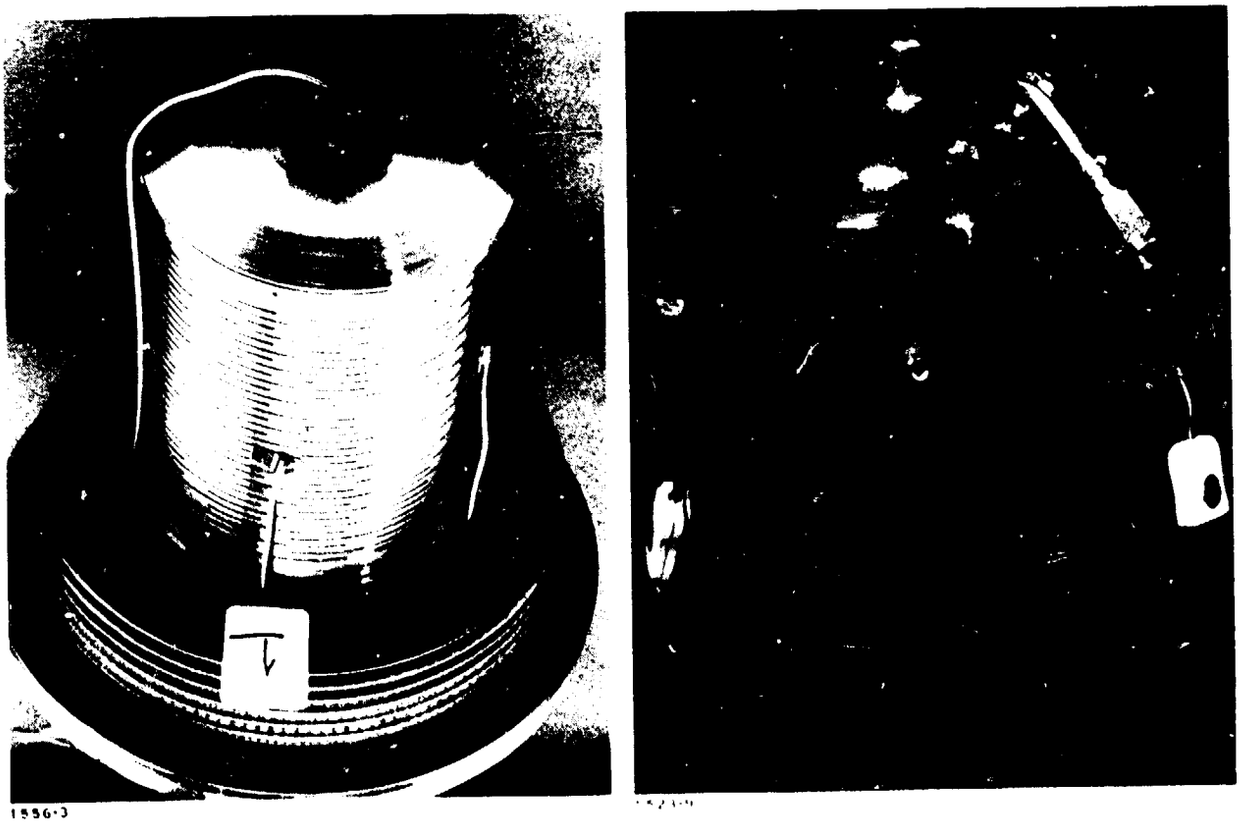

1556-3

11091-61

Figure 4-1

For the NASA tests, the gas generator was refurbished by use of 14- to 18-mesh Shell 405 catalyst for both inner and outer beds, whereas 25- to 30-mesh catalyst was used in the inner bed for the previous tests.

Prior to delivery of the reactor to NASA, a series of tests was conducted to demonstrate attitude insensitivity and hot restart capability of the gas generator under various thermal conditions.

The tests at RRC were conducted in accordance to the test plan (Ref. 4-1). All firings were at sea level. Continuous measurements were made of gas temperature (4 places), bedplate temperatures (4 places), nozzle inlet temperature, injector cavity temperature, outer wall temperatures, chamber pressure, and propellant flow rate.

The test procedures for the tests conducted at NASA-JSC are described in Reference 4-2.

4.2.1 Pressure-Modulated Tests

The test sequence employed for the pressure-modulated tests is presented in Figure 4-2. Prior to beginning the pressure-modulated tests, it was decided that the pulse-mode capability of the gas generator should be demonstrated. Consequently, one mission in pulse mode was conducted at a nominal flow rate of 0.23 lbm/sec. A Marotta MV100 valve was used for on/off control during this test. The mission duty cycle employed for the test is shown in Table 4-1. A schematic of the test set up is presented in Figure 4-3.

Table 4-1
DUTY CYCLES FOR
PULSE-MODE DEMONSTRATION

Power Level Simulation (%)	Number of Pulses	Pulse Width (sec)	Off Time (sec)
15	908	0.73	4.03
30	180	0.90	2.10
50	74	1.15	1.30
100	34	6.70	0.44

Following successful completion of the pulse-mode mission firing, the pressure-modulated mission firings were initiated. The throttle valve employed for these firings was a modified E-Systems valve supplied by NASA. A Marotta MV130 valve was used for on/off control. After completing five missions, the throttle valve malfunctioned and was subsequently replaced with four on/off valves manifolded in parallel lines and orificed to provide the required flow rates. Testing was resumed with an acceptance firing to check out the four-valve control system. The flow rates were slightly higher than predicted and were corrected by adjusting feed pressure. The remaining 15 missions were then conducted without incident. At the conclusion of the twentieth mission, a 500-second steady-state firing was conducted at a flow rate of 0.36 lbm/sec to demonstrate sustained maximum power output capability after 30 hours of operation.

Shown in Figure 4-4 is the mission power profile that was conducted for the pressure-modulated missions. Step throttling was used for the various power levels. Each mission consisted of two phases, with a shutdown and restart at 24 minutes into the mission. All starts were conducted with

PRESSURE-MODULATED TEST SEQUENCE

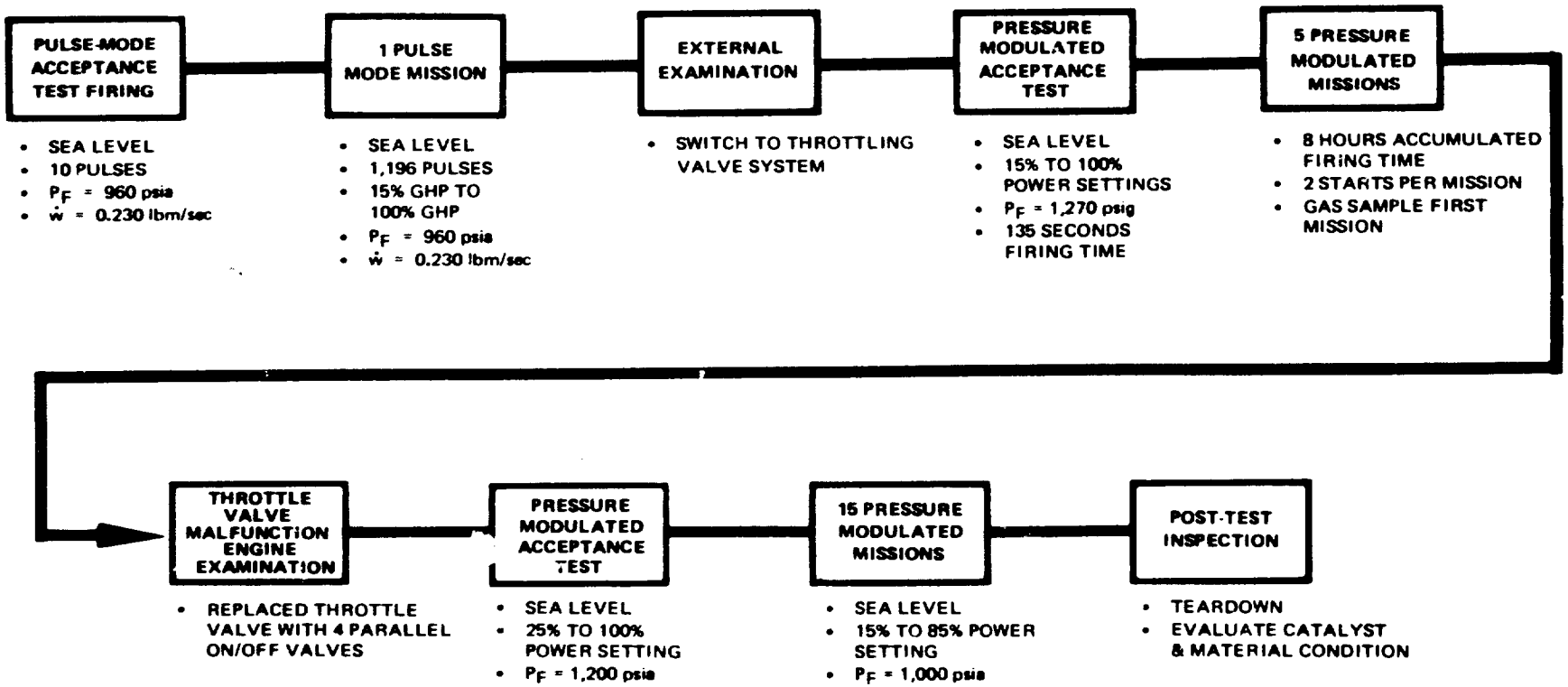

Figure 4-2

SPACE SHUTTLE APU GAS GENERATOR TEST SCHEMATIC

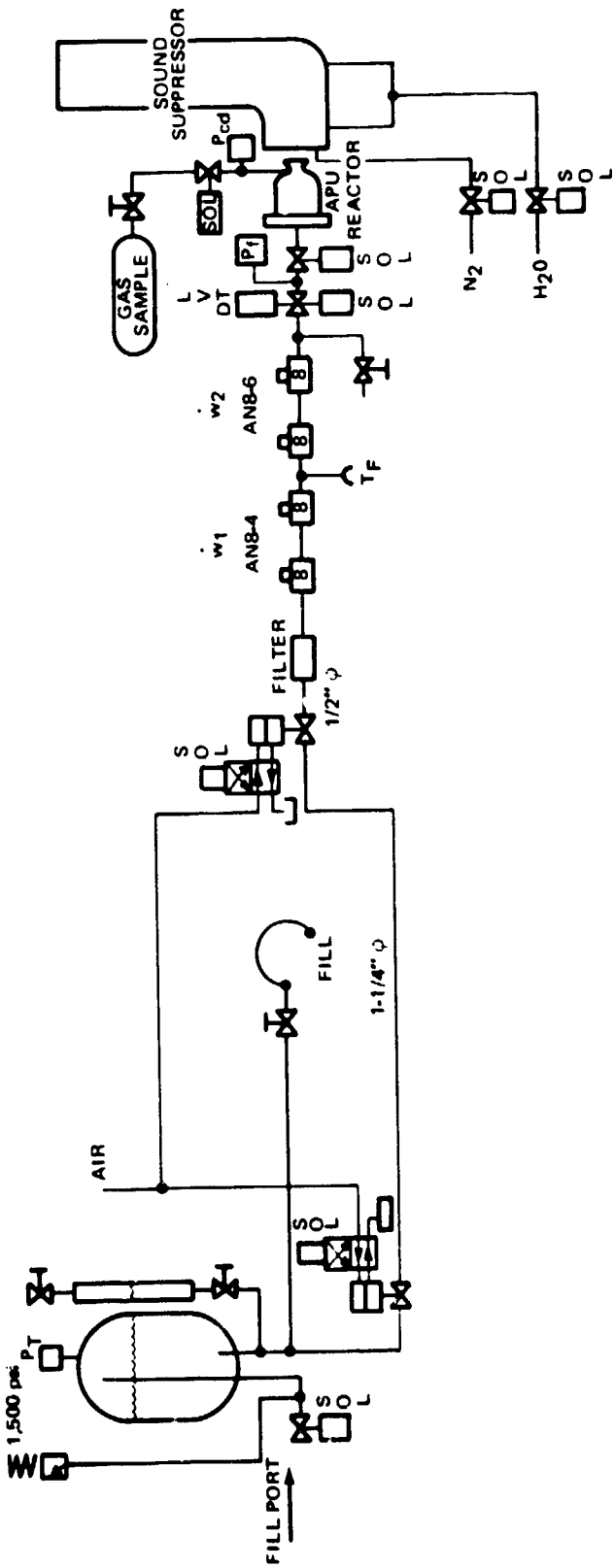

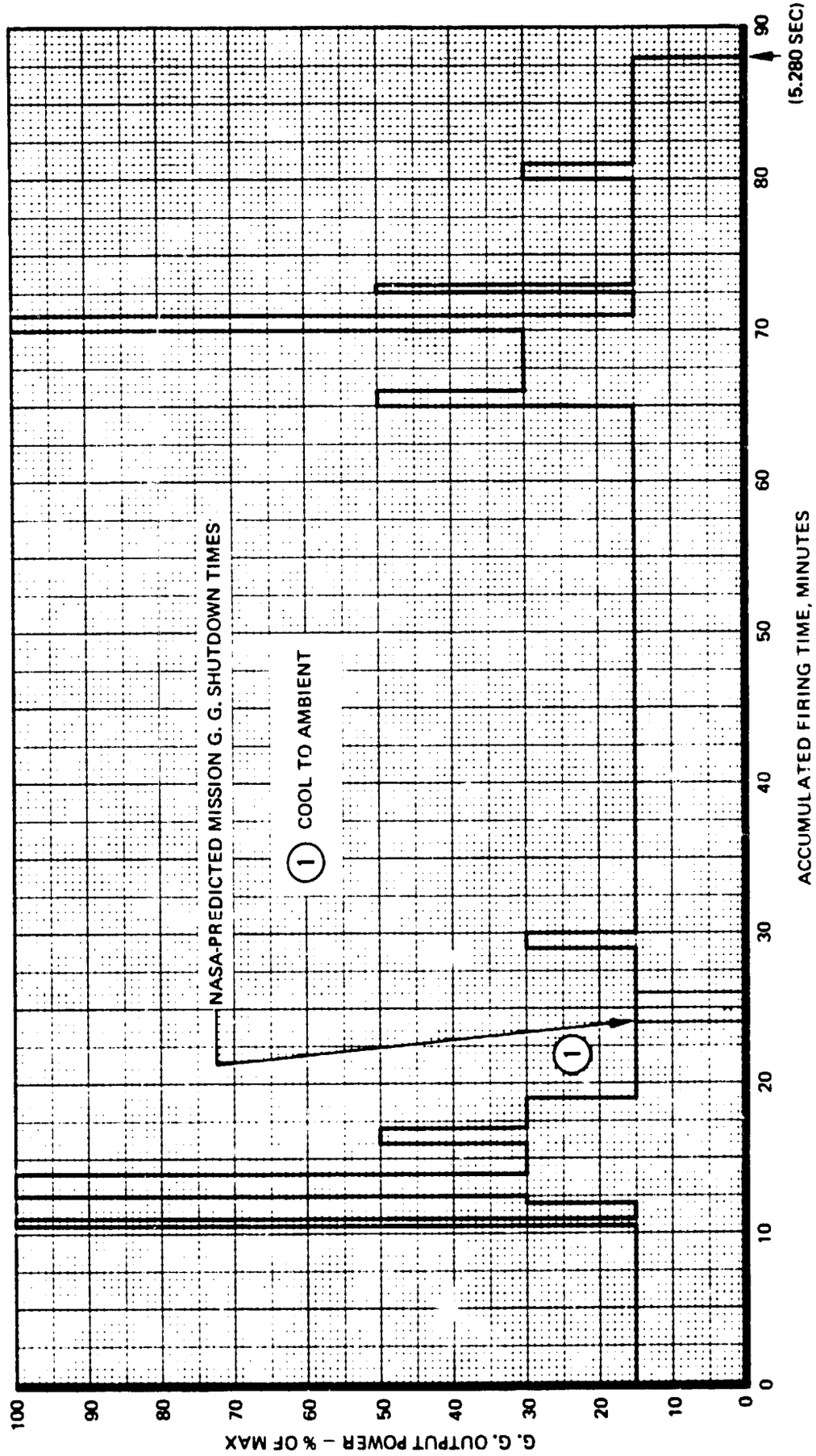

11072-94B

Figure 4-4

the reactor at 200°F. Cooldown between firings generally required 2 hours; no forced cooling was used. No purges were used to prevent air entering the catalyst bed or to remove propellant from the injector. All firings were conducted at sea level conditions. Each mission required 88 minutes of gas generator operation with the majority of the on-time accumulated at the 15% power level corresponding to a flow rate of 0.092 lbm/sec. Maximum design flow rate was 0.36 lbm/sec. A total of 12,500 lbm propellant was consumed during the tests, including the initial pulse-modulated mission.

4.2.2 Pulse-Modulated Tests

Following completion of the pressure-modulated tests, the gas generator was disassembled and inspected for damage and/or loss of catalyst. A minor change was made in the bedplate end-closure design and bedplate slot pattern. It was also decided to remove the catalyst bed spacers and to increase the density of the foam metal from approximately 1.5 to 3.0%. The gas generator was then refurbished using new catalyst, bedplate, and end closures. The injector and chamber were reused without refurbishment.

The test sequence for the pulse-modulated tests is shown in Figure 4-5. Reference firings were conducted after every [illegible] missions to serve as a basis for evaluating steady-state performance of the reactor throughout life tests. The mission duty cycle is presented in Table 4-2. The acceptance test firing sequence is presented in Table 4-3. As in the previous mission firings, each mission consisted of two phases corresponding to launch and reentry, with a cooldown period between phases. All starts were conducted with the reactor at 200°F. A Marotta MV100 on/off valve was used for the entire 20-mission demonstration test without refurbishment.

Table 4-2
PULSE-MODULATED MISSION DUTY CYCLE

Power Level Simulation (%)	Mission Time at Power Level (sec)	Pulse Characteristics			
		On Time (msec)	Off Time (msec)	Pulse Frequency (Hz)	Duty Cycle (%)
15 (Launch)	1,620	90	205	3.4	30.5
30 (Launch)	300	100	125	4.4	44.4
50 (Launch)	90	110	90	5.0	55.0
100 (Launch)	90	250	45	3.4	84.7
Cool to 200°F					
15 (Re-entry)	2,700	90	265	2.82	25.3
30 (Re-entry)	330	100	155	3.92	39.2
50 (Re-entry)	60	110	115	4.47	48.9
100 (Re-entry)	90	190	60	3.97	76.0

Total mission time = 88 minutes
Total on-time = 27.8 minutes
Total pulses = 17,112

PULSE MODULATED TEST SEQUENCE

11079-95A

Figure 4-5

Table 4-3
ACCEPTANCE TEST DUTY CYCLE

On-Time (Seconds)	Off-Time (Seconds)	Pulse Frequency (Hz)	Total Pulses
0.100	0.100	5	10
30.0	—	—	1
0.100	0.100	5	10

Each mission required in excess of 17,000 pulses at an average duty cycle of approximately 30 percent. Nominal steady-state flow rate was 0.23 lbm/sec at 750-psia chamber pressure and 1,000 psia inlet pressure. A total of 9,600 lbm propellant was consumed during the 20-mission demonstration test.

4.2.3 Hot Resta , and Attitude Sensitivity Tests

Upon completion of the pulse-modulation tests, a teardown analysis and inspection of the hardware and catalyst was accomplished. The unit was refurbished with new catalyst and bedplates. The chamber and injector were reused without refurbishment. The only change made in the assembly was to replace the inner bed catalyst with 14- to 18-mesh Shell 405 rather than the 25- to 30-mesh catalyst used in the previous tests.

Prior to delivery of the ga. generator to NASA-JSC, a series of tests was conducted to demonstrate attitude insensitivity and hot restart capability of the reactor under varying inlet pressure and thermal conditions. The test sequence for these tests is presented in Table 4-4. All previous testing of the gas generator was conducted with the reactor centerline horizontal. To demonstrate attitude insensitivity, two separate tests were conducted – one with the reactor rotated 120 degrees about its centerline, and the other with the reactor firing verically downward.

Hot restart capability of the reactor was demonstrated with the reactor in the horizontal attitude for two different feed pressure conditions. The first series of hot restarts was conducted with feed pressure maintained constant at the nominal design value (1,000 psia). The second series of hot

Table 4-4
ATTITUDE SENSITIVITY AND
HOT RESTART TEST SEQUENCE

Test No.	Configuration	Firing Duration
49	Horizontal	ATP
50	Rotated 120°	ATP
51	Vertical (down)	ATP
52	Bootstrap start	30 sec
53	Hot restart 400°F	30 sec
54	Hot restart 600°F	30 sec
55	Hot restart 800°F	30 sec
56	Hot restart 1,000°F	30 sec
57	Hot restart 1,200°F	30 sec
58	Steady-state restart	30 sec
59	Bootstrap start 400°F	10 sec
60	Bootstrap start 600°F	10 sec
61	Bootstrap start 800°F	10 sec
62	Bootstrap start 1,000°F	10 sec
63	Horizontal	ATP

restarts (bootstrap startup) was aimed at simulating the APU pump output pressure transient during startup. It was the goal to increase feed pressure from 200 to 1,000 psia in 4.5 seconds. All hot restart demonstrations were conducted by restarting at the various selected soakback temperatures obtained following a firing.

4.2.4 NASA-JSC Tests

The basic objective of the test program at JSC was to evaluate the life capability of the gas generator using 14- to 18-mesh Shell 405 catalyst in the inner bed and compare the results with previous life tests conducted at RRC using 25- to 30-mesh Shell 405 in the inner bed. The test was conducted at the JSC thermochemical test area during July and August 1974. The normal test conditions were as follows:

a. Ambient environment – sea level
b. Propellant temperature – uncontrolled
c. GG start temperature $\geqslant 200^{\circ}F$
d. Feed pressure – 1,000 to 1,050 psig
e. Propellant saturation – uncontrolled
f. GG orientation – horizontal

The duty cycles included acceptance tests and 20 simulated mission duty cycles identical to those used on previous pulse-modulation life testing at RRC. In addition, special tests were included in the program to investigate the APU 1/2-speed duty cycle and hot restarts at operating pressure (1,000-psig inlet). A Marotta MV100 valve was used for on/off control.

4.3 TEST RESULTS AND DISCUSSION

4.3.1 Pressure Modulation Test Results

Throughout the test program, continuous measurements were made of chamber pressure, flow rate, and gas temperature to monitor performance of the gas generator as a function of operating time. As noted previously, the goal of the test program was to demonstrate 20 simulated missions, following which the reactor was to be disassembled and examined for catalyst loss and nitriding damage. This goal was accomplished with the completion of 21 missions, including the initial pulse-modulated mission. A summary of the accomplishments achieved during the test program is presented in Table 4-5.

Table 4-5
SUMMARY OF PRESSURE MODULATED TEST ACCOMPLISHMENTS

Number of missions	
Pressure modulated	20
Pulse modulated	1
Number of starts	57
Number of pulses	1,196
Total on-time	30 hours
Total propellant consumed	12,500 lbm

Presented in Figure 4-6 is the effect of propellant flow rate on gas temperature for various mission firings. As can be seen, gas temperature increased by approximately 30°F during the 30 hours of testing. Gas temperature was measured with an Inconel-sheathed thermocouple located in the nozzle convergent section.

Characteristic velocity as a function of accumulated life is presented in Figure 4-7 for the

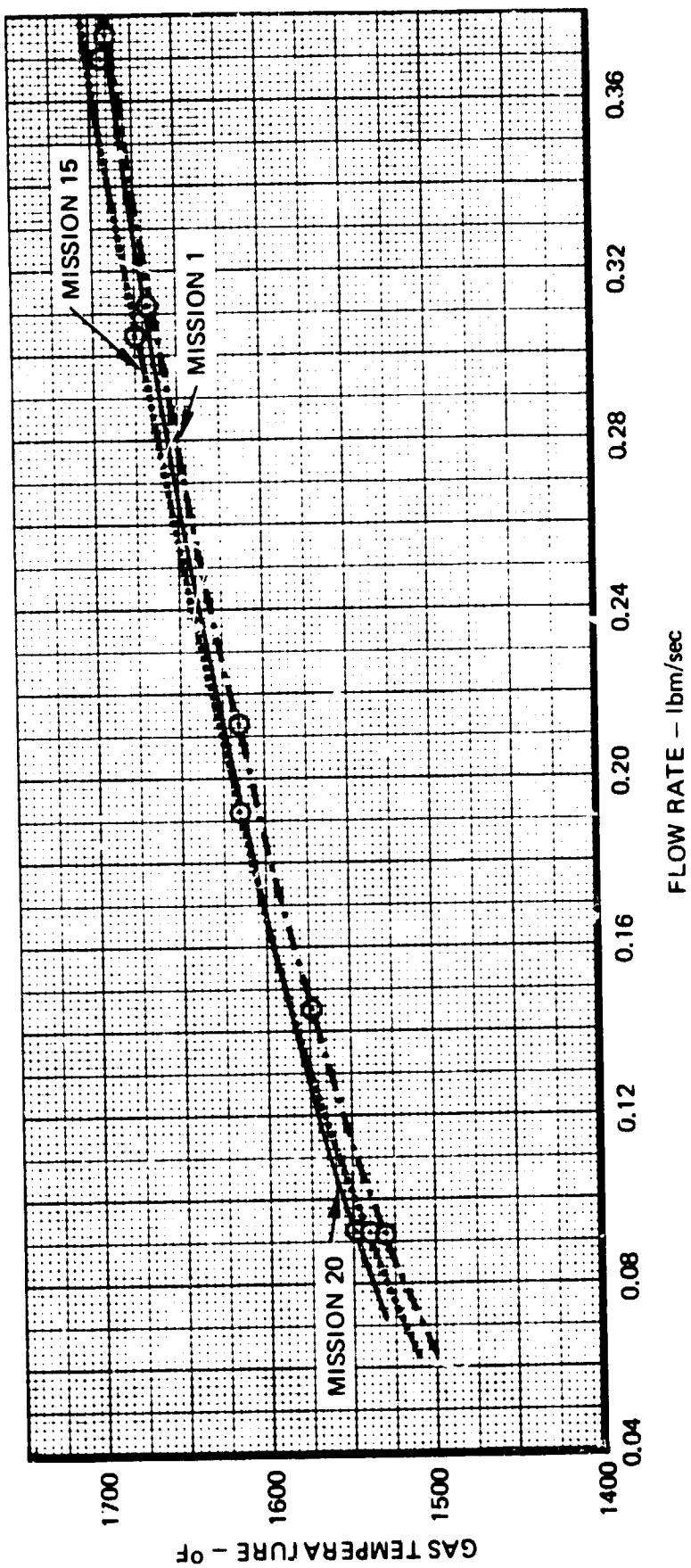
GAS TEMPERATURE VS FLOW RATE
MISSION 15
MISSION 1
MISSION 20
GAS TEMPERATURE – °F
1700
1600
1500
1400
FLOW RATE – lbm/sec
0.04
0.08
0.12
0.16
0.20
0.24
0.28
0.32
0.36

Figure 4-6

CHARACTERISTIC VELOCITY AS A FUNCTION OF RUN TIME

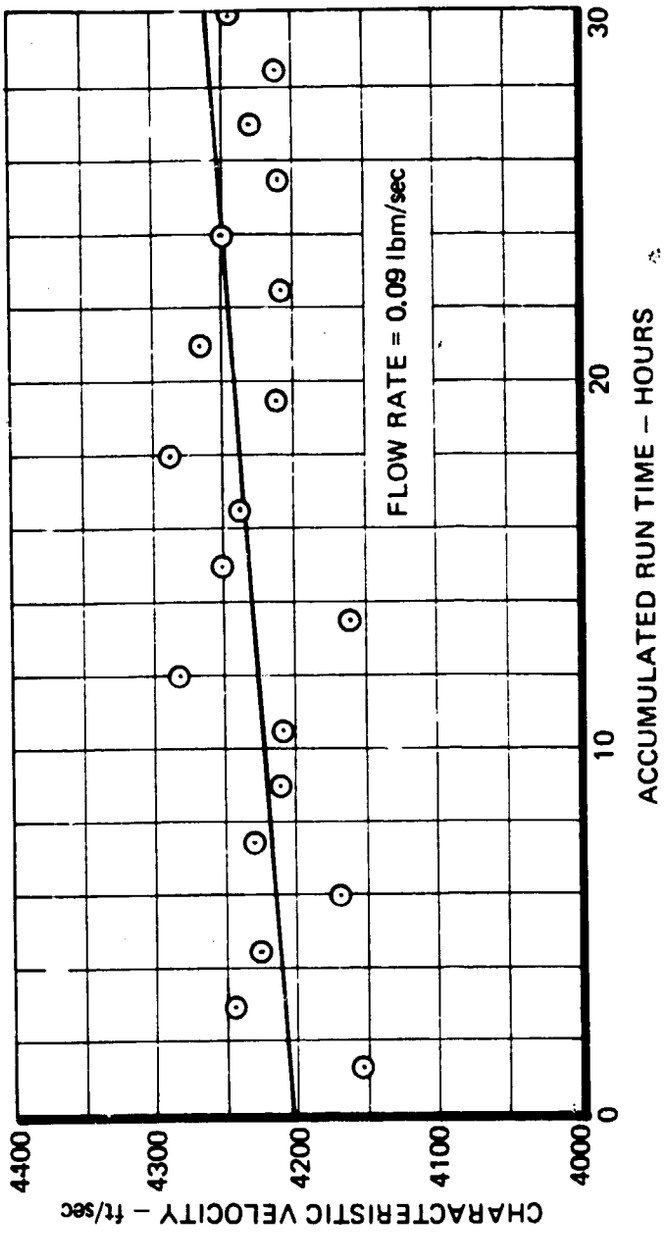

11085-37

Figure 4-7

minimum flow rate. Performance increased by approximately 1.3 percent during the test. Data scatter is approximately ±1.5 percent. Characteristic velocity at the higher flow rates was approximately 40 ft/sec higher than that shown in Figure 4-7 with data scatter less than ±1 percent.

Ignition delay time, defined as time from valve signal to 10 percent steady-state chamber pressure, is presented in Figure 4-8. All starts were conducted with the gas generator initially at 200°F at the minimum flow rate power level. It should be noted that the ignition delay is relatively large, which was due to the large chamber void volume and low flow rate.

Figure 4-9 shows the effect of accumulated life on reactor tailoff time, defined as the time interval between valve closure and when chamber pressure decays to 10 percent of the steady-state value. All shutdowns occurred during the minimum flow rate power level. The results show a marked increase in tailoff during the first 12 hours of operation but remained relatively constant throughout the remainder of the test. An increase in tailoff time is generally related to either catalyst void or a decrease in catalyst activity.

Nominal chamber pressure roughness (roughness values within one standard deviation of the mean) is shown in Figure 4-10 as a function of life for the maximum and minimum flow rate conditions. Maximum roughness (3 sigma value) was ±3-1/2 and ±21% at the maximum and minimum flow rates, respectively. It is noted that two chamber pressure values are identified at maximum flow rate, which was the result of the modified valve system providing lower maximum flow rate than that obtained during the initial mission firings. At the conclusion of 20 pressure-modulated missions, a 500-second steady-state firing was conducted at the initial maximum flow rate (0.36 lbm/sec). Reactor roughness during high flow rate operation remained consistently smooth. Although the relative roughness was much greater at lower flow rates, it is noted that the absolute pressure variations were approximately the same as those at the higher flow rate. A significant decrease in roughness is seen to occur as a result of removing the reactor from the test stand after 6 hours of operation. It is generally believed that roughness occurs as a result of small voids growing in the immediate vicinity about the injection elements. Redistribution of the catalyst during removal and handling of the reactor is postulated to have reduced these voids with resultant smoother operation. As life was accumulated, the voids again occurred due to propellant injection momentum forcing particles away from the injector, resulting in less stable operation. Oscillograph records of chamber pressure for various missions (at maximum flow) are presented in Appendix 6.1.

Following completion of the 30-hour test, a diagnostic teardown of the reactor was initiated. The reactor was removed from the test stand and the chamber examined in detail; no deformations or anomalies were noted (Figure 4-11). A photo of the catalyst bed assembly is shown in Figure 4-12. The threaded end-closure provided very easy access to the catalyst bed. Inspection of the reactor revealed no failure or cracking of any component; however, some distortion of the bedplates was detected (Figure 4-13). The injector was in excellent shape with no degradation of the individual injector elements (Figure 4-14). Water flow calibration of the injector for propellant mass flow distribution gave nearly identical results to those obtained prior to the demonstration test.

The catalyst bed was in excellent condition with only a small void observed in the inner bed (Figure 4-15). The foam metal, however, showed signs of degradation (Figure 4-16, see Volume III for additional photos). A summary of the catalyst weight data is presented in Table 4-6. Loss of

IGNITION DELAY TIME* VS ACCUMULATED BURN TIME

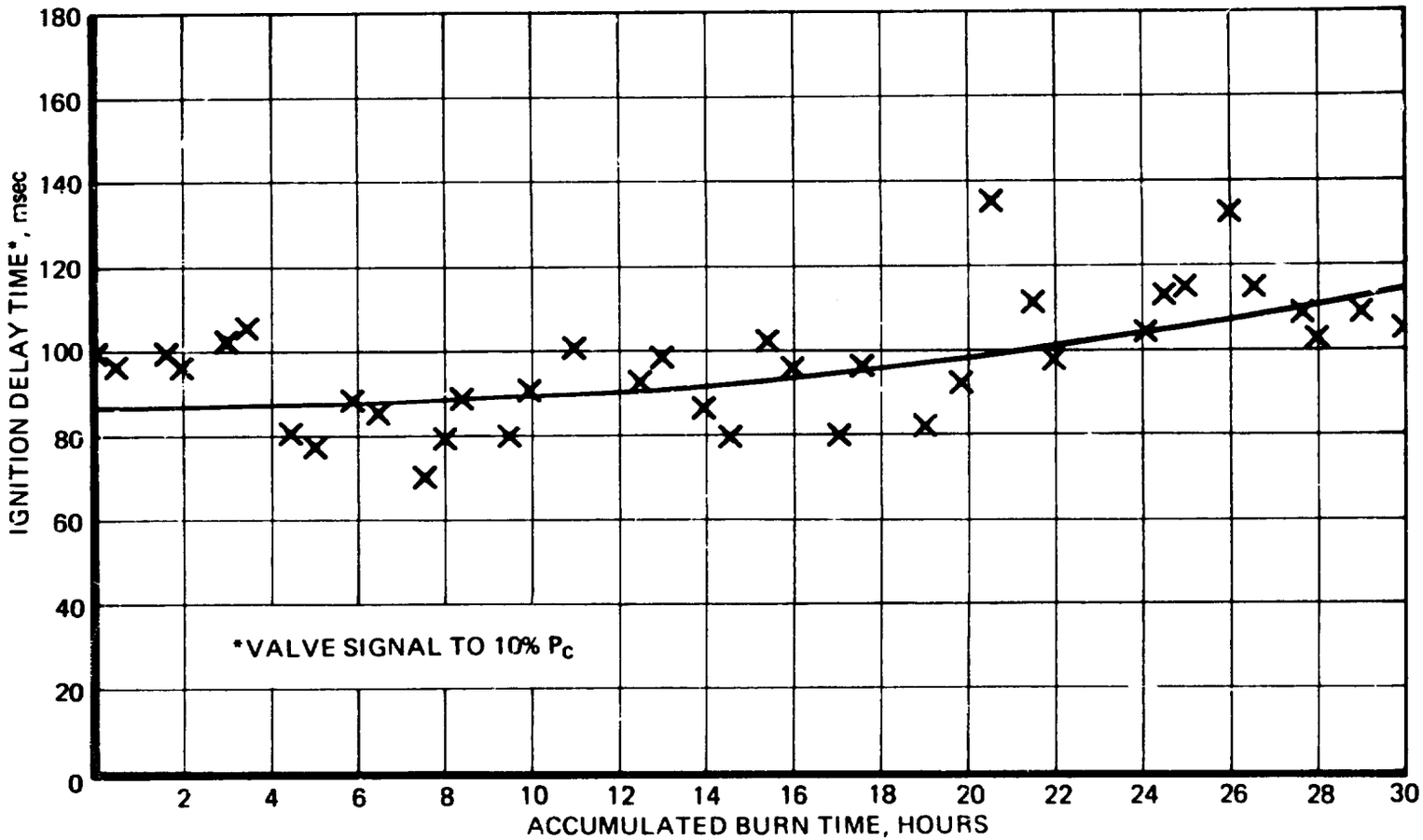

Figure 4-8

24001-63A

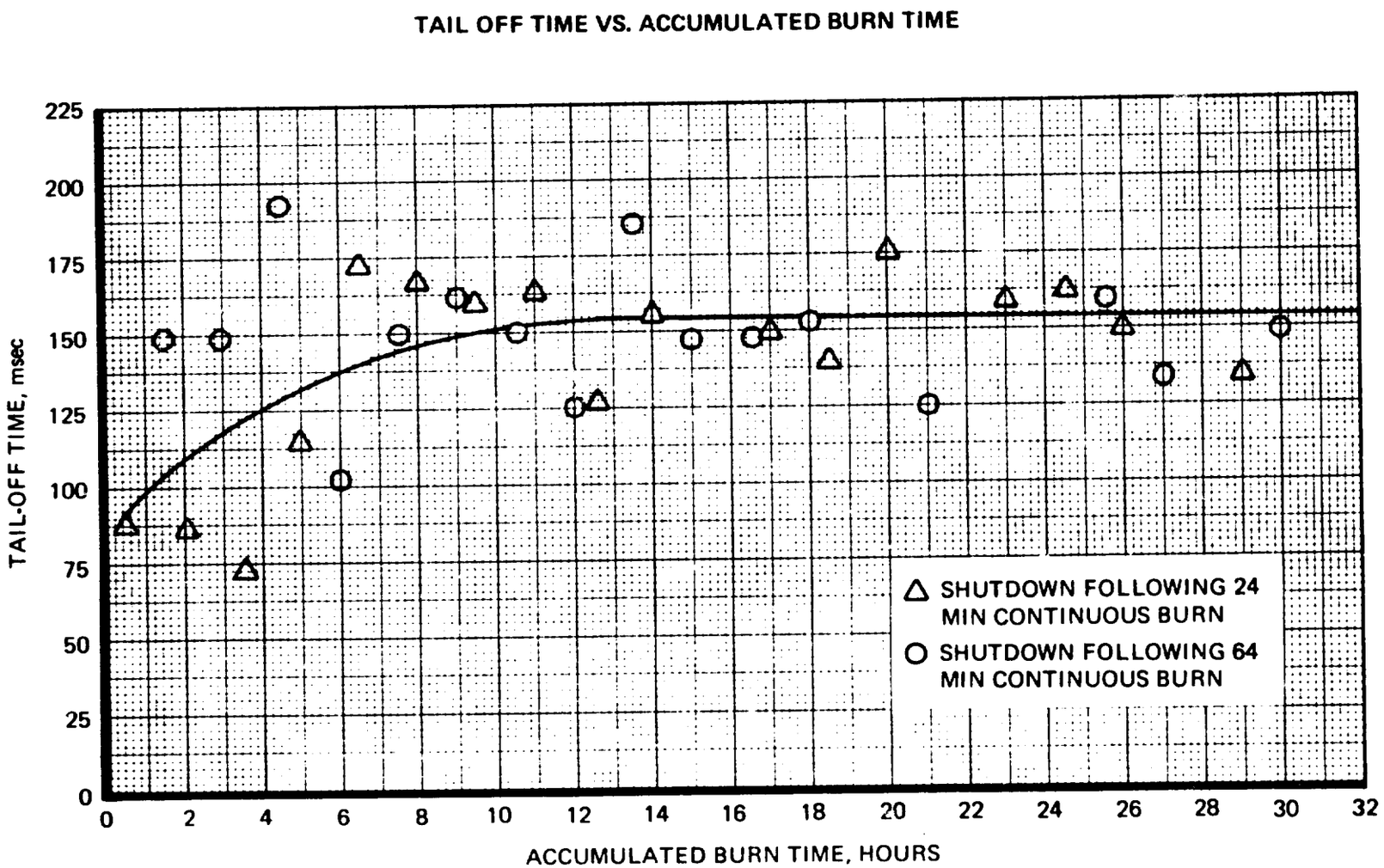
TAIL OFF TIME VS. ACCUMULATED BURN TIME
TAIL-OFF TIME, msec
225
200
175
150
125
100
75
50
25
0
0
2
4
6
8
10
12
14
16
18
20
22
24
26
28
30
32
ACCUMULATED BURN TIME, HOURS
SHUTDOWN FOLLOWING 24 MIN CONTINUOUS BURN
SHUTDOWN FOLLOWING 64 MIN CONTINUOUS BURN

Figure 4-9

NOMINAL ROUGHNESS VS LIFE

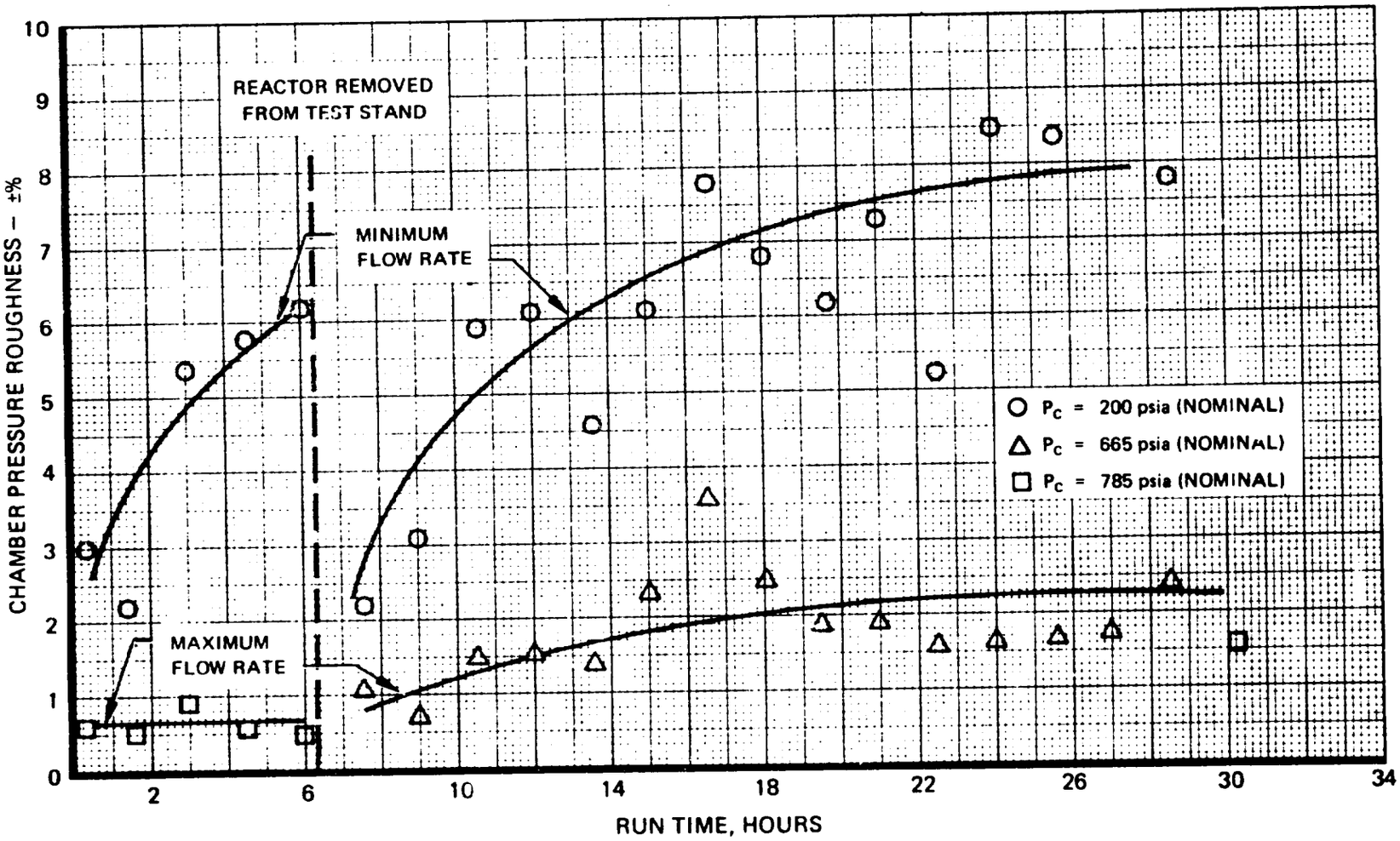

Figure 4-10

APU GAS GENERATOR CHAMBER

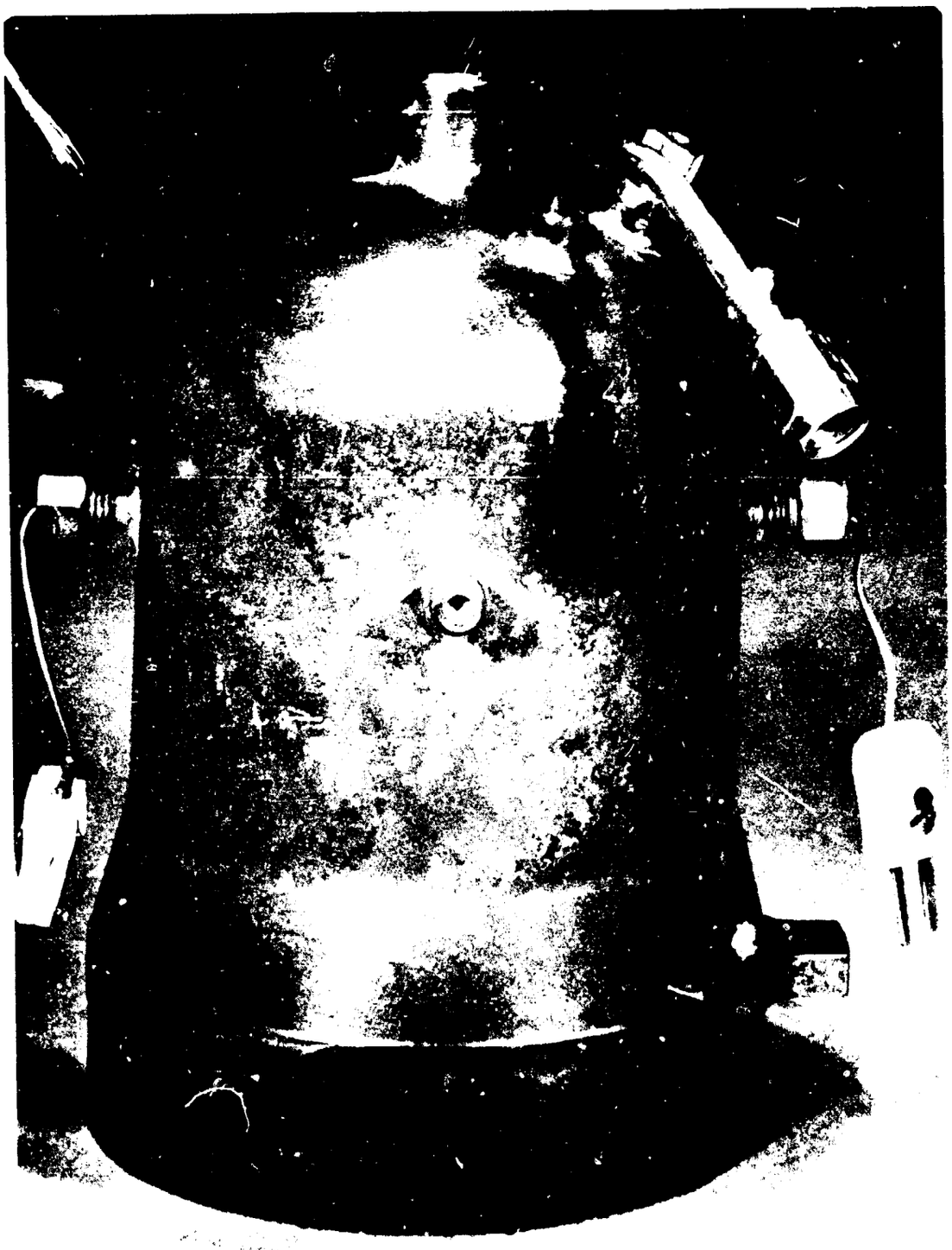

Figure 4-11

APU GAS GENERATOR MODULE

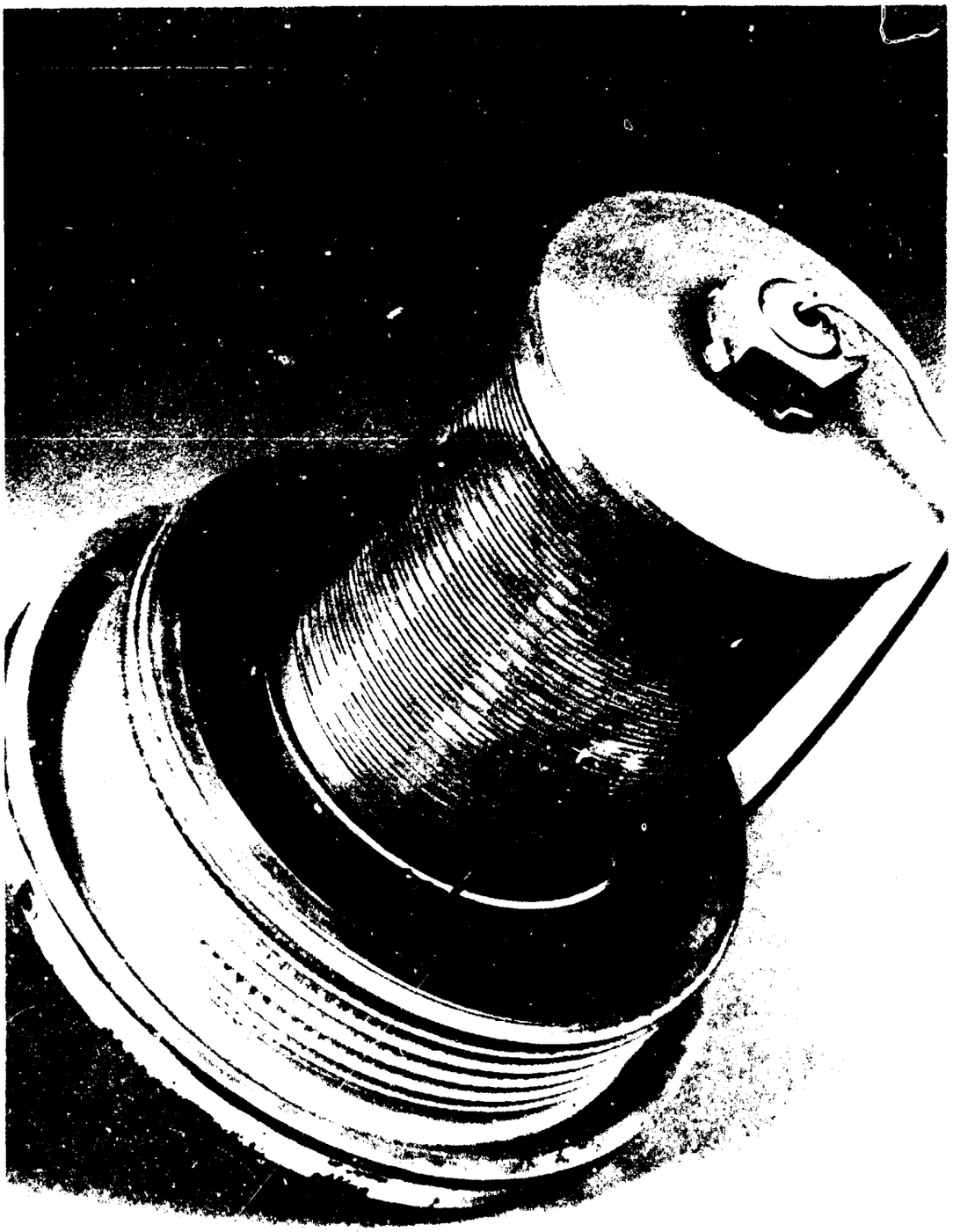

24001-30 1523-8

Figure 4-12

SPACE SHUTTLE APU GAS GENERATOR INNER BEDPLATE

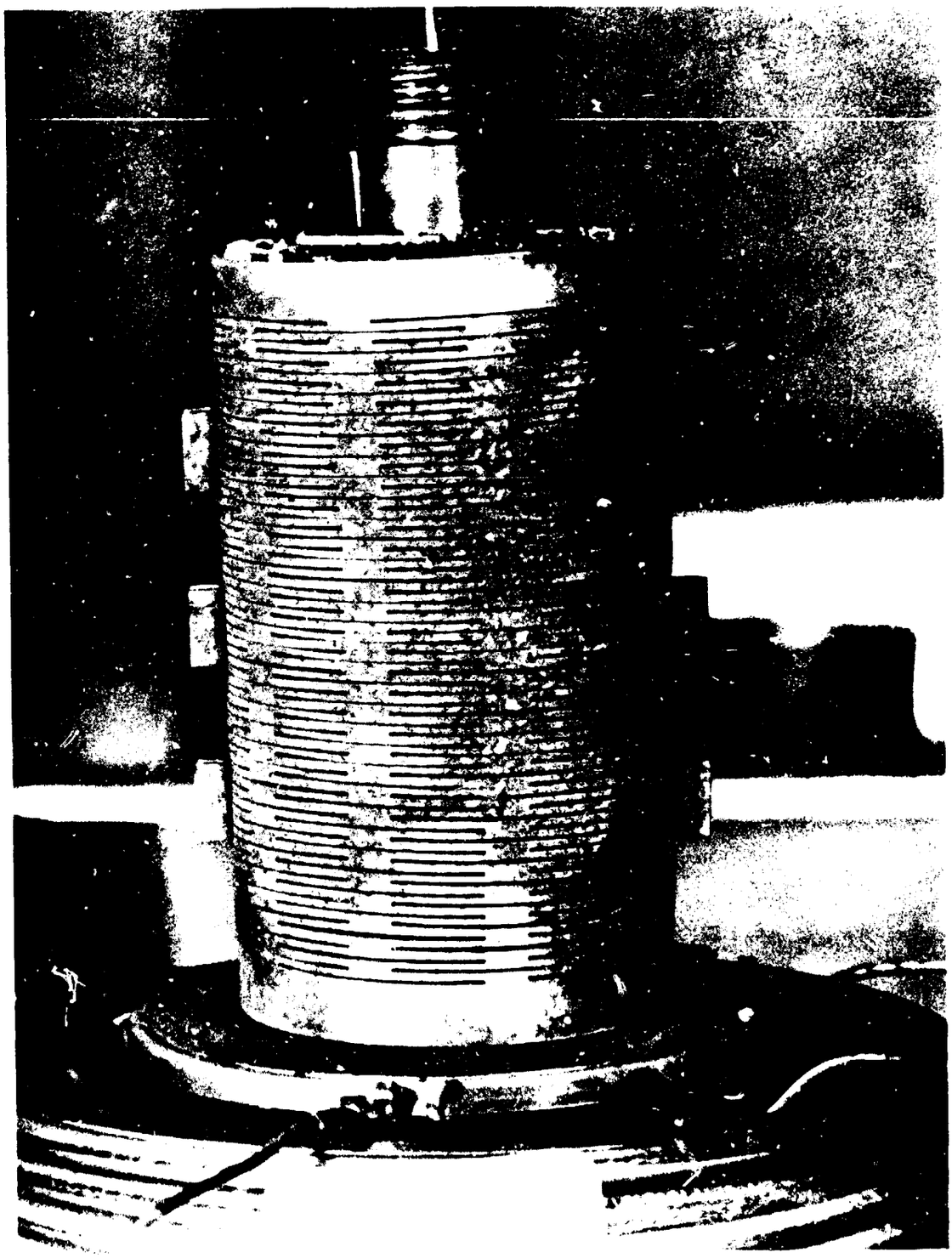

24001-45 1523-14

Figure 4-13

SPACE SHUTTLE APU GAS GENERATOR INJECTOR BODY

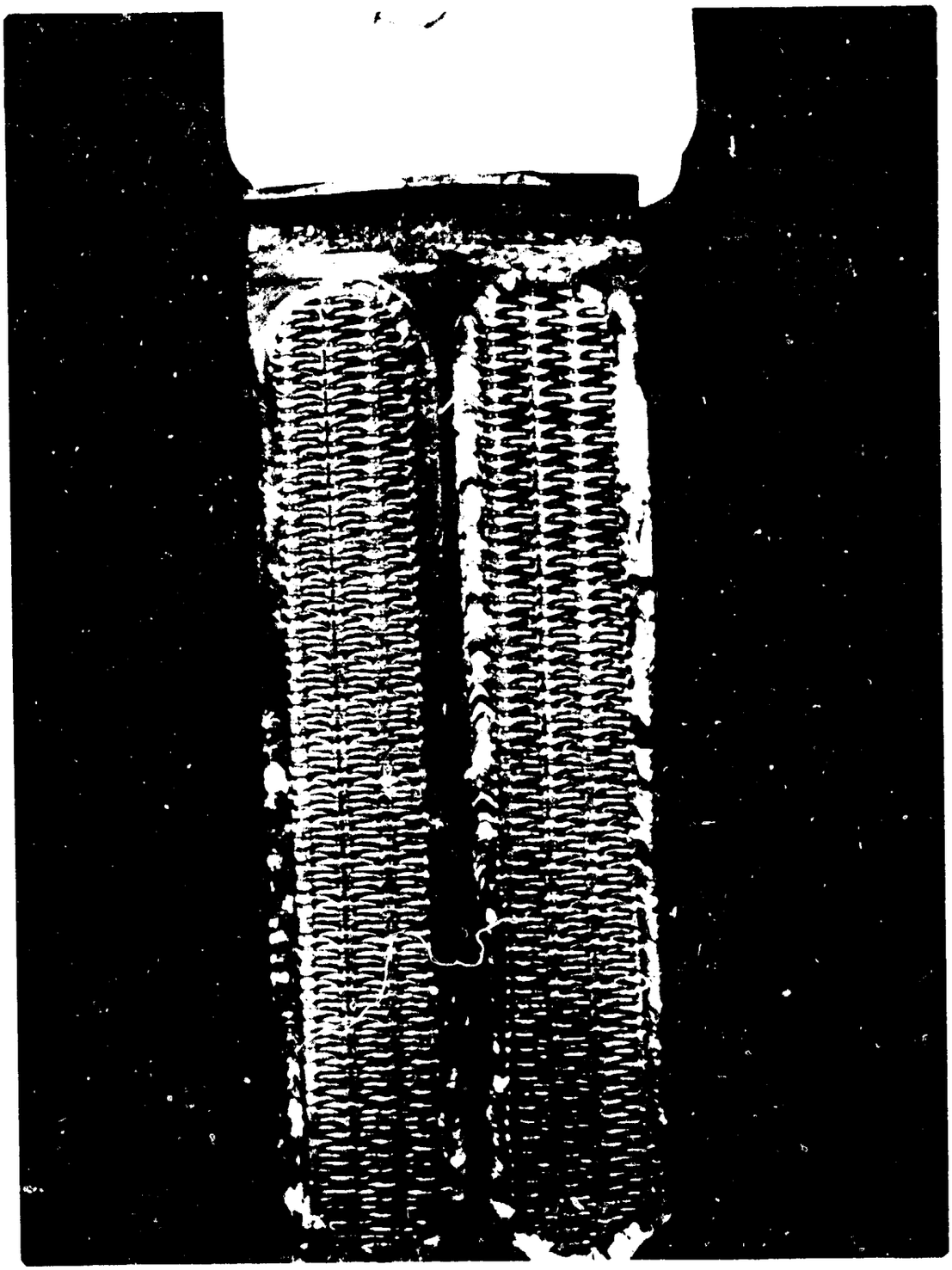

24001 47 1523-18

Figure 4-14

APU GAS GENERATOR CATALYST BED

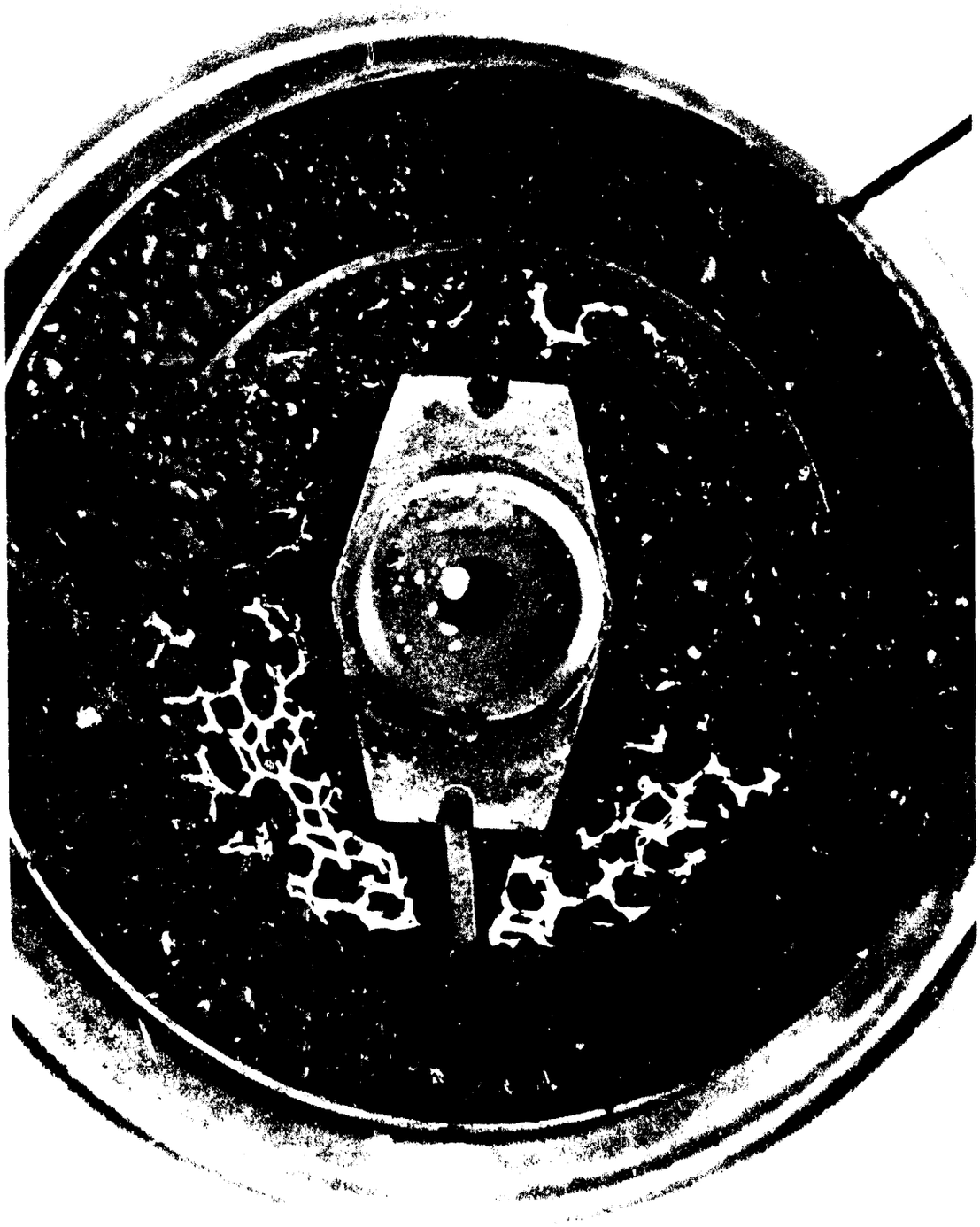

24001 33 1523 4

Figure 4 15

APU GAS GENERATOR FOAM STRUCTURE

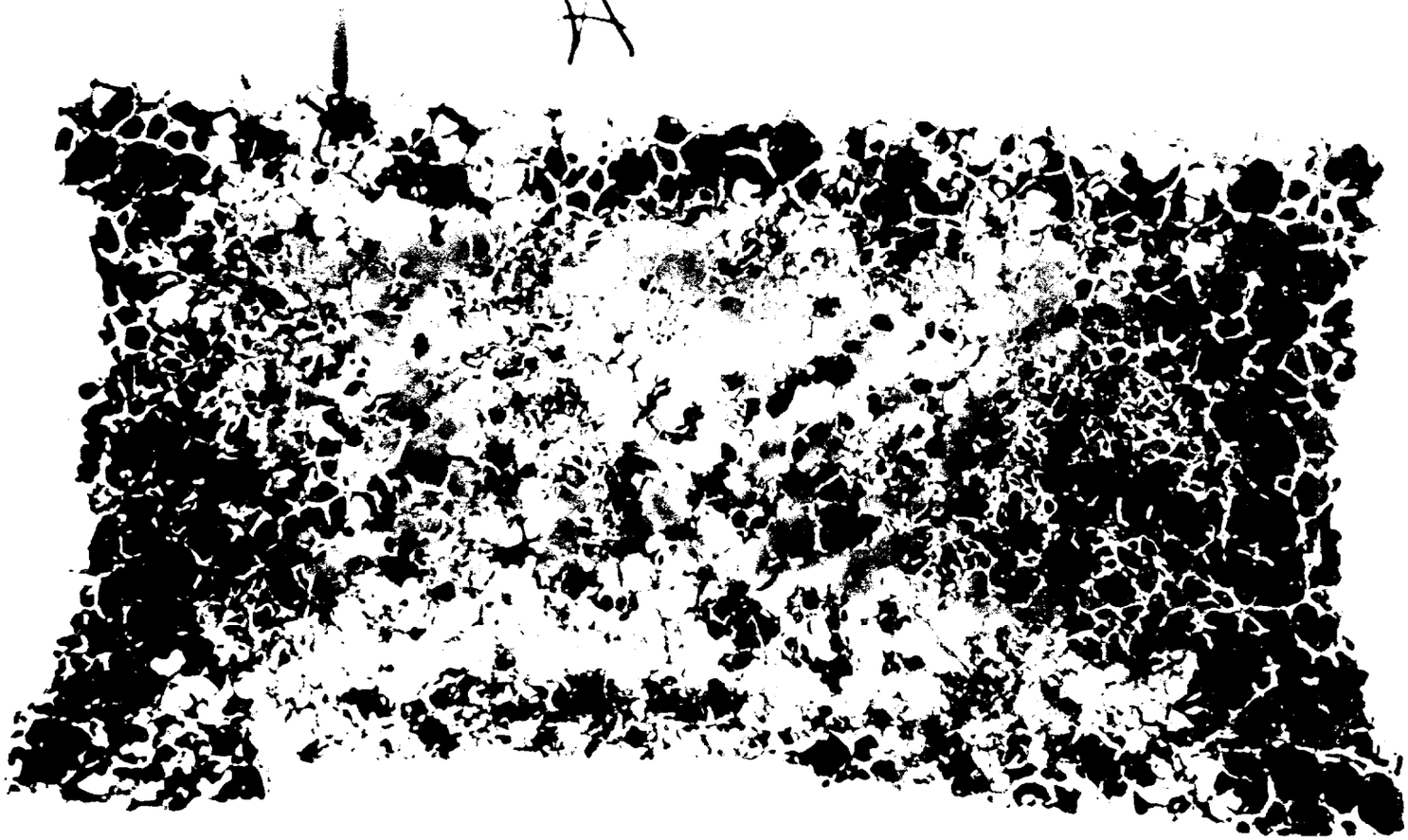

24001.35 1523-2

Figure 4-16

catalyst from the inner bed was only 2.25 percent. On a total weight basis, no catalyst was lost during the 30-hour test.

Table 4-6
CATALYST WEIGHT DATA FROM 30-HOUR TEST

Inner Bed, Shell 405 Catalyst, 25–30 mesh		
	Assembly	**Teardown**
Total weight	58.60	57.28
25–30 mesh, gm	58.60	49.64
30–35 mesh, gm		3.62
>35 mesh, gm		4.02
Loss, gm		1.32
Percent loss		2.25
Outer Bed, Shell 405, 14–18 mesh		
	Assembly	**Teardown**
Total weight, gm	90.31	92.02
14–18 mesh, gm	90.31	84.75
>18 mesh, gm		7.27
Loss (gain), gm		(1.71)

Hydrogen chemisorption measurement of the active metal surface area of the inner bed catalyst showed very little degradation – a value of 120 μ moles/g was measured for the post-test catalyst compared to 152 μ moles/g for unfired catalyst. Hydrogen chemisorption values for the outer bed catalyst, however, indicated a significant decrease in active metal surface area – a value of approximately 70 μ moles/g was measured. Atomic absorption analysis and an electron microprobe study of the catalyst failed to reveal the cause of the low hydrogen chemisorption values for the outer bed catalyst. Results of a trace metal analysis are presented in Table 4-7.

Based on the results of the teardown analysis, it was concluded that the life capability of the gas generator was substantially more than the demonstrated 30 hours. It was postulated that most of the inner bed catalyst loss occurred within the initial 12 hours of operation as evidenced by the tailoff time and chamber pressure roughness characteristics.

In order to eliminate bed cylinder distortion, it was recommended that the end-closure design be modified and that the bed spacers be removed as part of the gas generator refurbishment.

4.3.2 Pulse-Modulation Test Results

The objective of the pulse-modulated tests was to conduct 20 mission firings and to compare the results with those obtained from the corresponding pressure-modulated tests. Of primary interest was the effect on catalyst life of pulse-mode versus steady-state operation. A summary of the accomplishments achieved during the pulse-modulated mission firings is presented in Table 4-8.

Table 4-7

TRACE METAL ANALYSIS OF APU CATALYST – 30-HOUR TEST

Samples	ppm										
	Si	An	Ca	Fe	Mn	Ni	Cu	Cr	Co	Mg	Na
Catalyst from center part of foam; inner bed	320	269	ND	832	6.4	2,242	ND	44.8	ND	16	–
Catalyst from end part of foam; inner bed	147.8	51	ND	372	2.9	717	ND	14.3	7.2	4.3	192
25–30 mesh inner bed	100	25	ND	625	12.5	1,256	37.5	20	18	6.3	143
25–30 mesh inner bed	117.5	15	ND	487	ND	1,050	25	17.5	18	5	125
14–18 mesh extremity of outer bed	75	10	ND	57.7	ND	50	7.5	ND	ND	2.5	125
14–18 mesh outer bed	62.5	5	ND	150	ND	300	ND	ND	ND	2.5	150
14–18 mesh extremity of outer bed	62.5	5	ND	81.5	ND	137.5	ND	ND	ND	2.5	75
14–18 mesh outer bed	87.5	2.5	ND	137.5	ND	225	ND	ND	ND	3.75	17.5
New (14–18) catalyst	87.5	6.3	ND	62.5	ND	ND	ND	ND	ND	5	175
RA-1 carrier	112.5	5	ND	75	ND	ND	ND	ND	ND	5	175

V01760

Table 4-8
SUMMARY OF PULSE-MODULATED TEST ACCOMPLISHMENTS

Number of missions	20
Number of starts	48
Number of pulses	342,500
Total on time	9.3 hours
Total propellant consumed	9,600 lbm

As noted previously, steady-state reference firings were conducted at the conclusion of every five missions to monitor performance of the gas generator throughout the 20 missions. Presented in Figures 4-17 through 4-21 are the results for the steady-state reference firings. Comparison of these results with those of the pressure-modulated tests shows very similar trends. Gas temperature increased 30°F and characteristic velocity increased 40 ft/sec, which is nearly identical to the corresponding values for the pressure-modulated tests. Tailoff time and chamber pressure roughness increased markedly during the first five missions – a trend also observed during the previous mission firings. It is interesting to note that at the conclusion of 20 missions including 342,500 pulses, chamber pressure roughness was only slightly higher than that measured at the end of the steady-state mission firings.

A plot of gas temperature versus duty cycle is presented in Figure 4-22. It is noted that the recorded gas temperatures probably are not representative of the actual gas temperatures during pulse-mode operation, especially at the lower duty cycle. Pulse width at the low duty cycle was 90 milliseconds compared to 250 milliseconds at the higher duty cycle. Although the response characteristics of the sheathed thermocouples preclude accurate instantaneous measurement, the measurements are sufficiently accurate to monitor changes as a function of accumulated life.

Oscillograph traces of pulse shapes for the 50 percent power level are shown in Figure 4-23 for the first and last mission firings, respectively. Although there is a change in the pulse shape, the peak chamber pressure remained nearly constant. Integration of the pressure traces showed less than a 9 percent increase in the pressure-time integral during the 20 missions. Additional oscillograph traces are presented in Appendix 6.2.

Following completion of the 20 mission firings, a complete post-test teardown analysis of the gas generator was conducted. The catalyst in the outer bed was in excellent condition. A small void was observed in the inner bed. The bedplates and injector were also in excellent condition, with only minor deformation of the bedplates. Photomicrographs of the inner bedplate revealed it to have more nitriding damage than that from previous tests. The material was found to be brittle and failed at a bend angle of less than 5 degrees. Photographs of the gas generator during disassembly are presented in Figures 4-24 through 4-27. Degradation of the foam metal is evident in Figure 4-28.

Results of the post-test catalyst weight analysis are presented in Table 4-9. Catalyst loss from the inner bed was 3.3 percent. Outer bed weight measurements indicated a slight weight gain (<0.3 gm) during the test, which could be attributed to catalyst migration from the inner bed. Data for breakup of the catalyst in the inner bed revealed that approximately 87 percent of the catalyst was within the original 25- to 30-mesh size. Hydrogen chemisorption values of the inner and outer beds were 116 and 134 μ moles/g, respectively.

SPACE SHUTTLE APU GAS GENERATOR
STEADY-STATE GAS TEMPERATURE VS LIFE

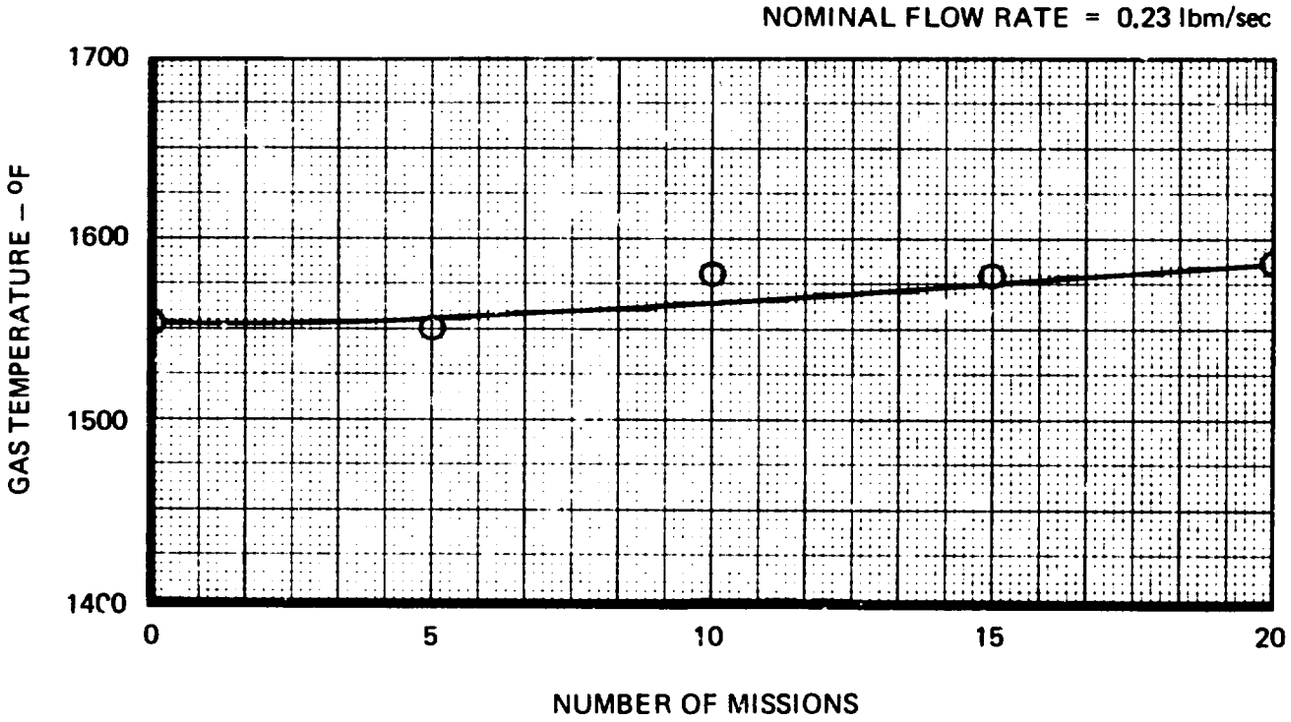

Figure 4-17

SPACE SHUTTLE APU GAS GENERATOR
CHARACTERISTIC VELOCITY VS LIFE

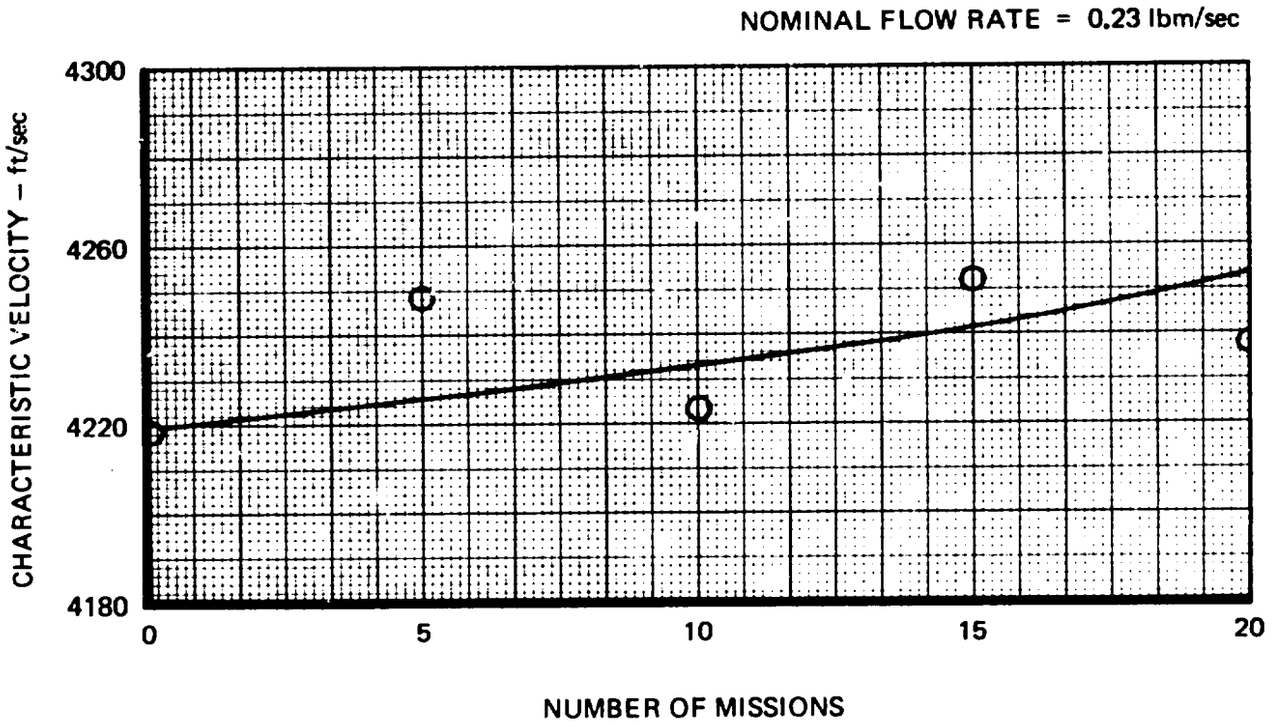

Figure 4-18

11079-67

SPACE SHUTTLE APU GAS GENERATOR
IGNITION DELAY VS LIFE

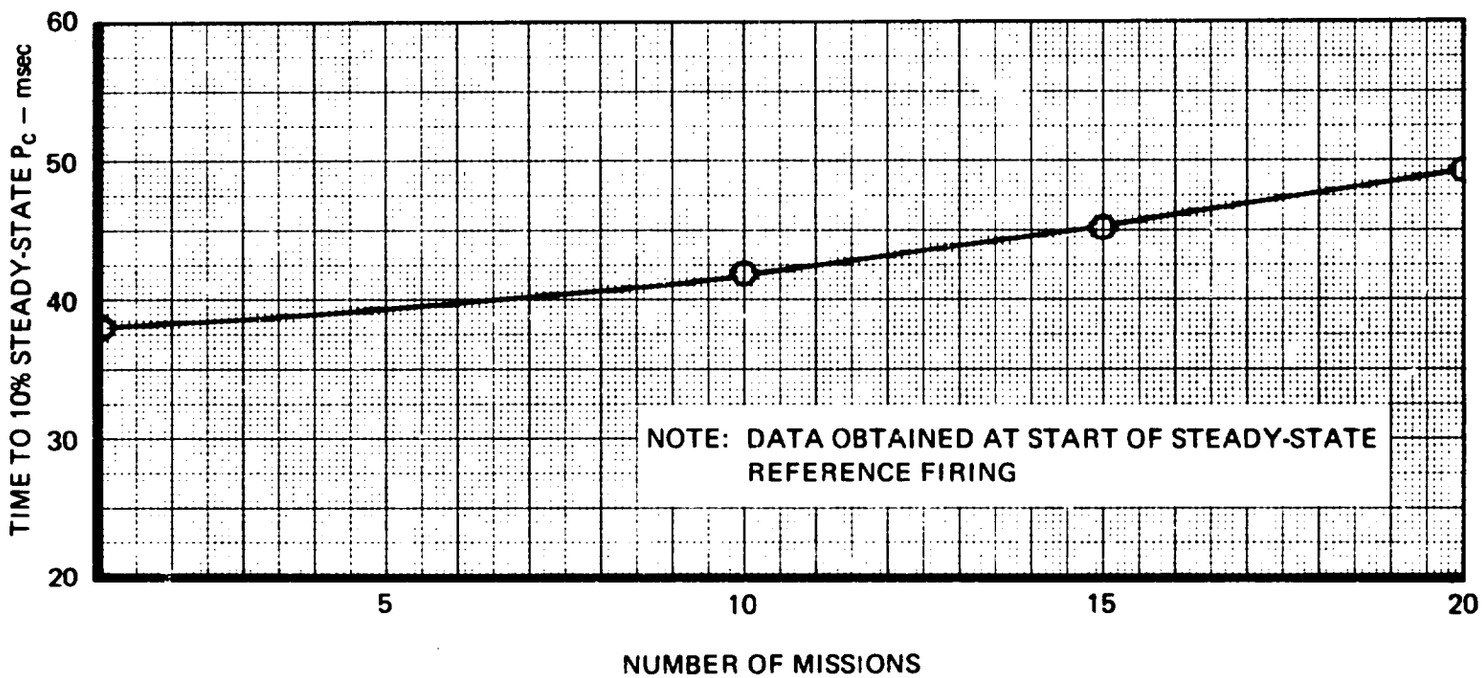

Figure 4-19

SPACE SHUTTLE
APU GAS GENERATOR
TAIL-OFF TIME VS LIFE

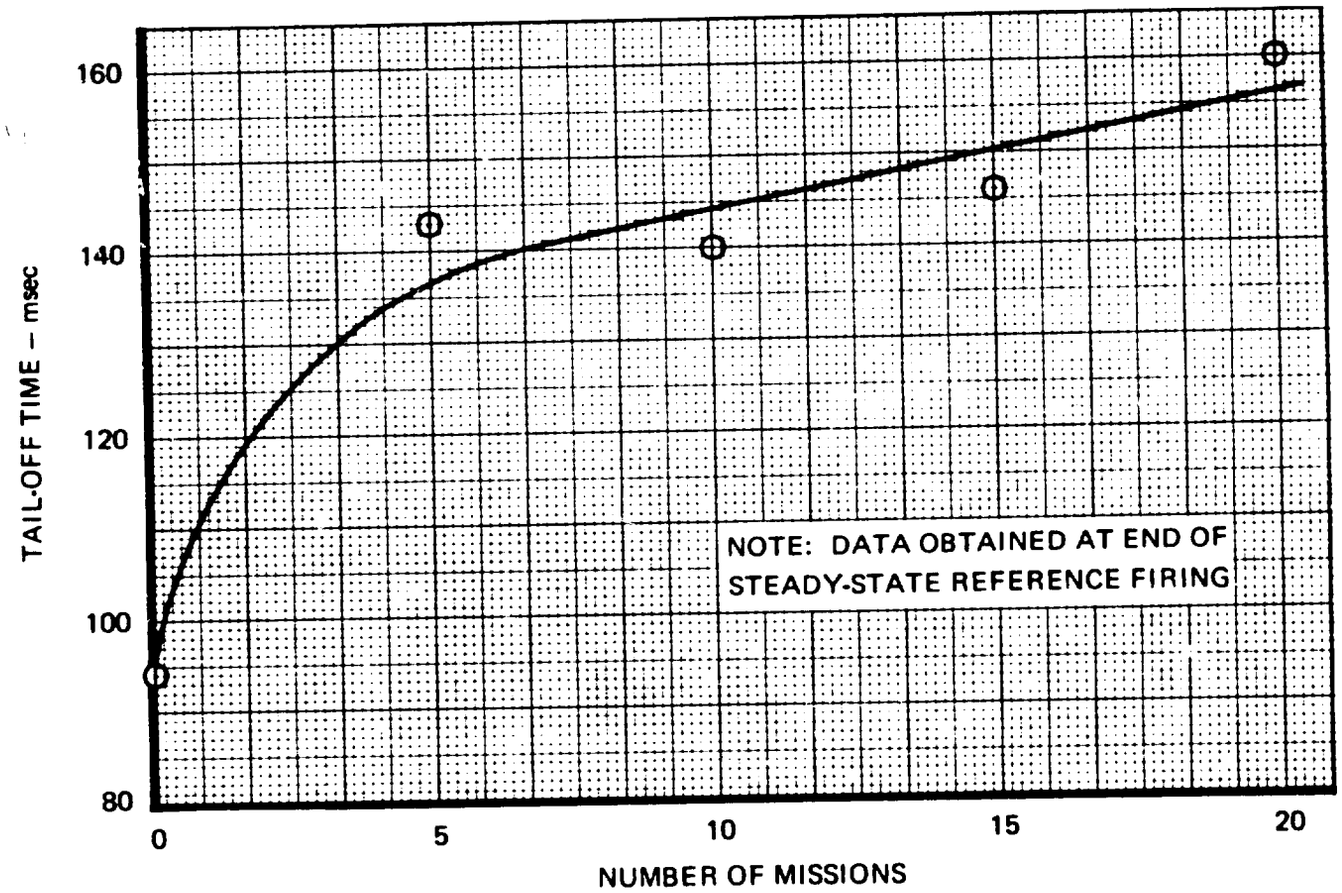

11079-61

Figure 4-20

SPACE SHUTTLE APU GAS GENERATOR
CHAMBER PRESSURE ROUGHNESS VS LIFE

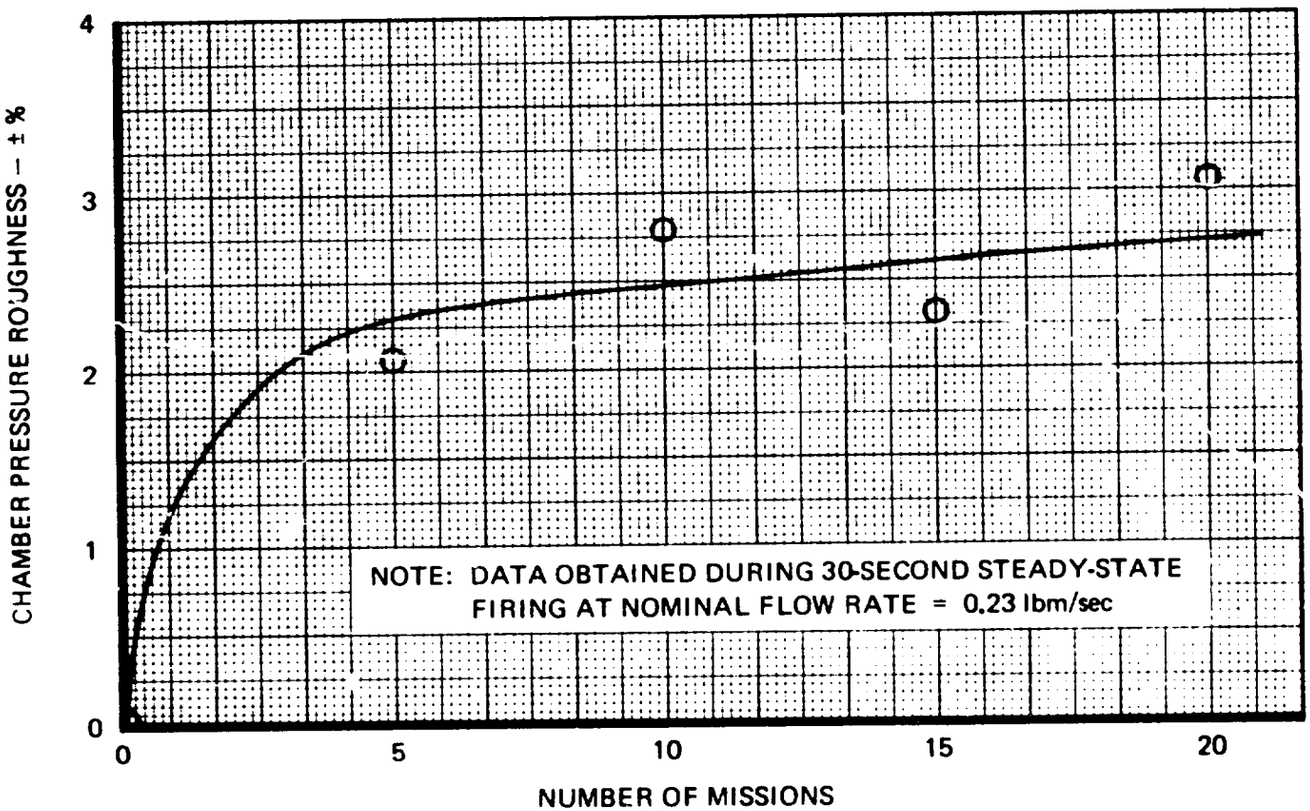

Figure 4-21

SPACE SHUTTLE
APU GAS GENERATOR
GAS TEMPERATURE VS DUTY CYCLE

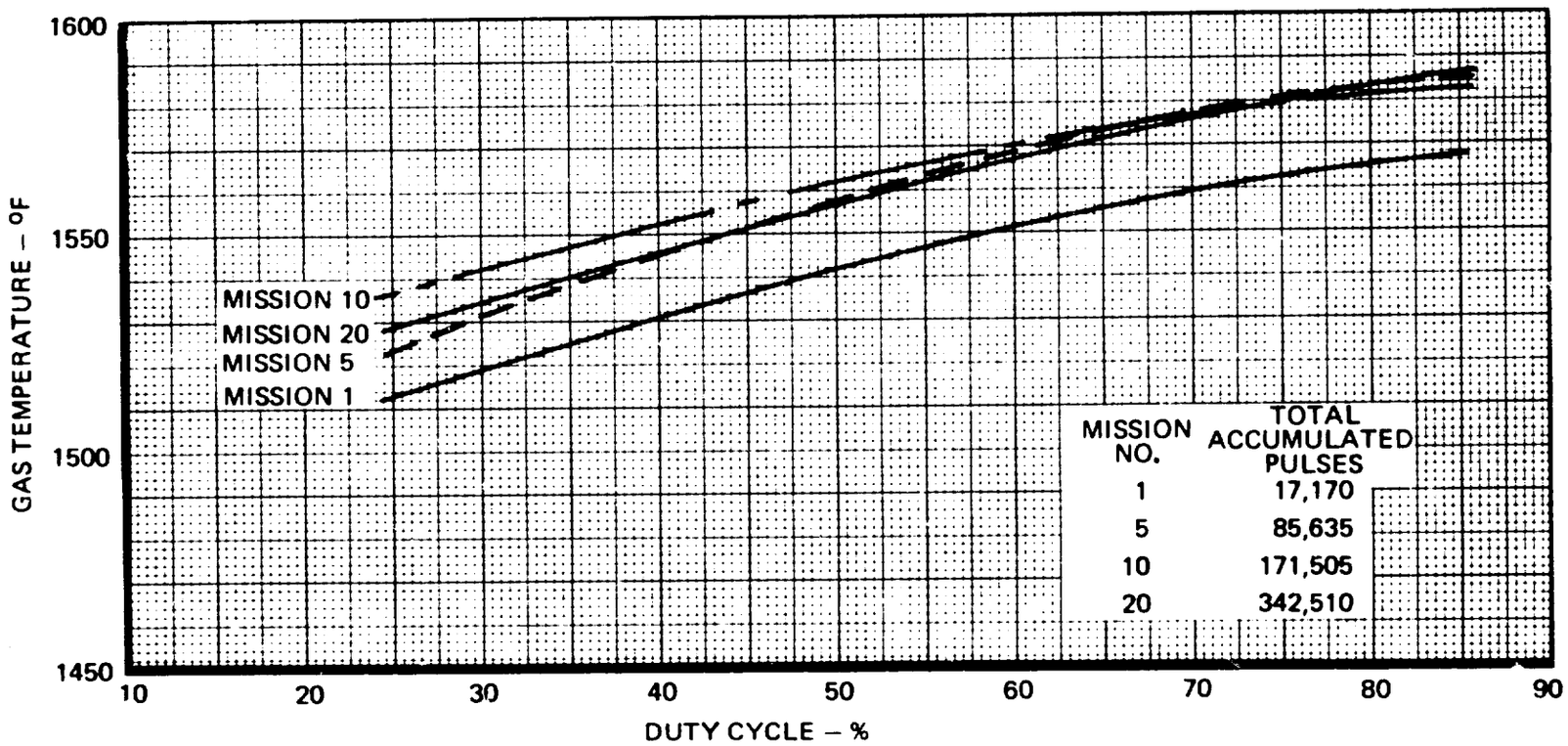

Figure 4-22

PULSE SHAPE VERSUS LIFE

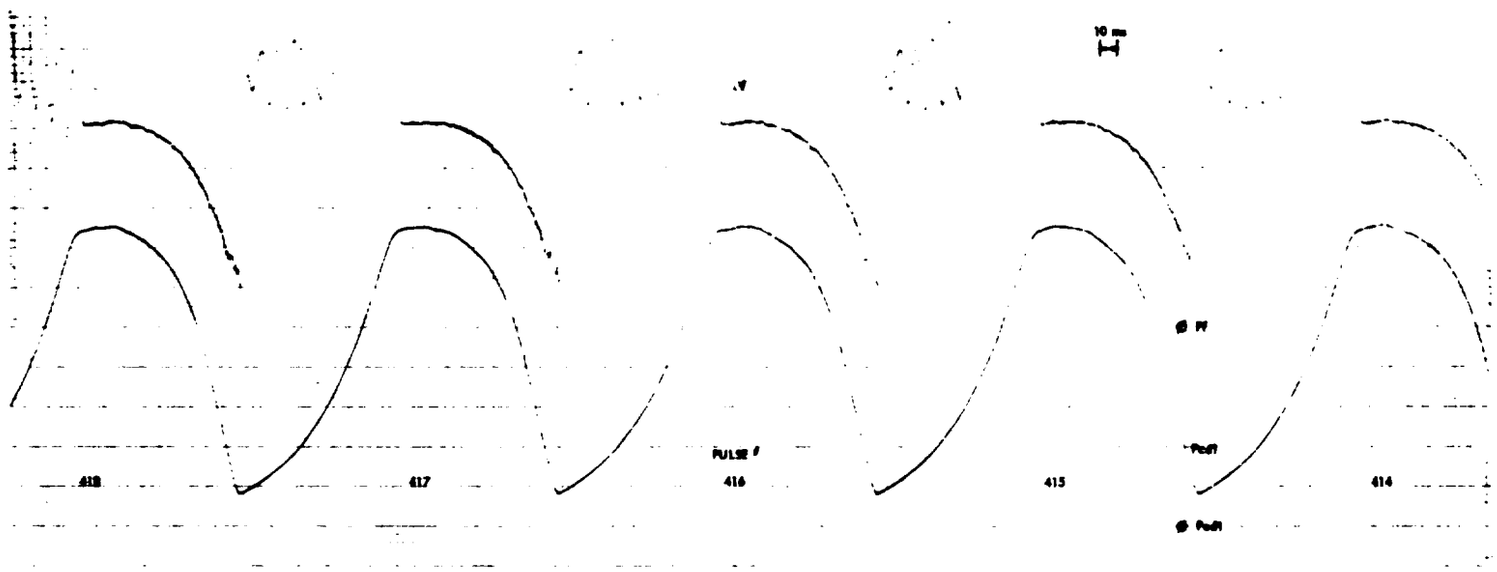

Mission 1 – 50 Percent Power Level

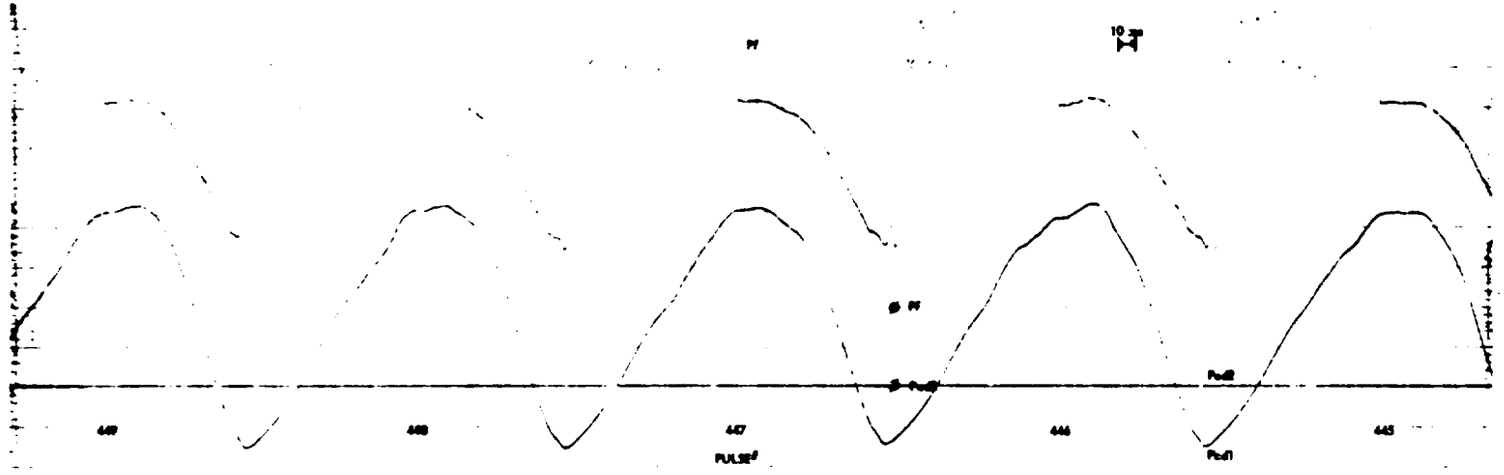

Mission 20 – 50 Percent Power Level

Figure 4-23

GAS GENERATOR MODULE AFTER 20 MISSION PULSE MODE TEST

GAS GENERATOR INNER BEDPLATE

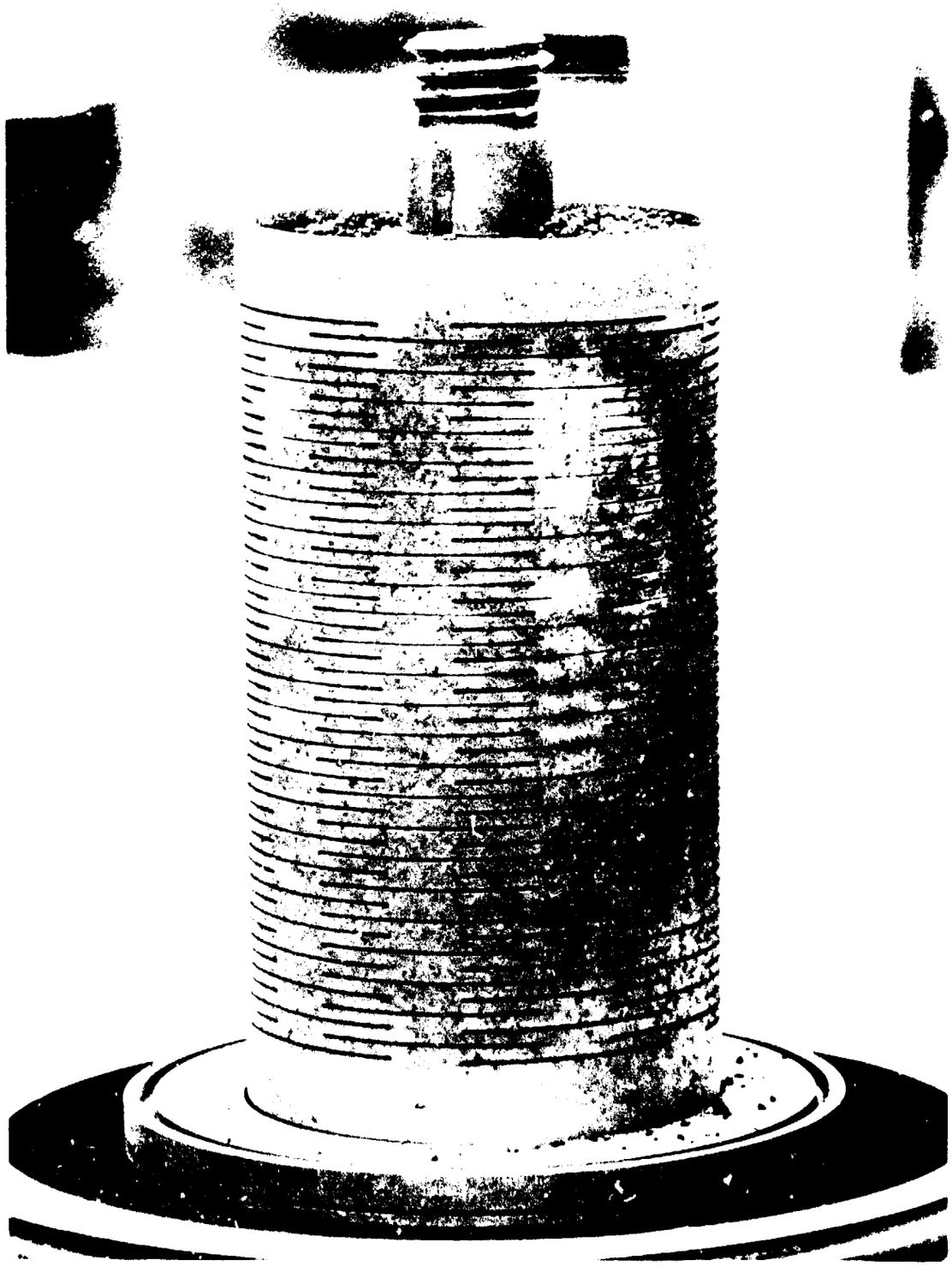

11079-91 1591-2

Figure 4-25

GAS GENERATOR CATALYST BED

GAS GENERATOR INJECTOR

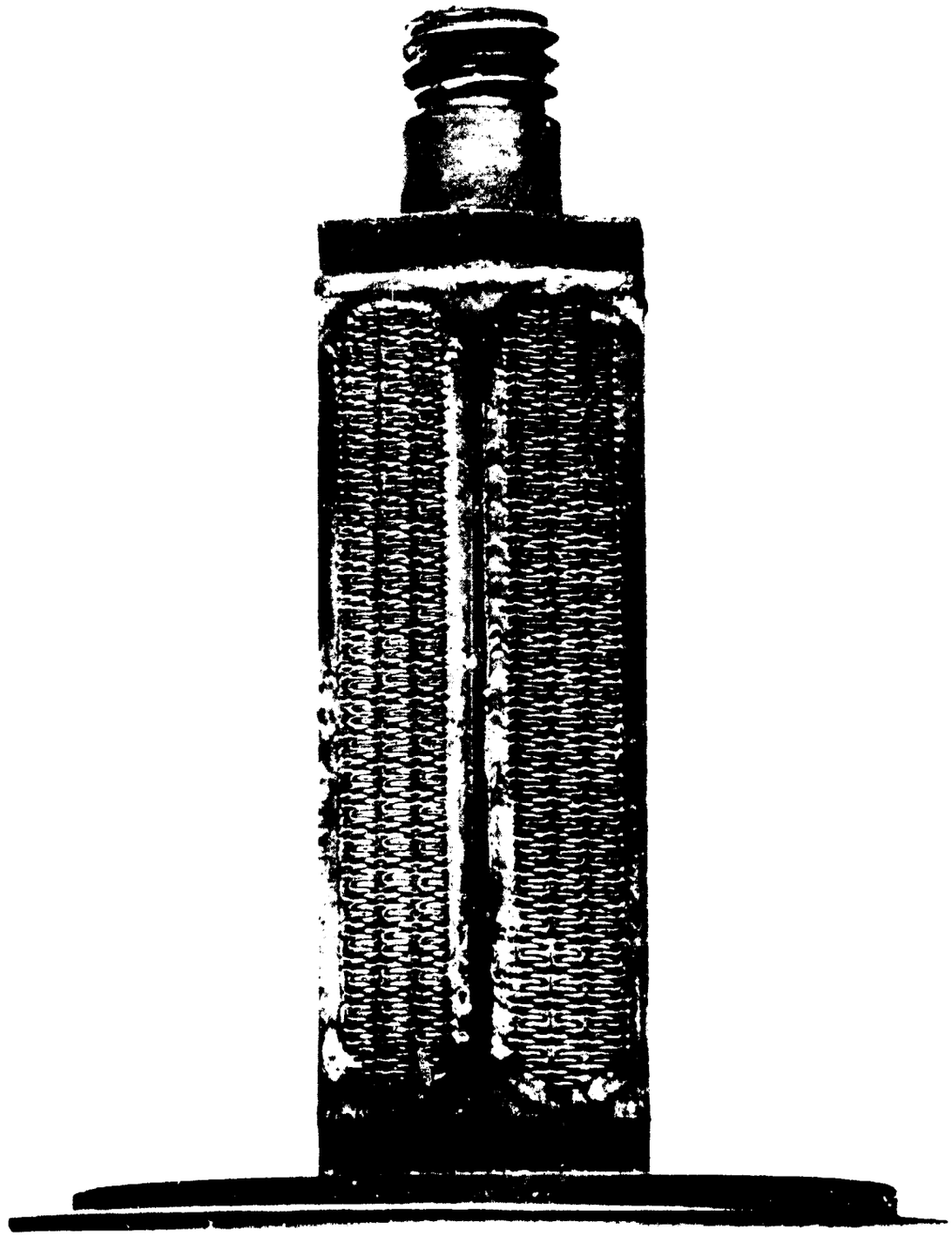

11079-88 1591-7

Figure 4-27

GAS GENERATOR FOAM STRUCTURE, VIEW FROM DOWNSTREAM SIDE

11079-87 1591-4

Figure 4-28

Table 4-9
CATALYST WEIGHT DATA FROM
PULSE-MODULATED LIFE TEST

Inner Bed, Shell 405, 25–30 mesh:

	Assembly	Teardown
Total weight	58.37	56.43
25–30 mesh (gm)	58.37	49.15
>30 mesh (gm)		7.28
Loss (gm)		1.94
% loss		3.3%

Outer Bed, Shell 405, 14–18 mesh:

	Assembly	Teardown
Total weight	91.35	91.58
14–18 mesh (gm)	91.35	86.67
>18 mesh (gm)		4.91
Gain (gm)		0.23

4.3.3 Attitude Sensitivity and Hot Restart Tests

The first test in this series (Table 4-4) was conducted to serve as a baseline for comparison of data for subsequent tests. The results of that test are presented in Table 4-10 showing a comparison with results obtained with 25- to 30-mesh catalyst in the inner bed. The desired goal of increasing gas temperature was achieved. However, ignition delay, tailoff time, and roughness also increased.

Table 4-10
EFFECT OF CATALYST MESH SIZE
ON GAS GENERATOR PERFORMANCE

	Inner Bed Catalyst Mesh Size	
	25–30	14–18
Ignition delay time (msec)	38	62
Tailoff time (msec)	94	126
T_G (°F)	1,525	1,605
P_c (psia)	770.1	784
$\dot{w}$ (lbm/sec)	0.2484	0.2438
C* (ft/sec)	4,112	4,262
P_c roughness (±%)	0	1.0

No discernible difference in the performance or operating characteristics of the gas generator was observed during firings with the reactor in the different orientations. Startup and shutdown transients were nearly identical for all three reactor orientations.

The hot restart demonstrations were conducted by restarting at various soakback temperatures obtained following a firing. No pressure spikes were observed during any of the hot restart tests; however, chamber pressure was somewhat rougher during the initial second of the 800°F restart at maximum feed pressure. Roughness during this start transient was approximately ±8 percent, whereas roughness at the end of the steady-state firings was typically ±1 percent. Roughness during startup at 1,000°F and 1,200°F was significantly less than that at 800°F (approximately ±2 percent).

The initial bootstrap start test required 16 seconds for feed pressure to reach the maximum value. Ullage volume in the propellant tank was adjusted for the subsequent runs to achieve the desired pressurization rate. During the initial bootstrap tests, coupling between the feed system and reactor pressures was observed during the start transient. As bed temperature was increased, the coupling effect became more pronounced with the result that at 800°F, flow to the reactor was momentarily stopped during the initial 0.1 second. The reactor continued to operate throughout the remainder of the test without incident; however, roughness was observed to be higher than normal for the initial 2 seconds (±10 percent), whereupon operation smoothed to normal. During the 1,000°F startup, flow was stopped twice during the start transient; however, no spikes were observed, and roughness was significantly less than that observed during the startup at 800°F. A planned bootstrap startup at 1,200°F was not conducted due to the coupling problem.

Based on the test results obtained during the hot restart tests, it was concluded that the reactor can be safely restarted at any temperature; however, at 800°F, there is indication that a potential problem exists due to the observed roughness during the start transient which warrants additional studies. Under bootstrap startup, a serious problem was encountered due to coupling with the feed system. For the current APU pump-fed system, however, the problem may be less pronounced due to the continuous flow output provided by the pump.

4.3.4 NASA-JSC Test Results

The gas generator successfully completed the planned test program at JSC. The unit completed 20 simulated Space Shuttle APU mission duty cycles including approximately 29.3 hours of operation, 9.4 hours of accumulated valve on-time, and approximately 347,000 total pulses. During the test program, approximately 8,700 pounds of hydrazine were consumed. The unit was subjected to 56 starts at 200°F and performed over a duty cycle range from 9 percent to 85 percent. Table 4-11 summarizes the performance variation from the initial acceptance test duty cycle to the final acceptance test duty cycle.

Figure 4-29 illustrates the variation in hot gas temperature with life. The hot gas temperature shown was taken at the end of the 30-second steady-state firings performed for reference data after every five missions. It should be noted that the unit had not reached thermal equilibrium at the end of 30 seconds; however, the temperatures should be good for comparative purposes. The figure indicates that the gas temperature peaked after five missions and decreased somewhat as additional life was accumulated.

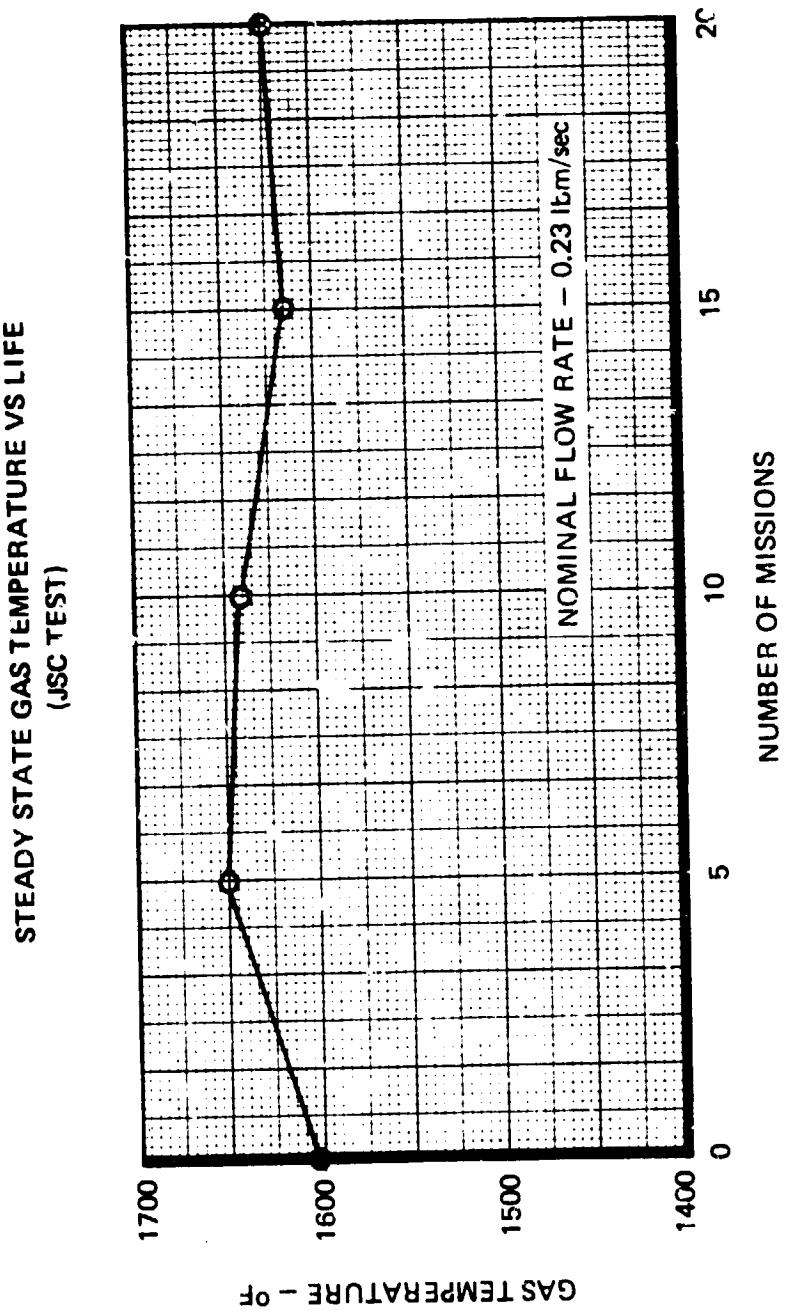
STEADY STATE GAS TEMPERATURE VS LIFE
(JSC TEST)
NOMINAL FLOW RATE – 0.23 lbm/sec
GAS TEMPERATURE – °F
1700
1600
1500
1400
0
5
10
15
NUMBER OF MISSIONS

Figure 4-29

Table 4-11
NASA-JSC TEST SUMMARY

Parameter	First Acceptance Test	Final Acceptance Test
Gas temperature (°F)	1,600°F	1,625°F
P_c roughness (percent)	±0.05%	±9.5%
Hot ignition delay (msec)	15	31
Cold ignition delay (msec)	38	47
Tail off time (msec)	113	163
Characteristic velocity (ft/sec)	4,290	--
Total catalyst weight (gm)	144.75	142.6

The characteristic exhaust velocity was 4,290 ft/sec on the first 30-seconds reference firing. This agrees fairly well with the predicted C* based on gas temperature. Subsequent C* readings were of questionable accuracy. Apparently, there was a small error in either the chamber pressure or the flow rate reading which caused the calculated C* to be too high. The C* readings should have increased with life approximately as a function of the square root of the gas temperature. There was no evidence of washout during any of the 30-second runs

Ignition delay and tailoff time are illustrated in Figures 4-30 and 31. The ignition delay increased 16 milliseconds during the test program. Ignition delay was defined as the time from valve opening to 10 percent steady-state chamber pressure. The increase in hot ignition delay was probably caused primarily by the presence of bed voids. The activity of the catalyst bed did not decrease significantly with life since only a 9-millisecond increase was noted in cold bed (200°F) ignition delay. The tailoff time, time from valve closure to 10 percent chamber pressure, increased 50 milliseconds during the test program. This is also believed to be an indication of the presence of voids in the catalyst bed. It should be noted that the increases in both ignition delay and tailoff time are similar to those experienced in the previous life test using 25- to 30-mesh catalyst in the inner bed.

Figure 4-32 shows the increase in chamber pressure roughness with life. As can be seen, chamber pressure roughness increased rapidly during the first five missions but then stabilized at around ±9 percent for the remaining 15 missions. This trend is similar to the trends seen on previous life tests with 25- to 30-mesh catalyst; however, the roughness with 14- to 18-mesh catalyst stabilized at a much higher value (9 percent versus 3 percent). The gas temperature and ignition delay also changed more rapidly during the first five missions than on subsequent missions.

The gas temperature variation with life and duty cycle is illustrated in Figure 4-33. The gas temperature at equilibrium ranged from about 1,610°F at 15 percent power level (25 to 30 percent

IGNITION DELAY VS LIFE
(JSC TEST)

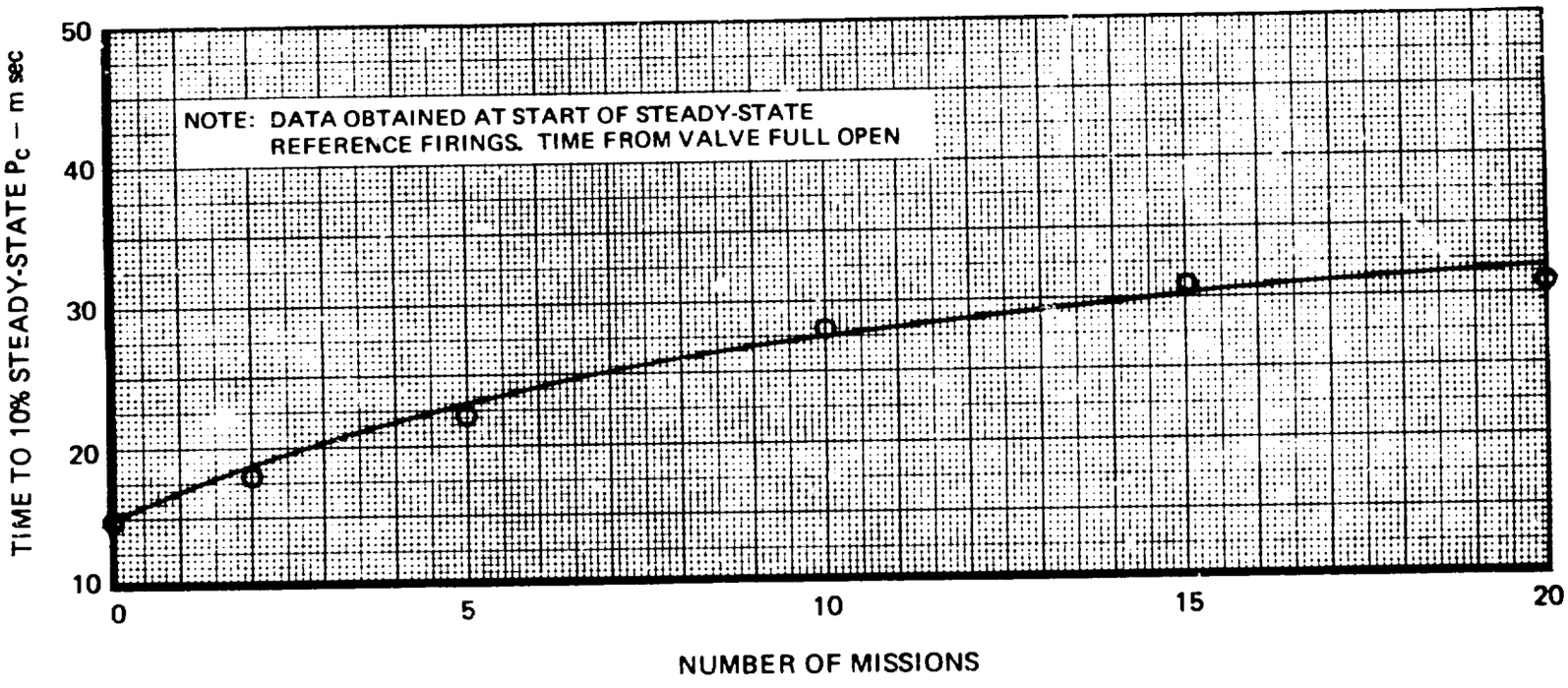

Figure 4-30

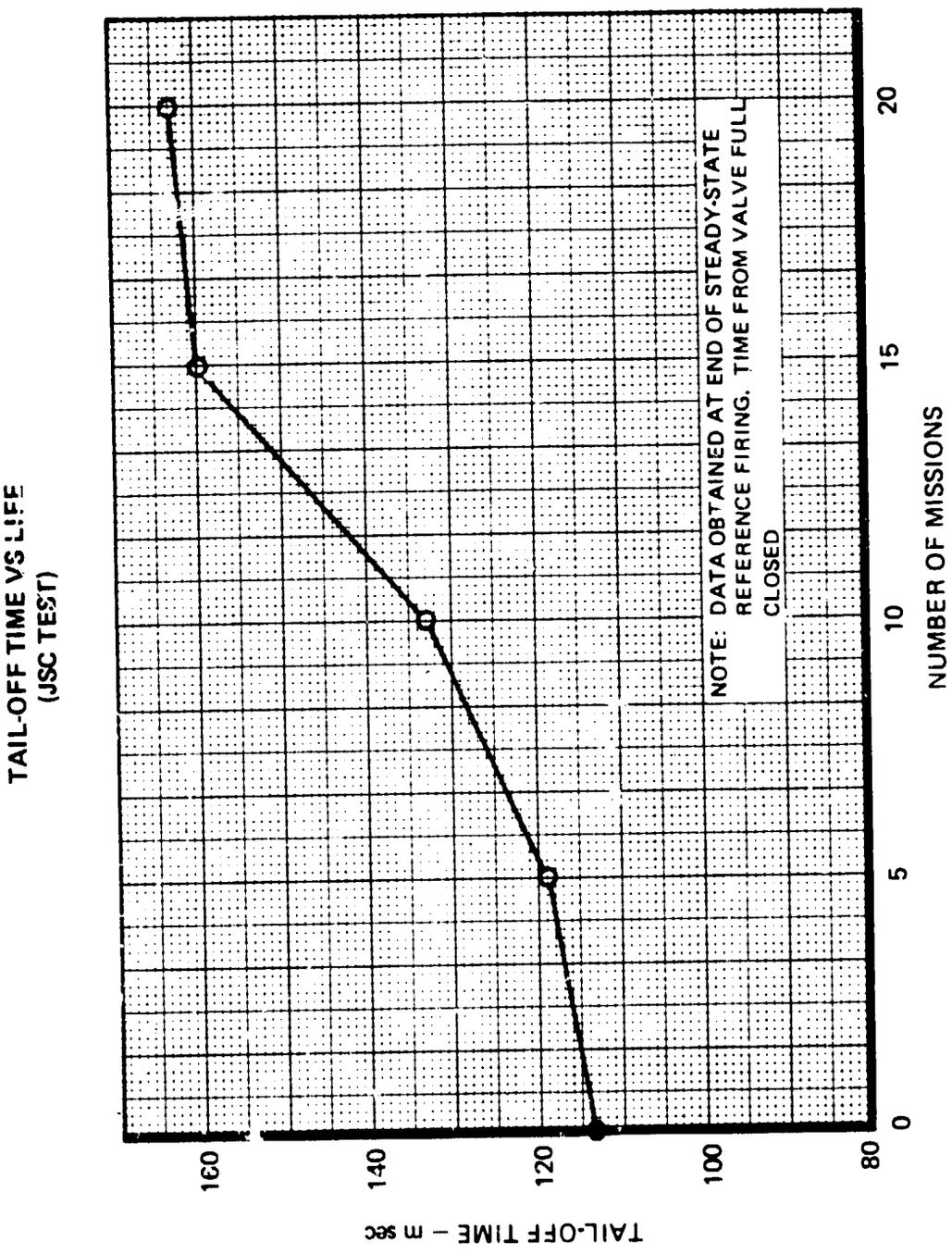
TAIL-OFF TIME VS LIFE
(JSC TEST)
NOTE: DATA OBTAINED AT END OF STEADY-STATE REFERENCE FIRING. TIME FROM VALVE FULL CLOSED
TAIL-OFF TIME – m sec
160
140
120
100
80
0
5
10
15
20
NUMBER OF MISSIONS

CHAMBER PRESSURE ROUGHNESS VS LIFE
(JSC TEST)

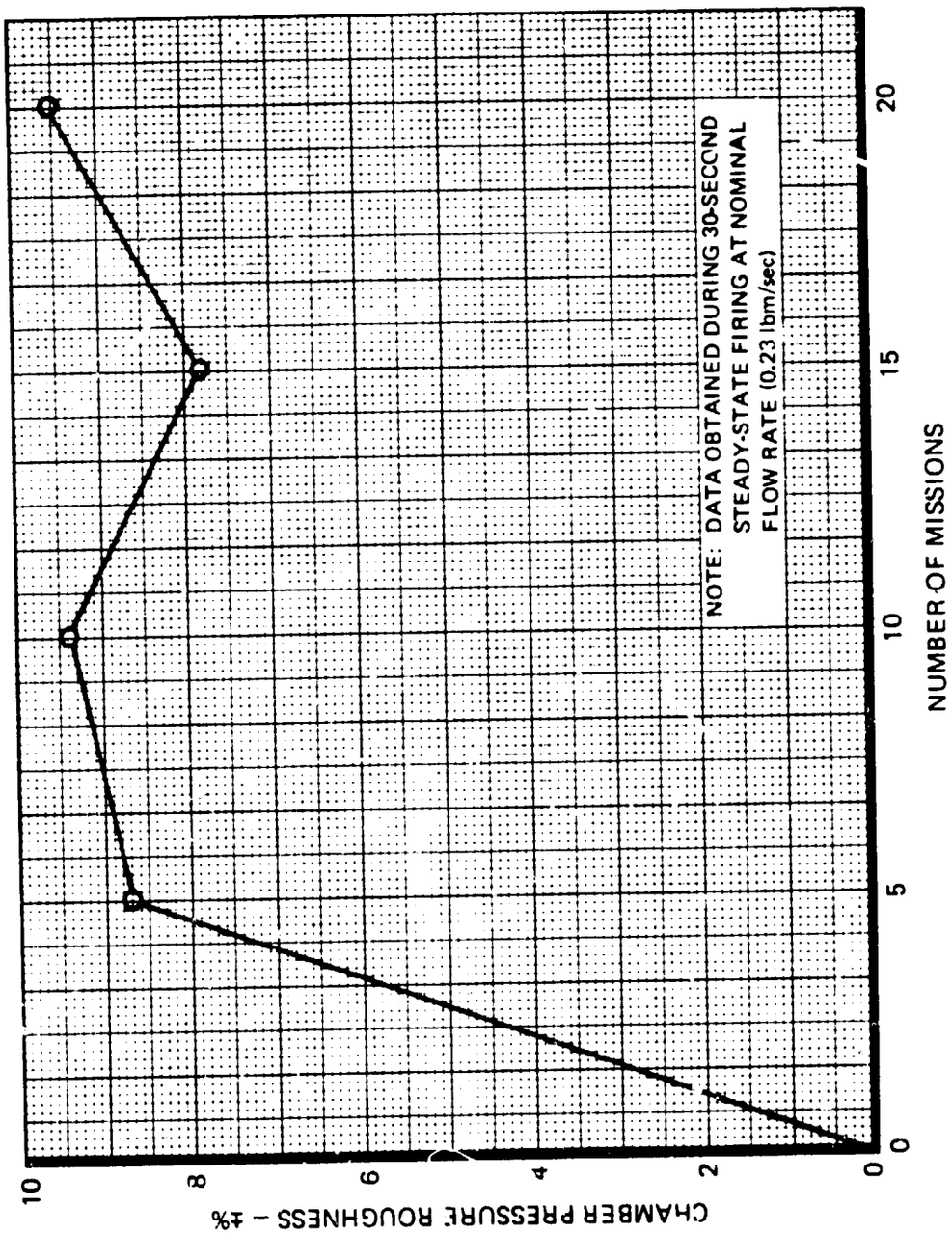

Figure 4-32

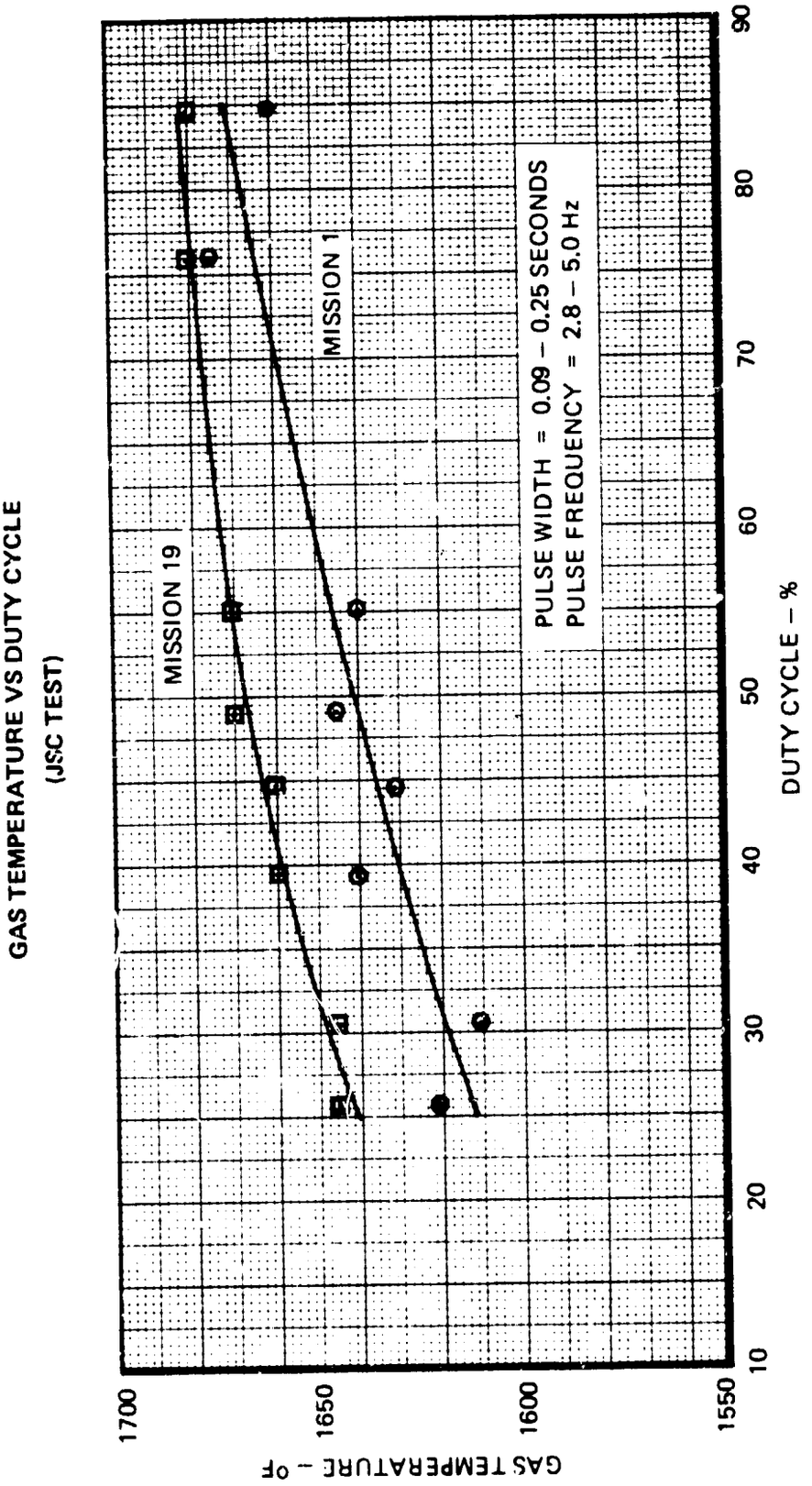

24001-82

Figure 4-33

duty cycle) to about 1,670°F at 100 percent power level (75 to 85 percent duty cycle) on the first mission duty cycle. The temperature increased by about 30°F at 15 percent power and 10°F at 100 percent power during the test program. The increase in gas temperature with life was small and should tend to help APU performance without exceeding material temperature limitations. It should be noted that the 1,670 to 1,680°F hot gas temperature at 100 percent power is very close to the design goal of 1,700°F.

The maximum variation in gas temperature with angular position was 60°F, and the maximum variation in bedplate temperature with angular position was 95°F. These values were recorded during mission duty cycle 20. The variation in bedplate temperature with angular position during the steady-state runs increased from 10°F on the first 30-second run to 165°F on the final 30-second run. The bottom of the catalyst bed was the coolest location during the final run, indicating that the catalyst had shifted somewhat due to gravitational force.

The changes in chamber pressure characteristics with life are illustrated in Figures 4-34 and 4-35. Figure 4-34 shows the change in pulse shapes between the first mission and the final mission. The peak pressure increased by about 250 psi, and the rise and decay slopes changed. It should be noted that the first mission was run with 1,050-psig inlet pressure and the final mission with 1,000-psig inlet. Also, the calibration constant for chamber pressure was changed; therefore, the pulse shapes are not directly comparable as shown. However, the different shapes are still evident and are most likely the result of voids in the catalyst bed which caused a longer ignition delay and then caused higher peak pressures as the propellant in the voids was rapidly decomposed. The overshoot was less as the power level (duty cycle) increased such that there was no appreciable overshoot at 100 percent power. This was apparently the result of the shorter off times, which did not allow the voids to clear between pulses. Figure 4-35 illustrates the change in chamber pressure roughness between the first 30-second steady-state firing and the last 30-second firing. Again, the change in roughness was probably the result of voids in the catalyst bed. As mentioned previously, the roughness seemed to stabilize after about five mission duty cycles.

Special tests were run to investigate the predicted APU 1/2-speed duty cycle and the gas generator hot restart capability. The 1/2-speed duty cycle used was a 9 percent duty cycle with 0.085 second on time and 0.850 second off time. The inlet pressure was reduced to 700 psig. The gas generator completed the 1/2-speed duty cycle with no problems. The hot gas temperature decreased to about 1,570°F during the 1/2-speed duty cycle.

Hot restarts were performed to investigate conditions not tested in the previous hot restart duty cycles performed at RRC. Hot restarts were performed during the time when the injector temperature was rising due to soakback after a firing. The object was to determine if the unit could be restarted while the injector "dribble volume" propellant was evaporating. The unit was restarted after off-times from 5 to 300 seconds. No significant pressure spikes were seen during the restarts, however, there was evidence of the effects of vapor in the injector. The pressure rise time on startup was more rapid than normal, some of the restarts had small pressure overshoots, and some had abnormal chamber pressure roughness. These restarts were made with 1,000-psig propellant inlet pressure since the bootstrap inlet pressure profile could not be simulated because of facility limitations.

PULSE SHAPES ON MISSION DUTY CYCLES 1 AND 20

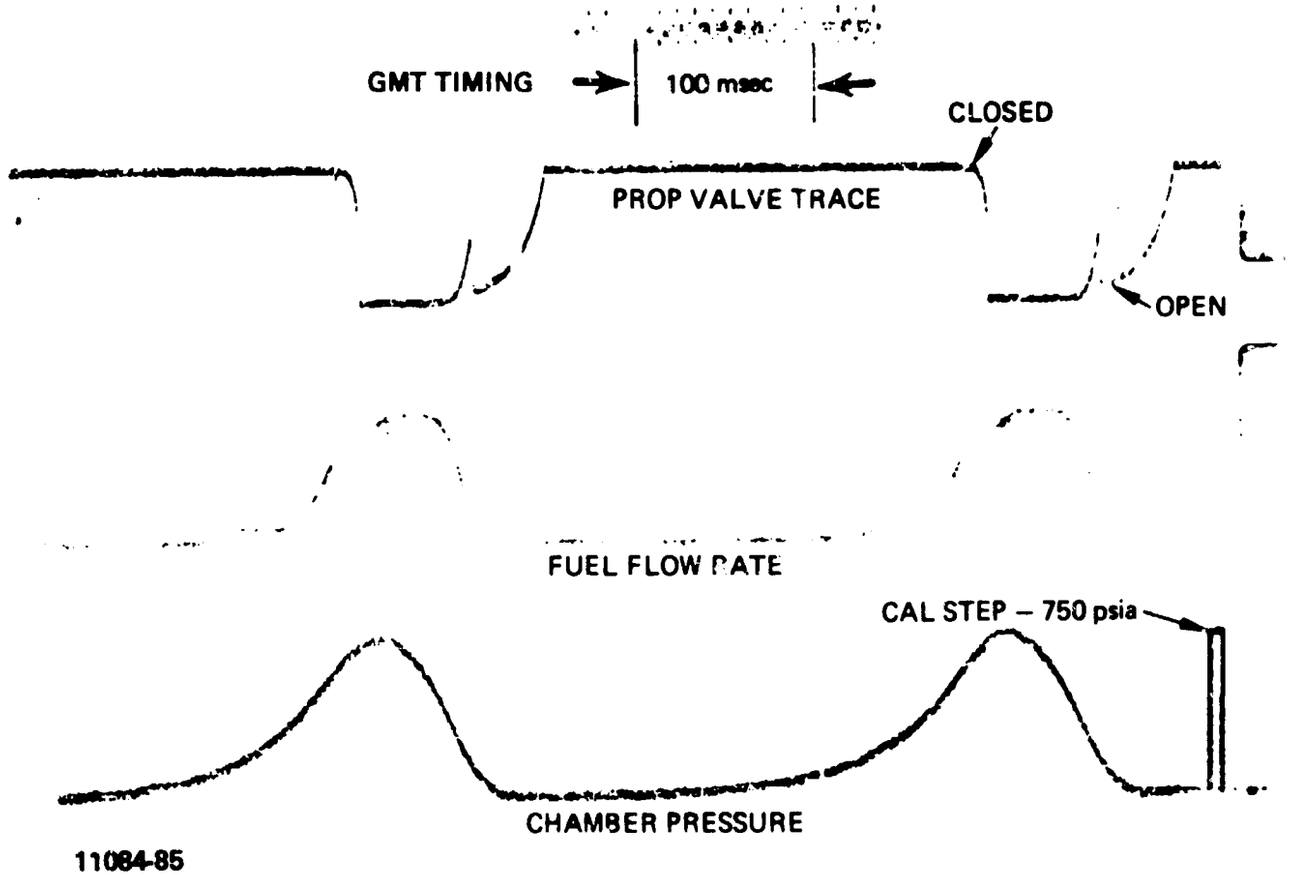

11084-85

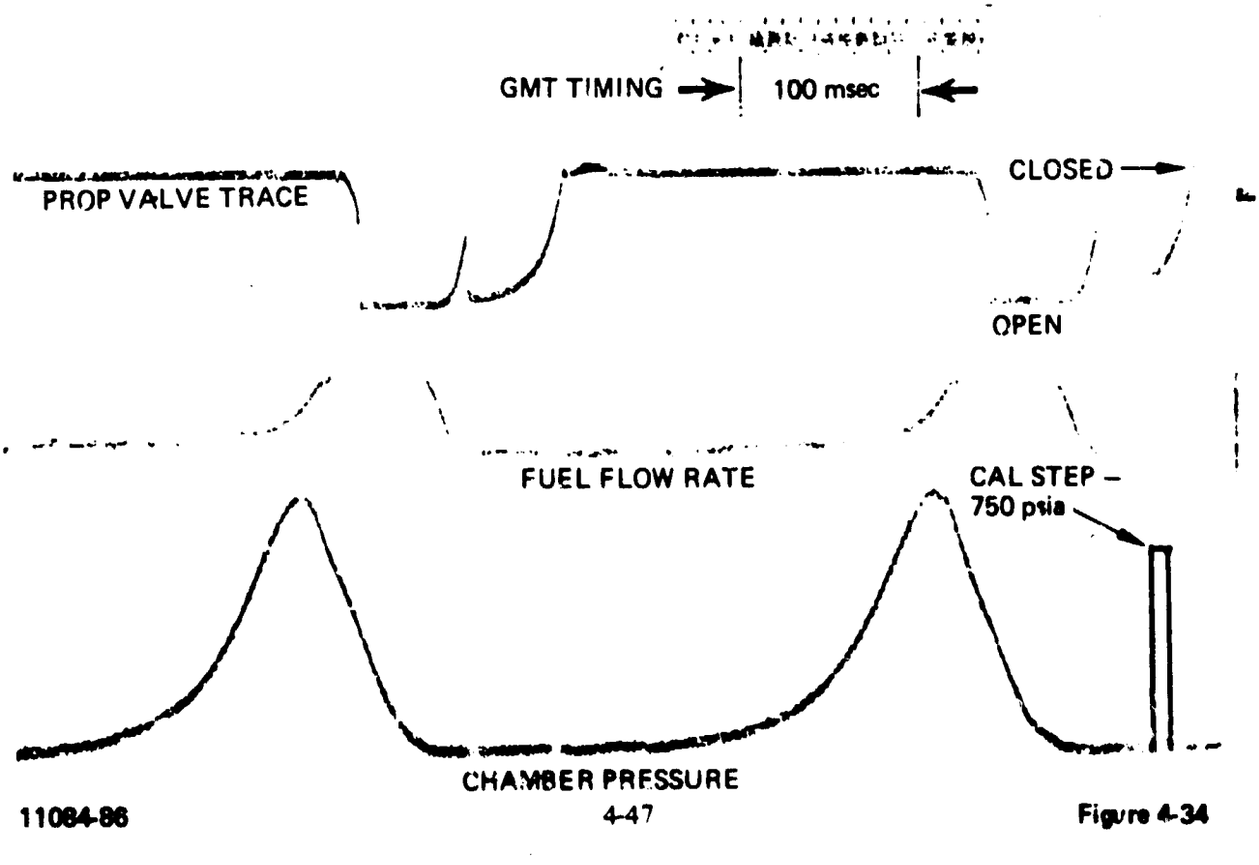

11084-86

Figure 4-34

STEADY-STATE CHAMBER PRESSURE AT BEGINNING AND END OF TEST

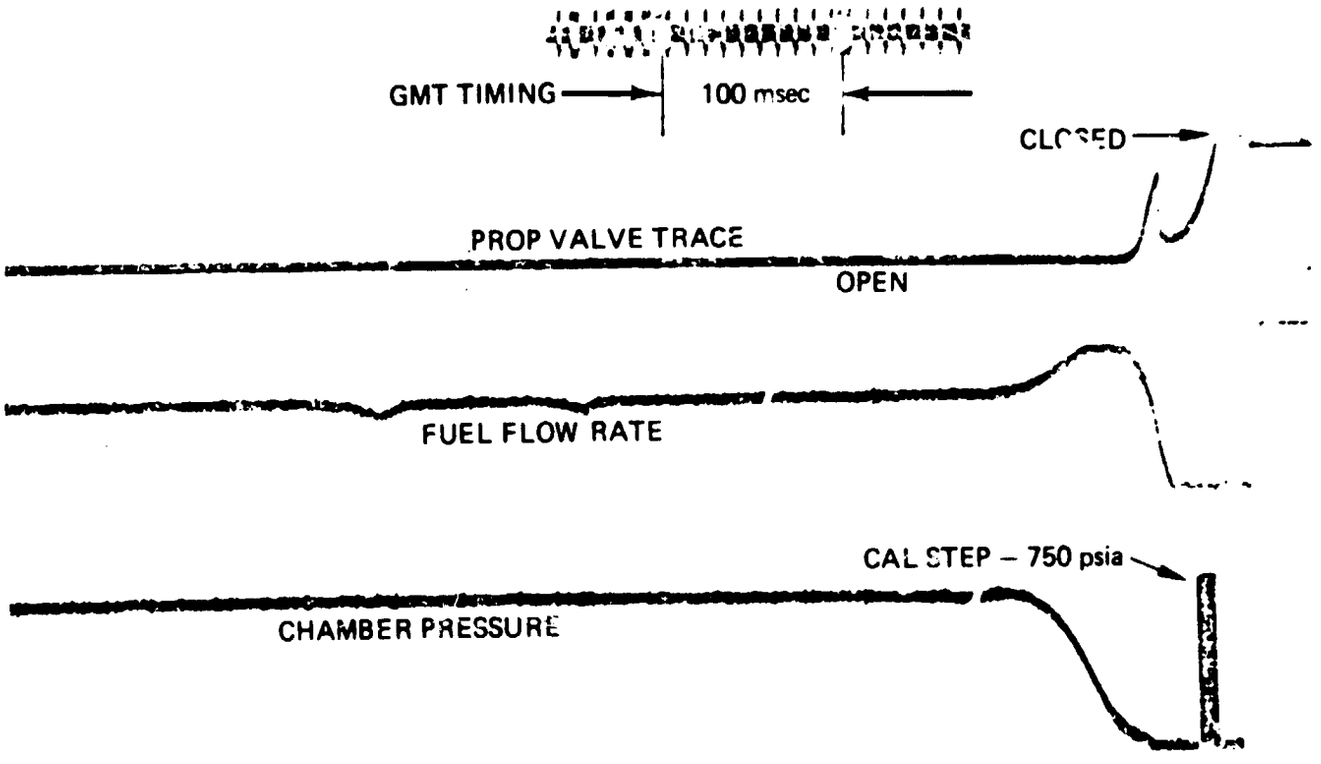

11084-87

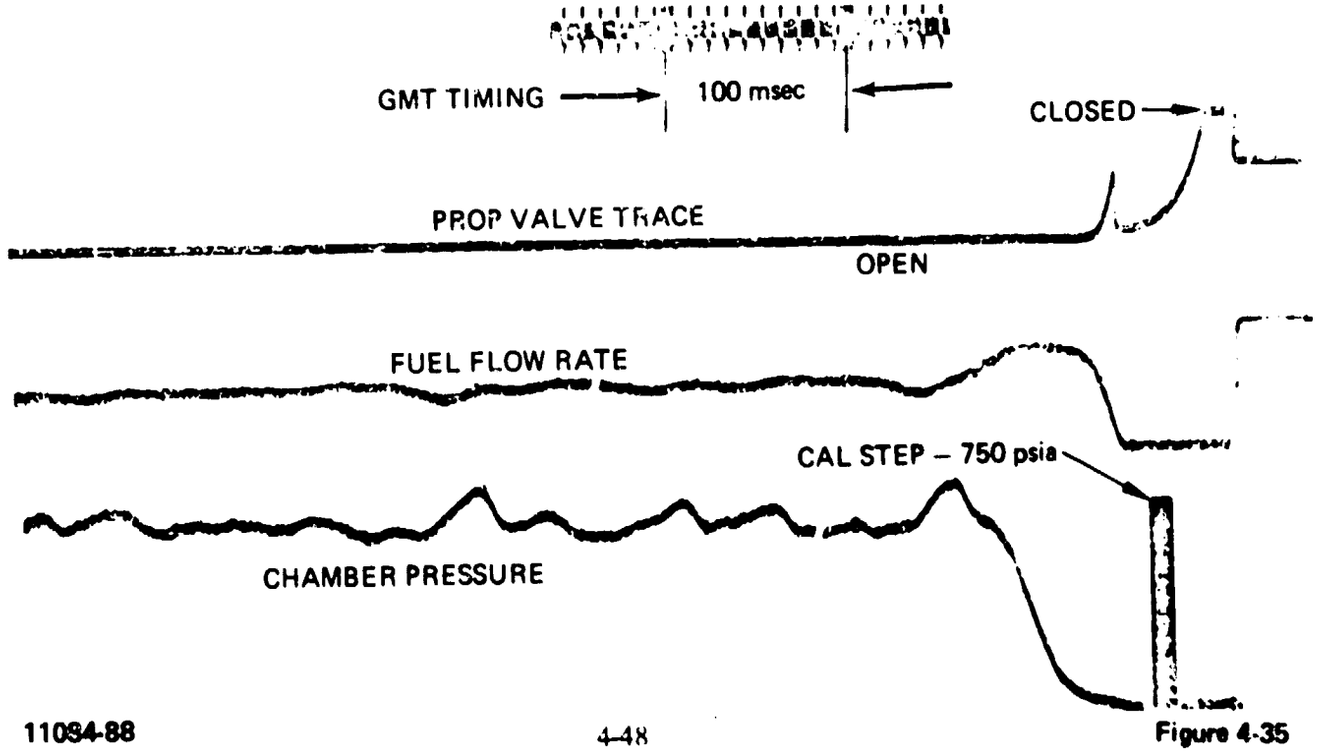

11084-88

Figure 4-35

An interesting phenomenon occurred during the JSC testing. As the catalyst bed began to degrade, as evidenced by chamber pressure roughness and pulse shapes, a visible flame began to appear at the exit of the nozzle between pulses on the lower power duty cycles (15 percent). The flame was also visible after shutdown at the end of a mission sequence and was accompanied by an audible "pop." The flame did not appear in a run until the unit was approaching equilibrium temperature. High-speed movies were made so that the flame phenomenon could be fully analyzed. These movies indicated that the flame started as a small, bluish-white flame (3 to 4 inches long) about 200 milliseconds after voltage was removed from the valve. The flame burned at a low level until the next pulse was initiated. At a time corresponding to the start of chamber pressure rise, the flame expanded to a large (yellowish-white) flame which lasted for about 10 milliseconds. As the chamber pressure continued to rise, the flame went out, and the exhaust was no longer visible. This sequence was repeatable whenever the off-time was sufficient to allow the small flame to occur (greater than 150 to 200 milliseconds). However, if the small flame did not occur due to insufficient off-time, the large flame on startup did not occur and the exhaust was not visible. Apparently, the flame resulted from the burning of exhaust gases in air as the velocity and pressure of the gases decreased between pulses. The most probable cause of the flame was delayed decomposition of hydrazine trapped in bed voids. This would explain why the flame did not occur early in the test before the bed had degraded. However, the flame could also have been caused or influenced by a change in reaction products as life was accumulated and/or hotter reactor and injector temperatures as the gas temperature increased with life. Regardless of the cause, the phenomenon should not be a problem on the Space Shuttle APU application since the gas generator exhausts into a turbine and exhaust duct without being exposed to air.

The results of the teardown and inspection which were conducted by RRC indicated that a sizeable void had been created in the inner catalyst bed corresponding to a loss of 7.1 percent of the inner bed catalyst. A 9 to 10 percent weight loss of the nickel foam retention structure was also reported. Table 4-12 summarizes the teardown and inspection results. Photographs of the components are presented in Figures 4-36 through 4-39.

The bedplates, chamber, and injector were in good condition with some minor distortion of the inner bedplate. The chamber and injector had accumulated run times of 120 and 90 hours, respectively, at the time of teardown. It is surprising to note that the 14- to 18-mesh inner bed suffered more loss and more breakup than the similarly tested 25- to 30-mesh inner bed. This probably resulted from the fact that the packing density for the 14- to 18-mesh catalyst with foam retention was lower than the packing density with 25- to 30-mesh catalyst with foam. Consequently, the inner bed probably had some small voids before it was fired such that foam degradation or catalyst breakup due to firing could result in larger voids, thus causing greater catalyst breakup.

Table 4-12
TEARDOWN RESULTS

	Assembly	Teardown
Inner Bed, Shell 405, 14–18 mesh		
Total weight (gm)	52.2	48.5
14–18 mesh	52.2	39.5
>18 mesh		9.0
Loss		3.7
Percent loss		7.1
Outer Bed, Shell 405, 14–18 mesh		
Total weight (gm)	92.55	94.0
>18 mesh		6.9
Gain		1.45
Percent gain		1.6
Total catalyst (gm)	144.75	142.55
Nickel foam (gm)	13.56	12.28
Hydrogen chemisorption μ moles/g		
Inner bed	152	135
Outer bed	152	122

CATALYST BED ASSEMBLY

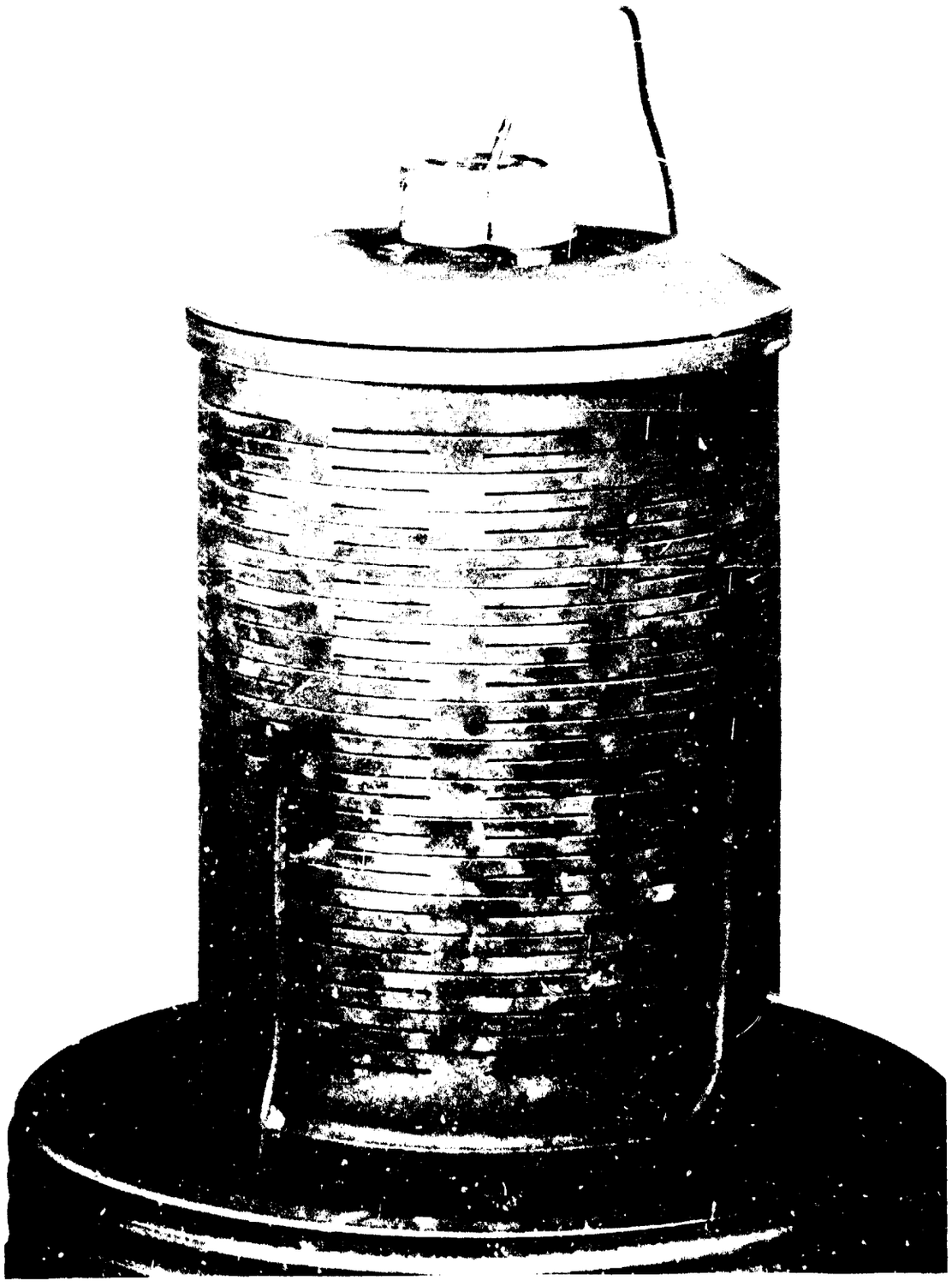

11092-64 1661-4

Figure 4 36

CATALYST BED ASSEMBLY - ENCLOSURE REMOVED

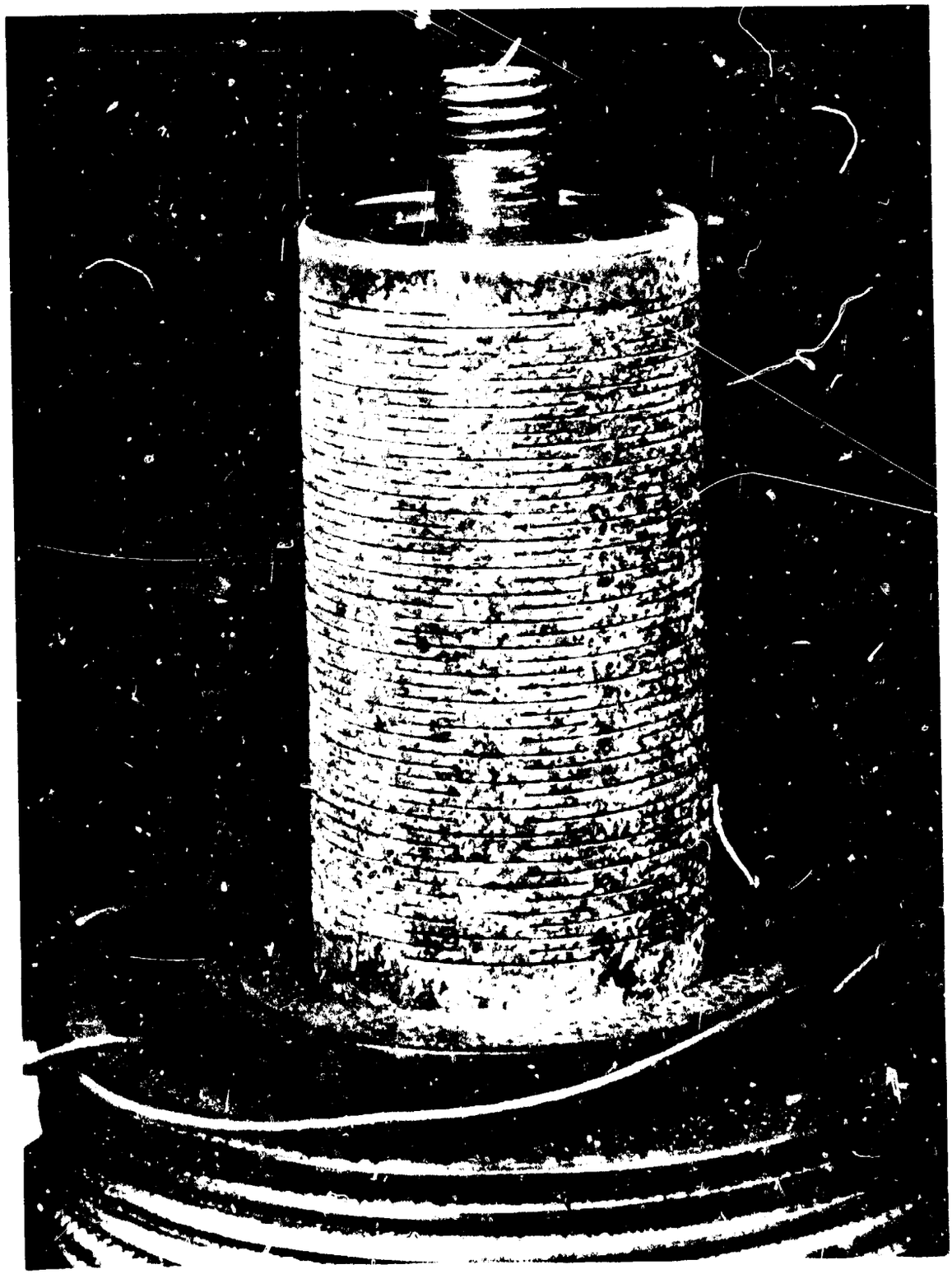

11092 63 1661 2

Figure 4 37

END VIEW OF CATALYST BED ASSEMBLY

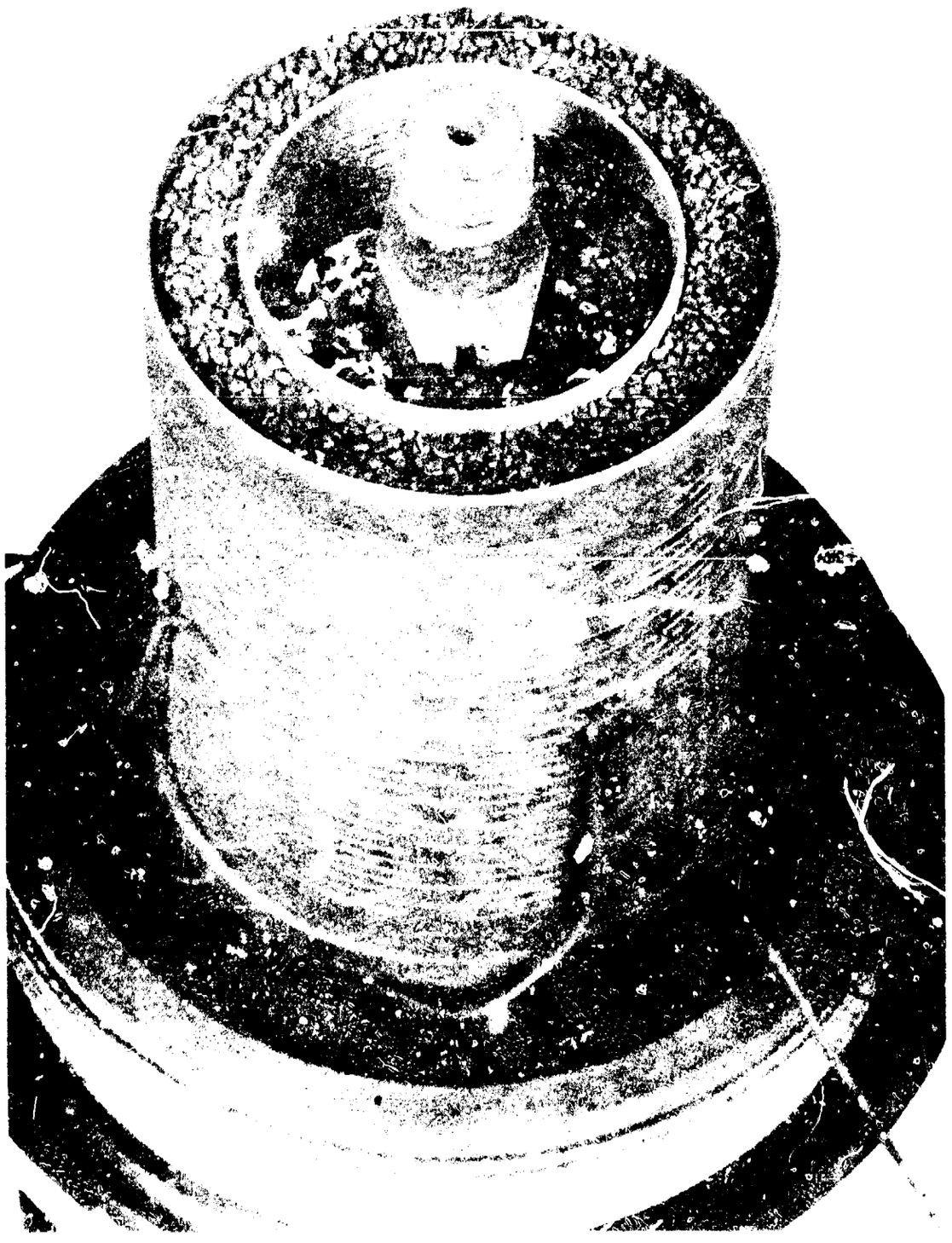

11092 65 1661 1

Figure 4.38

INJECTOR SIDE VIEW

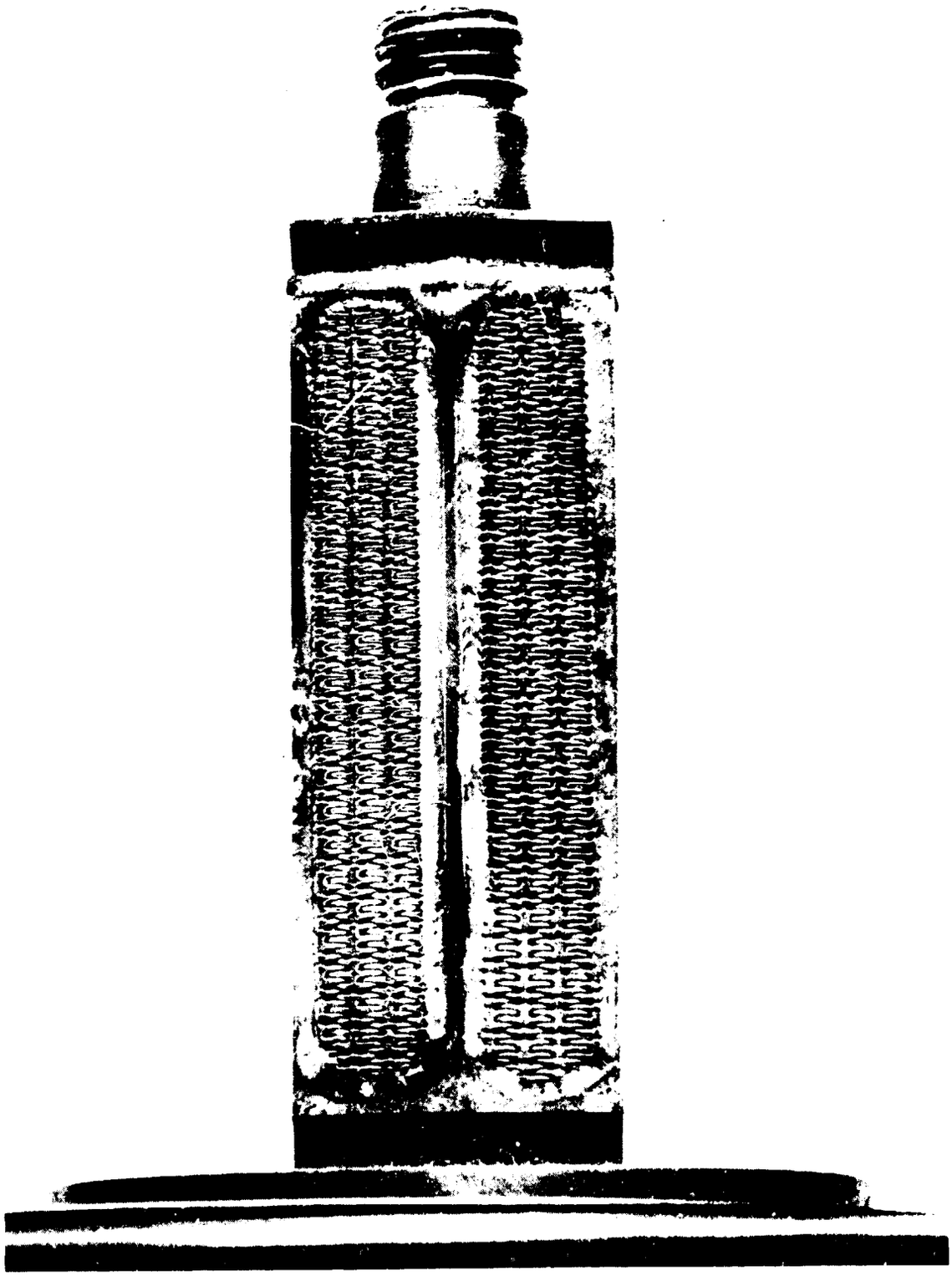

Figure 4-39

5.0 CONCLUSIONS AND RECOMMENDATIONS

The major results, conclusions, and recommendations of the catalytic gas generator investigation are as follows:

1. The results of this program have shown that a catalytic gas generator can be designed to meet the requirements of the Space Shuttle APU. A total of 60 simulated missions was conducted during three separate tests using the same injector and chamber. Although the catalyst bed was refurbished after each 20-mission test, the post-test teardown results indicated that significantly more life capability existed. On the basis of an extrapolation of gas temperature to a limiting value of 1,700°F, a life capability of 100 missions (150 hours) was projected for the pulse-modulated mode of operation. It should be noted, however, that vibration testing of the GG was not conducted and that its effect on life is therefore unknown.

2. A comparison of the test results revealed no significant difference in the mission life capability for the gas generator operating in pulse-mode or steady-state. Inner bed catalyst loss was 2.3 percent for the steady-state missions compared to 3.3 percent for the pulse-mode missions.

3. Tests conducted with the gas generator in various orientations (vertical down and various horizontal attitudes) revealed no discernible effect of attitude on performance or operating characteristics. Hot restart tests were successfully conducted with the gas generator initially at temperatures ranging from 200 to 1,200°F. A potential problem exists under bootstrap startup conditions when the bed temperature exceeds 600°F.

4. The effect of replacing the inner bed 25- to 30-mesh catalyst with 14- to 18-mesh catalyst was to increase gas temperature by 80°F with a small increase in chamber pressure roughness. Contrary to initial predictions, attrition of the coarser mesh catalyst was somewhat more than that encountered with the 25- to 30-mesh catalyst. It was postulated, however, that the relatively low packing density of the coarse-mesh catalyst in the foam metal may have been a factor in the higher attrition rate.

5. The foam metal used for retention of the catalyst showed evidence of degradation during the tests. The Hastelloy B material used for fabrication of the major components showed very little degradation with the exception of the bedplates which showed evidence of nitriding attack. The chamber had an accumulated exposure time of 120 hours while the injector had 90 hours. The same injector was used throughout the test program with a total propellant throughput of 30,800 lbm.

6. It is recommended that vibration testing be conducted with the gas generator firing to identify potential problems associated with Space Shuttle launch conditions.

7. It is recommended that bootstrap startup with a hot injector be thoroughly investigated to define the limits of safe reliable operation.

8. Additional testing of the 14- to 18-mesh inner bed catalyst is recommended. A larger pore size foam, however, should be developed for the larger catalyst granules.

APPENDIX 6.1

PRESSURE MODULATED OSCILLOGRAPH RECORDS

Presented in this section are oscillograph records for the pressure modulated tests at various times during the test series. The data show chamber pressure traces for the maximum flow rate condition. The accumulated burn time for each figure is shown at the top of the oscillograph record.

SPACE SHUTTLE APU GAS GENERATOR
OSCILLOGRAPH TRACE OF HI-FLOW RATE
AT ONE-HALF HOUR ACCUMULATED BURN

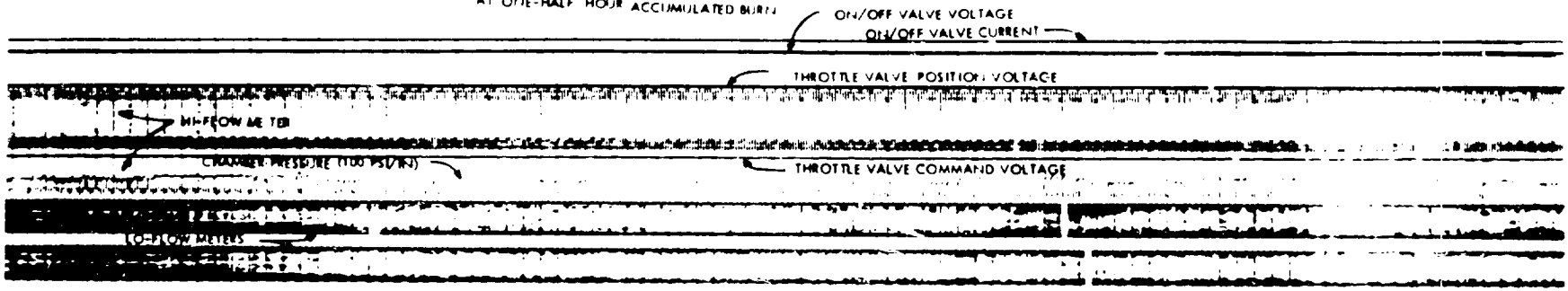

CHAMBER PRESSURE (200 PSI/IN)

5A

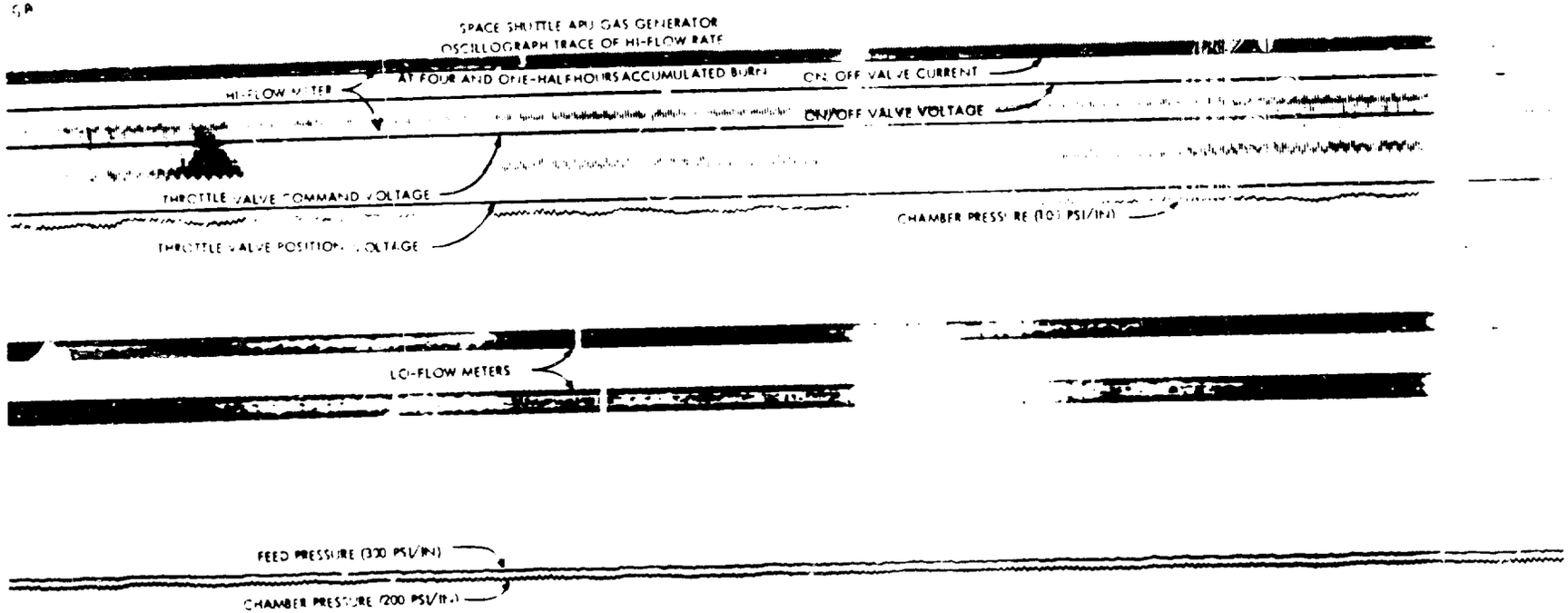
SPACE SHUTTLE APU GAS GENERATOR
OSCILLOGRAPH TRACE OF HI-FLOW RATE
AT FOUR AND ONE-HALF HOURS ACCUMULATED BURN
HI-FLOW METER
ON/OFF VALVE CURRENT
ON/OFF VALVE VOLTAGE
THROTTLE VALVE COMMAND VOLTAGE
THROTTLE VALVE POSITION VOLTAGE
CHAMBER PRESSURE (100 PSI/IN.)
LO-FLOW METERS
FEED PRESSURE (300 PSI/IN.)
CHAMBER PRESSURE (200 PSI/IN.)

24001 56

10A

SPACE SHUTTLE APU GAS GENERATOR
OSCILLOGRAPH TRACE OF HI-FLOW RATE
AT NINE HOURS ACCUMULATED BURN

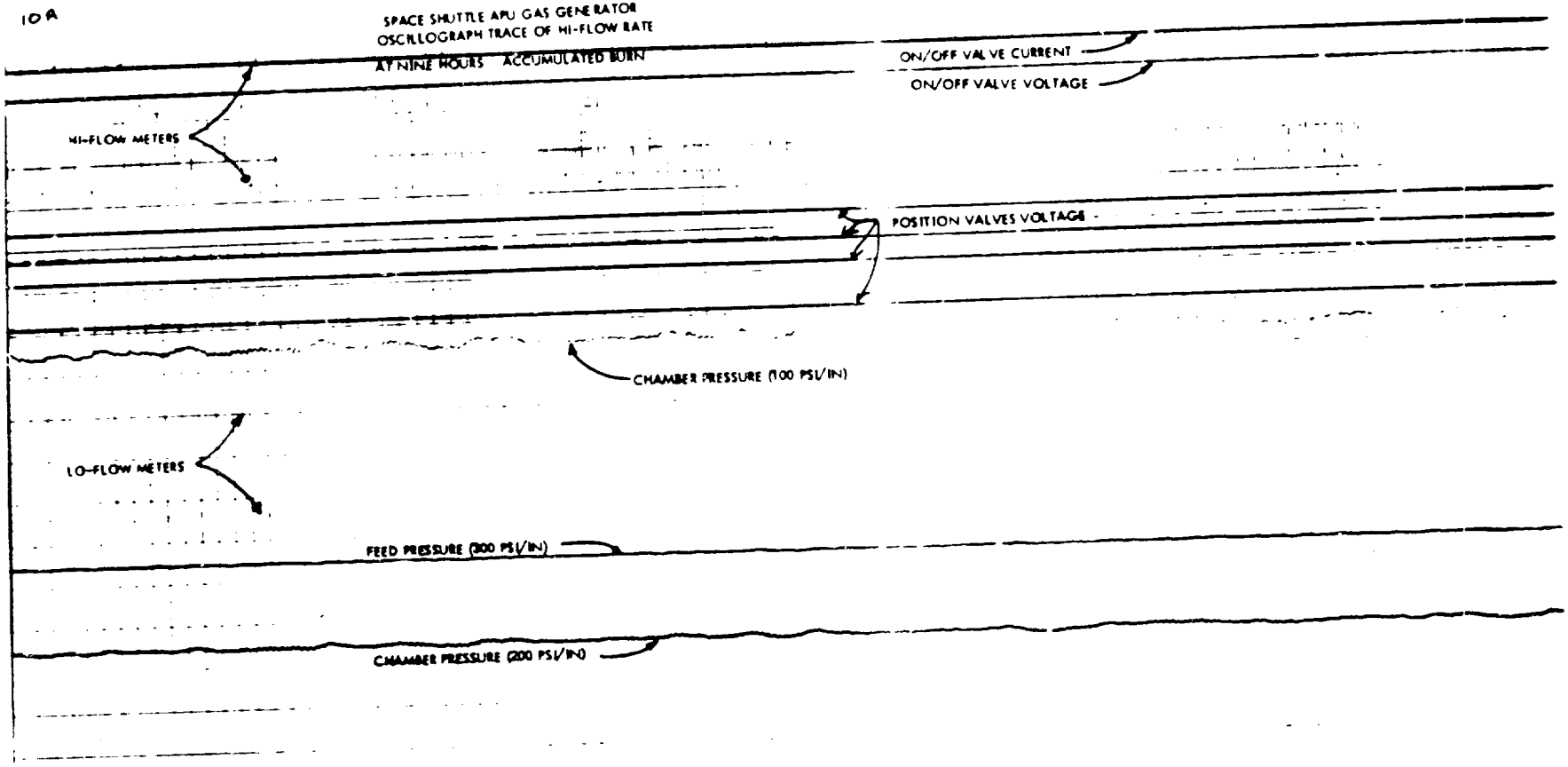

26001 63

12A

SPACE SHUTTLE APU GAS GENERATOR
OSCILLOGRAPH TRACE OF HIGH FLOW RATE
[illegible] HOURS ACCUMULATED BURN

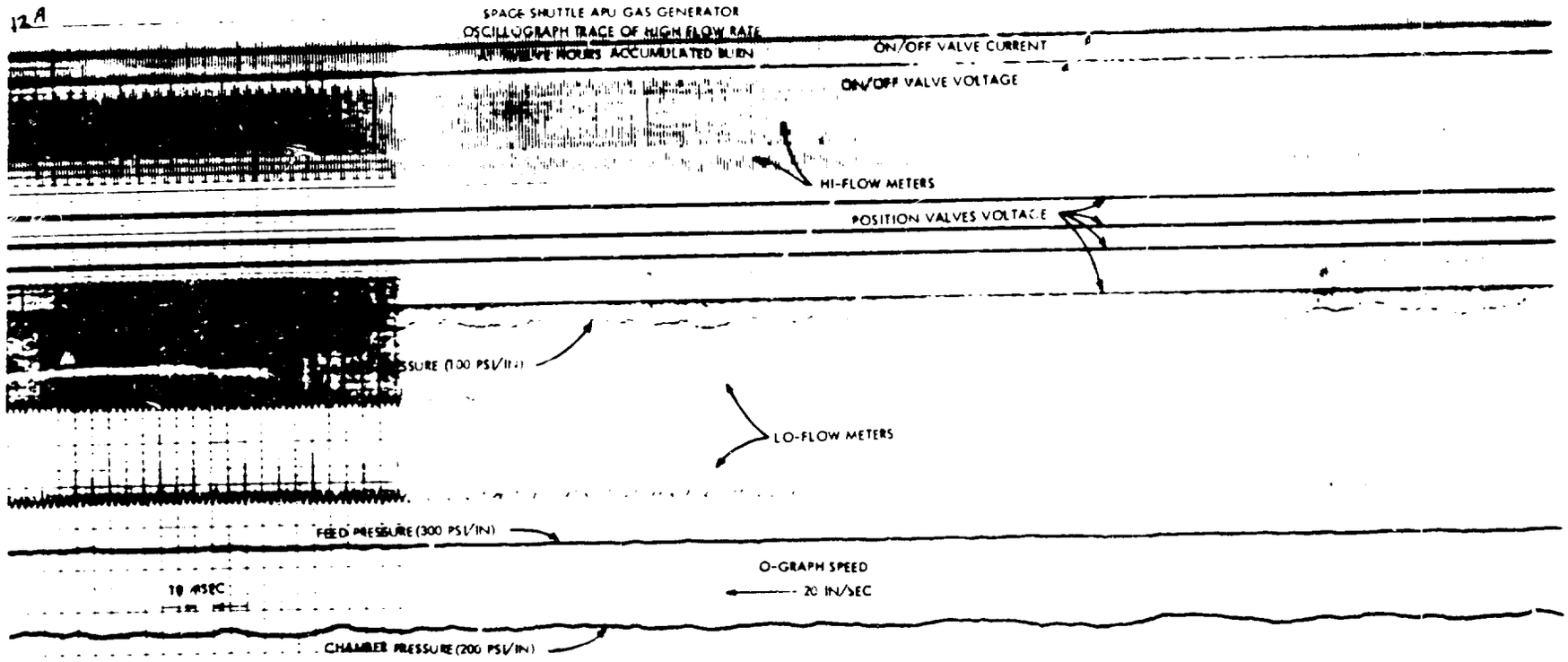

24001 57

14A

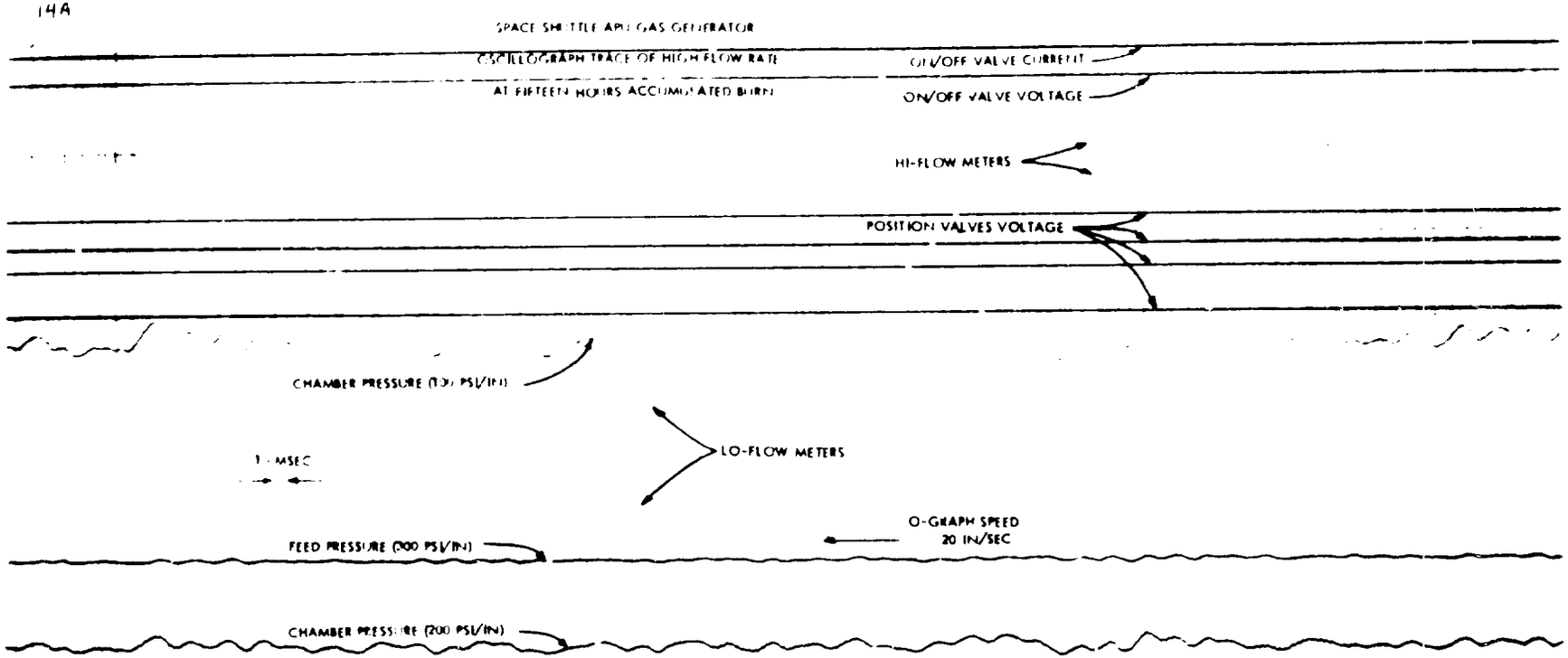
SPACE SHUTTLE APU GAS GENERATOR
OSCILLOGRAPH TRACE OF HIGH FLOW RATE
AT FIFTEEN HOURS ACCUMULATED BURN
ON/OFF VALVE CURRENT
ON/OFF VALVE VOLTAGE
HI-FLOW METERS
POSITION VALVES VOLTAGE
CHAMBER PRESSURE (100 PSI/IN)
1 MSEC
LO-FLOW METERS
O-GRAPH SPEED
20 IN/SEC
FEED PRESSURE (200 PSI/IN)
CHAMBER PRESSURE (200 PSI/IN)

18A

SPACE SHUTTLE APU GAS GENERATOR
OSCILLOGRAPH TRACE OF HI-FLOW RATE
AT TWENTY-ONE HOURS ACCUMULATED BURN

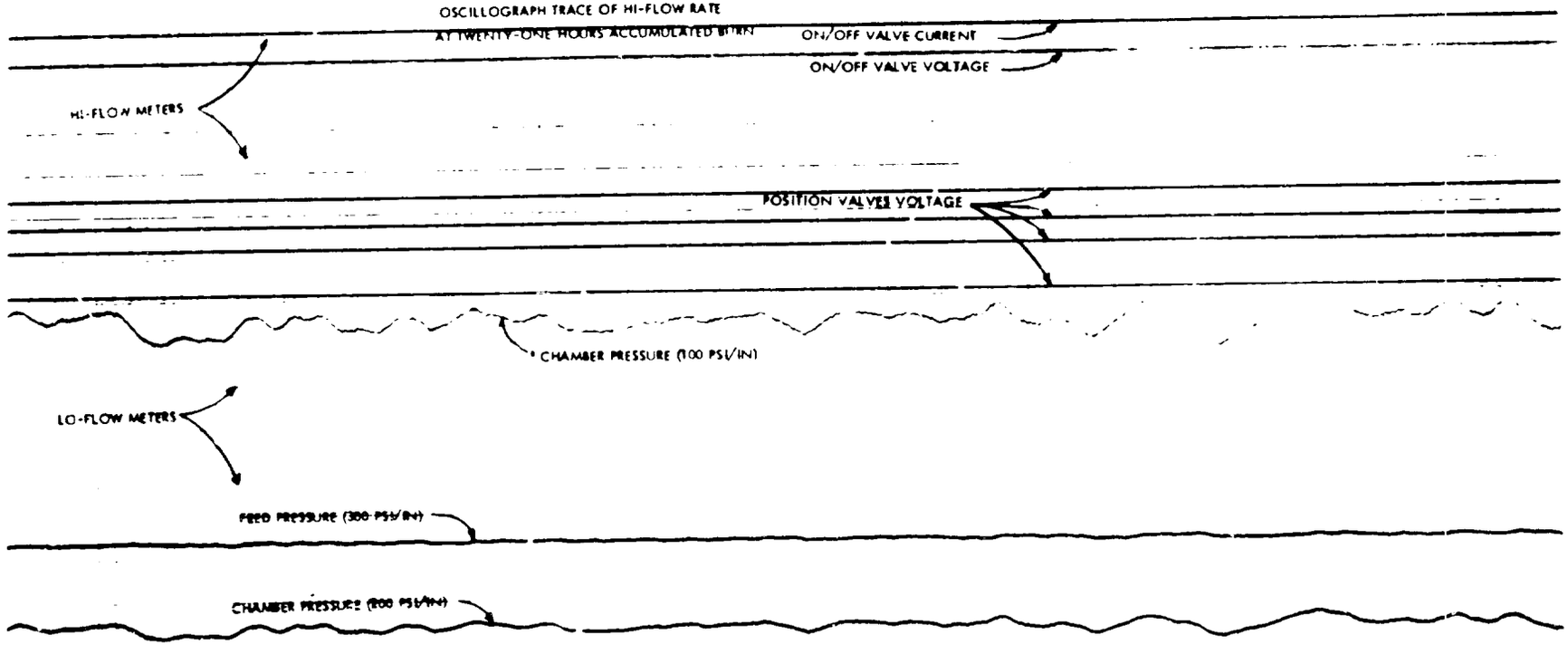

24001 60

20 A-B

SPACE SHUTTLE APU GAS GENERATOR

OSCILLOGRAPH TRACE OF HIGH FLOW RATE

AT TWENTY-FOUR HOUR ACCUMULATED BURN

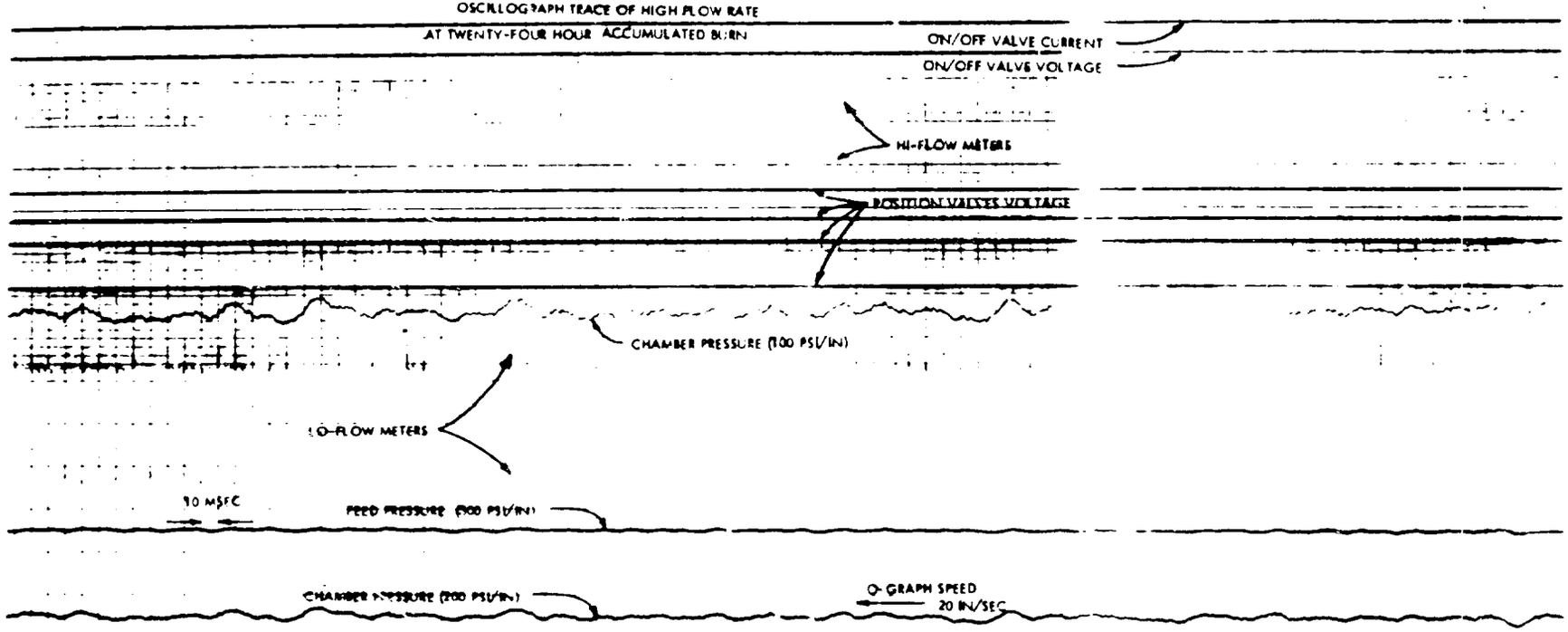

24001 61

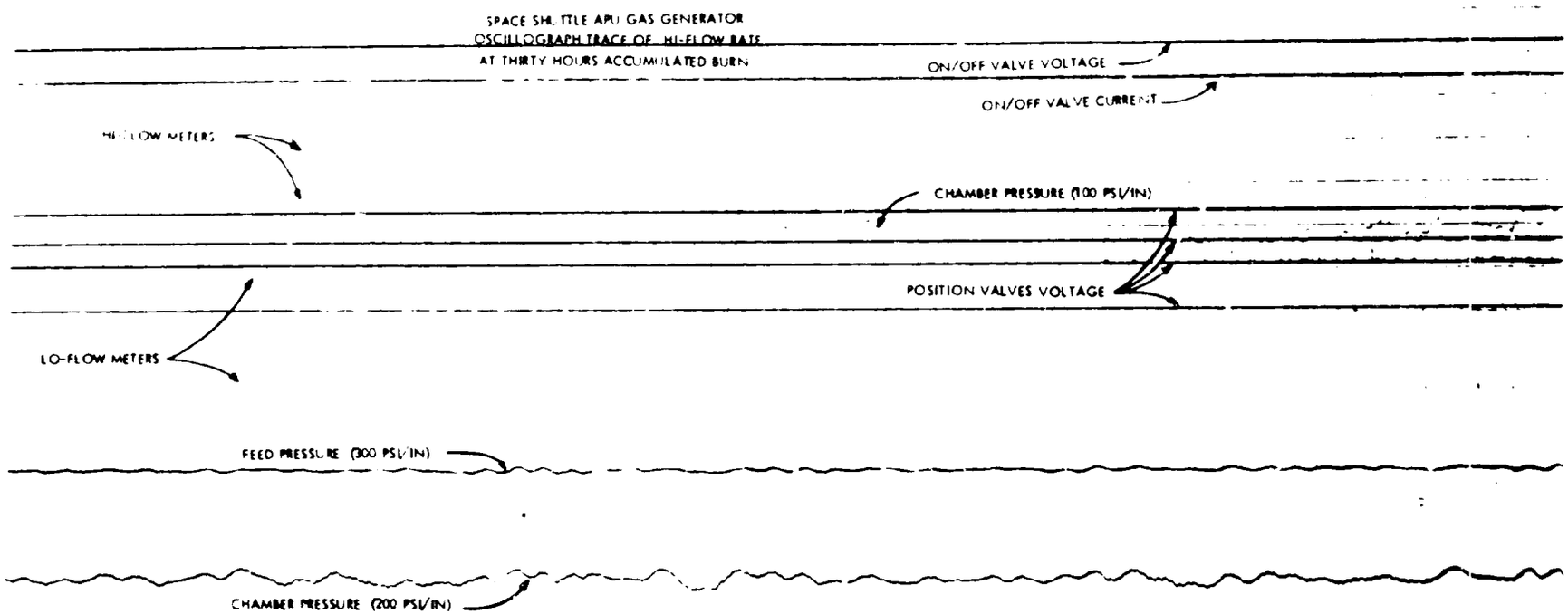
SPACE SHUTTLE APU GAS GENERATOR
OSCILLOGRAPH TRACE OF HI-FLOW RATE
AT THIRTY HOURS ACCUMULATED BURN
ON/OFF VALVE VOLTAGE
ON/OFF VALVE CURRENT
HI-FLOW METERS
CHAMBER PRESSURE (100 PSI/IN)
POSITION VALVES VOLTAGE
LO-FLOW METERS
FEED PRESSURE (300 PSI/IN)
CHAMBER PRESSURE (200 PSI/IN)

24001 62

APPENDIX 6.2
PULSE-MODULATED OSCILLOGRAPH RECORDS

Presented in this section are the oscillograph records obtained during the pulse-modulated tests. The first two figures are the pressure traces obtained during the initial and final steady-state reference firings. The subsequent oscillograph records show pulse traces at various power levels obtained during various mission firings throughout the test program. The mission number and power level are denoted at the bottom of each figure.

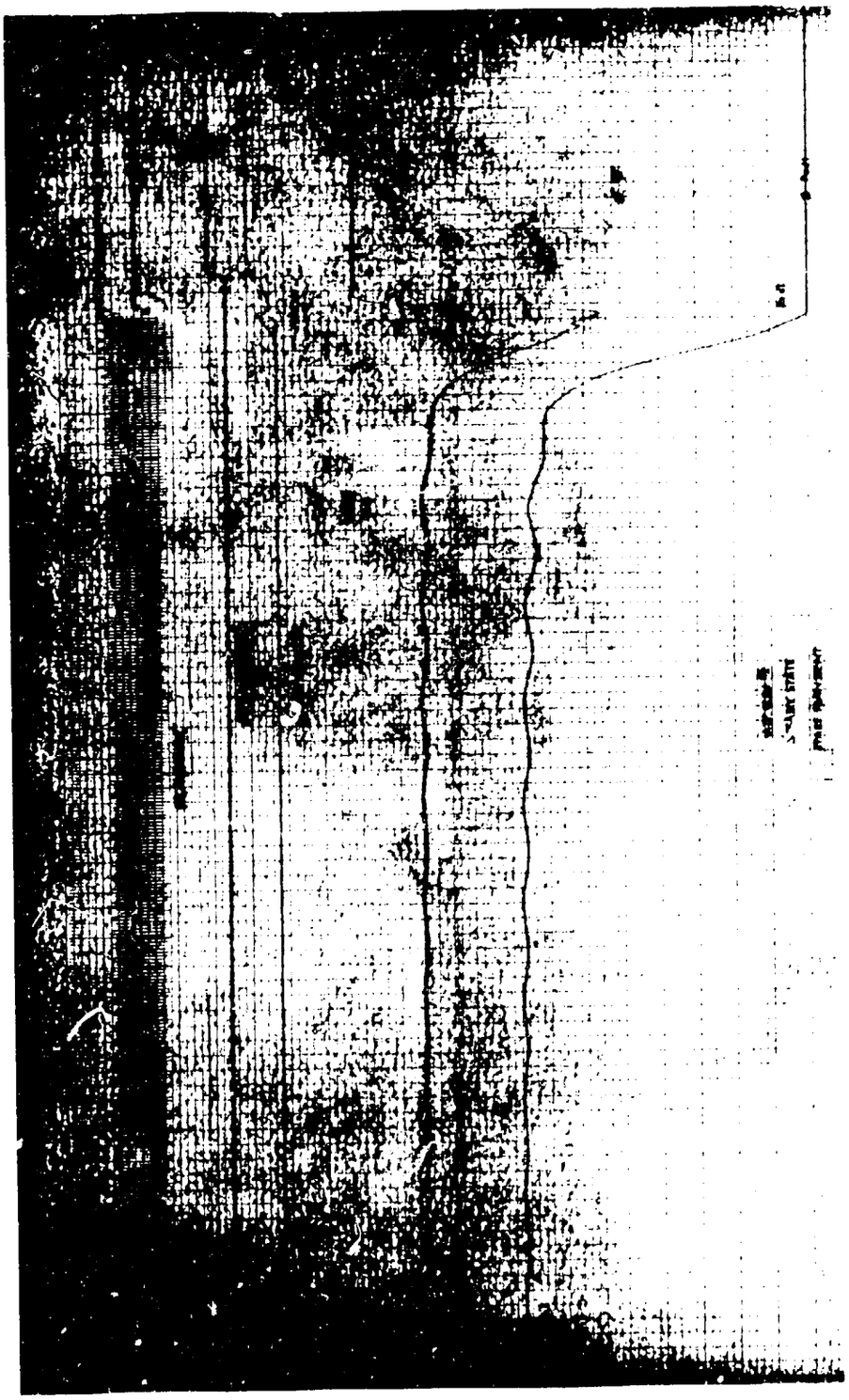

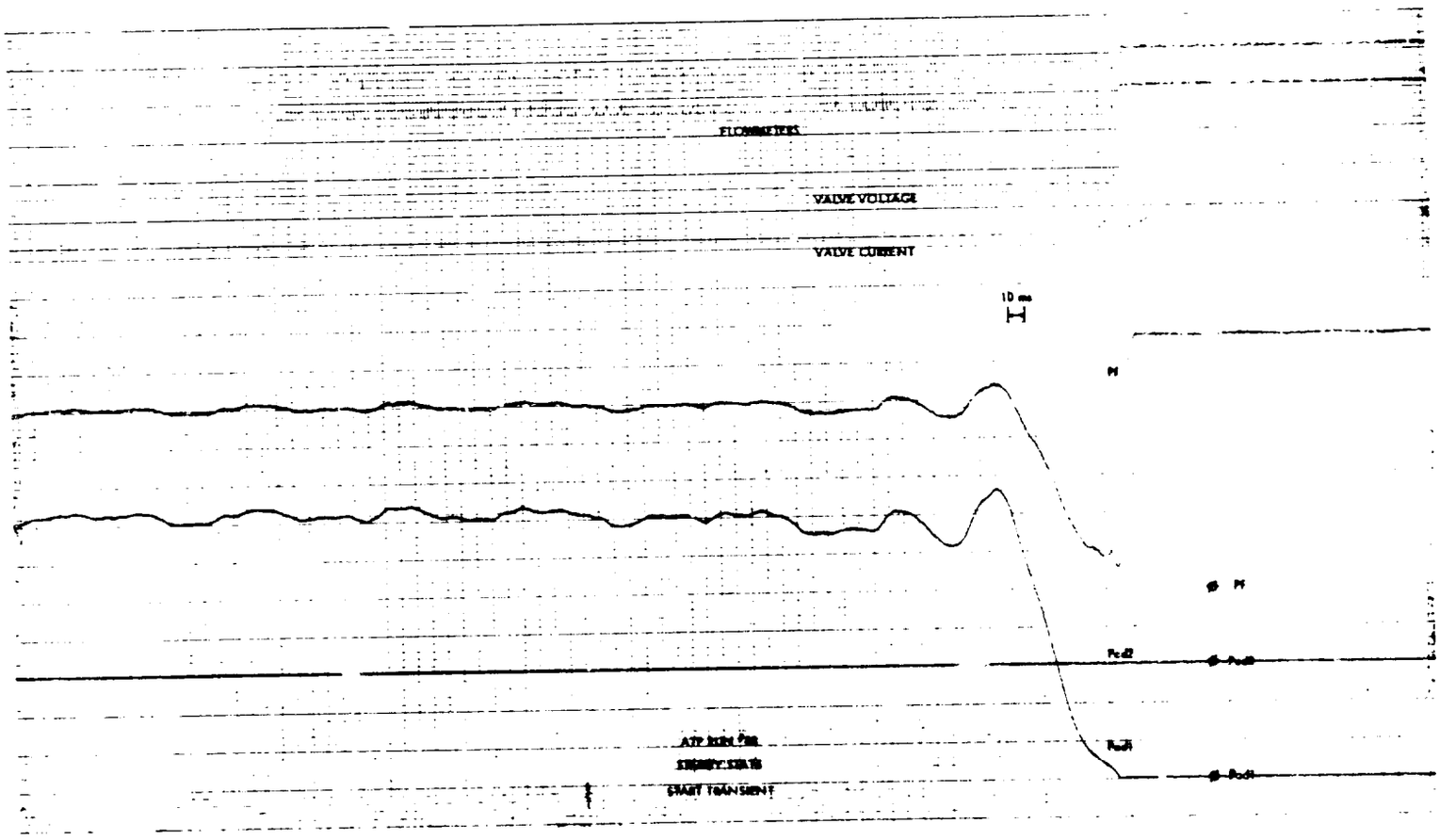
FLOWMETERS
VALVE VOLTAGE
VALVE CURRENT
10 ms
START TRANSIENT

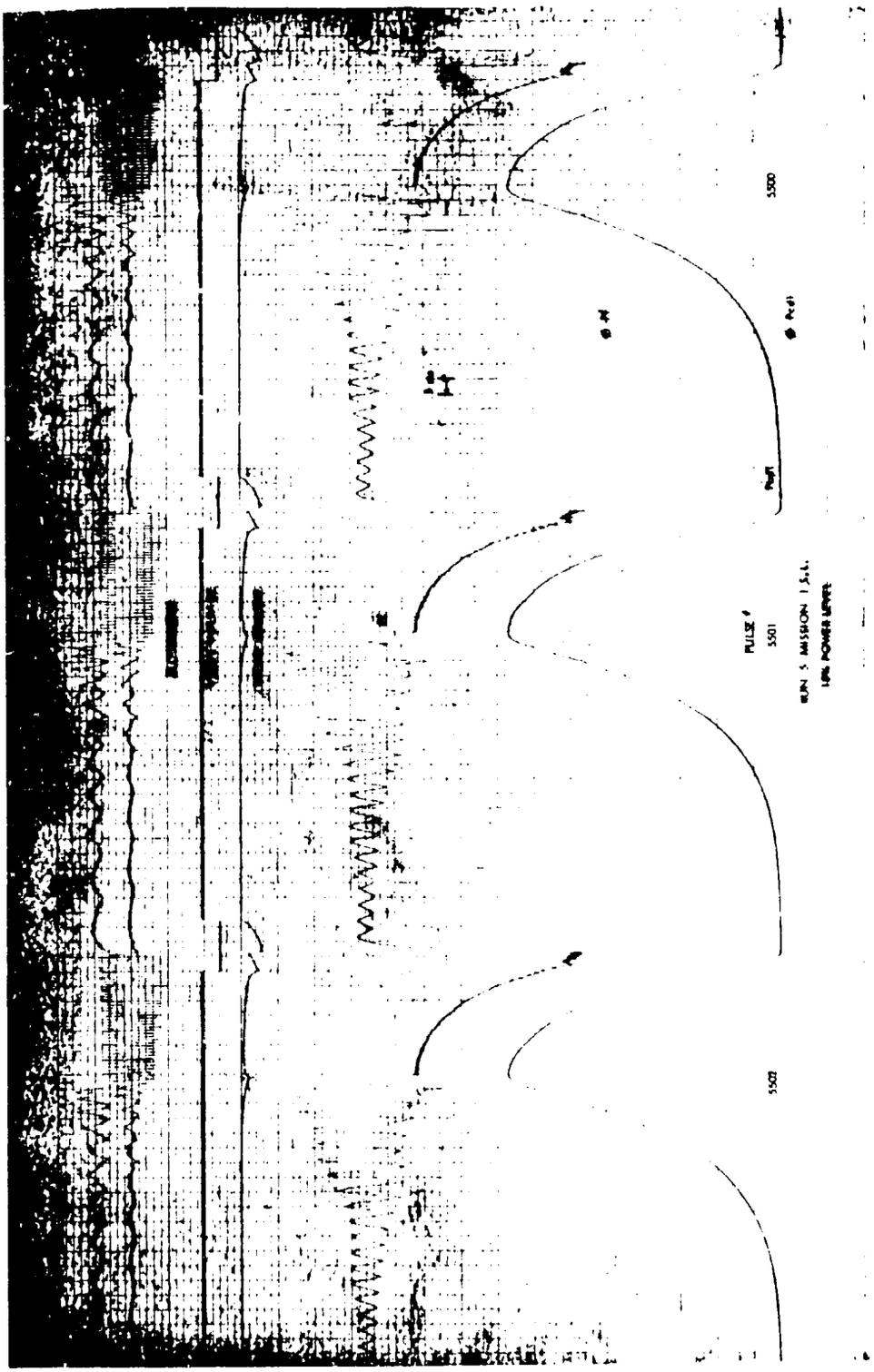

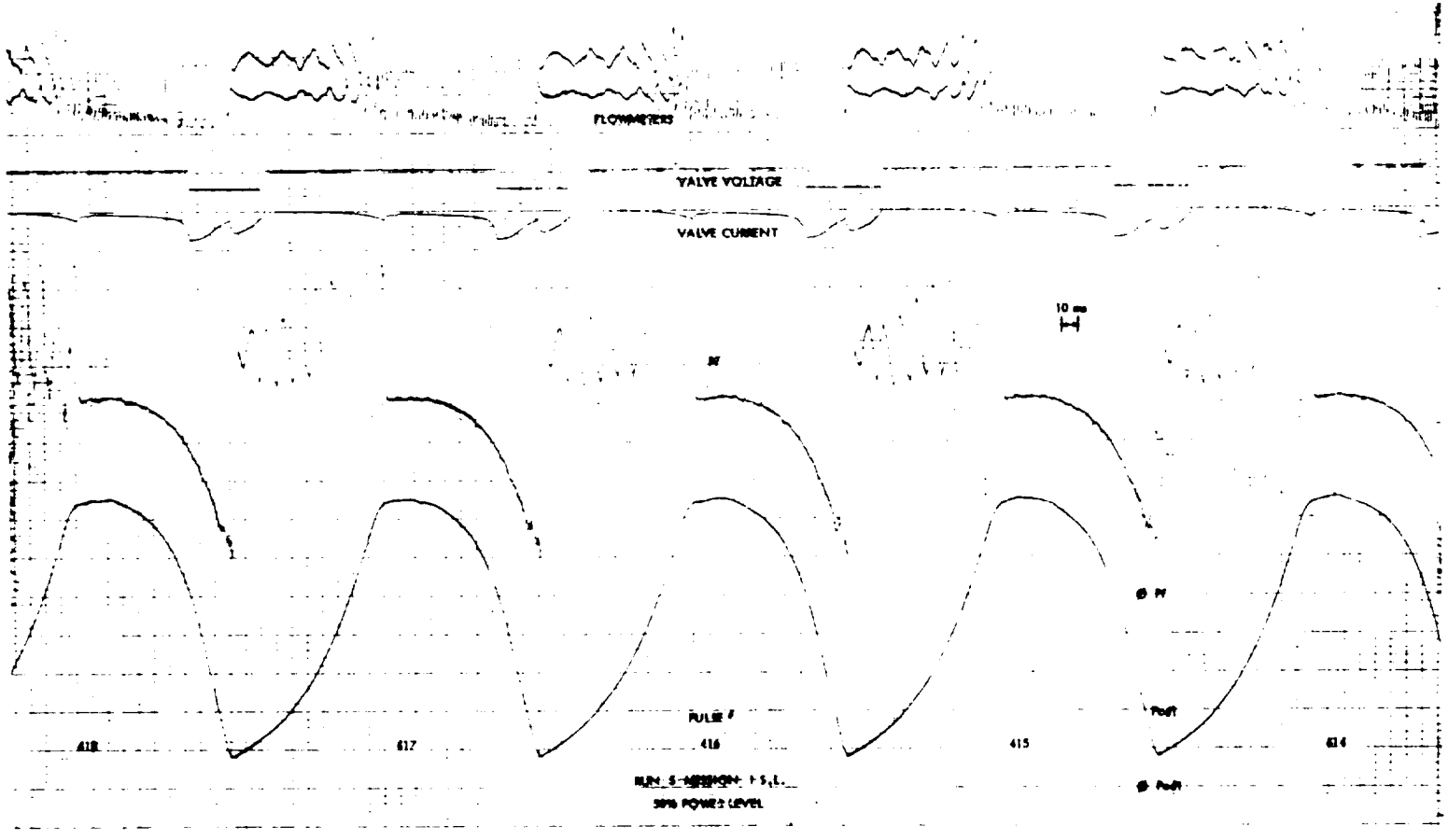

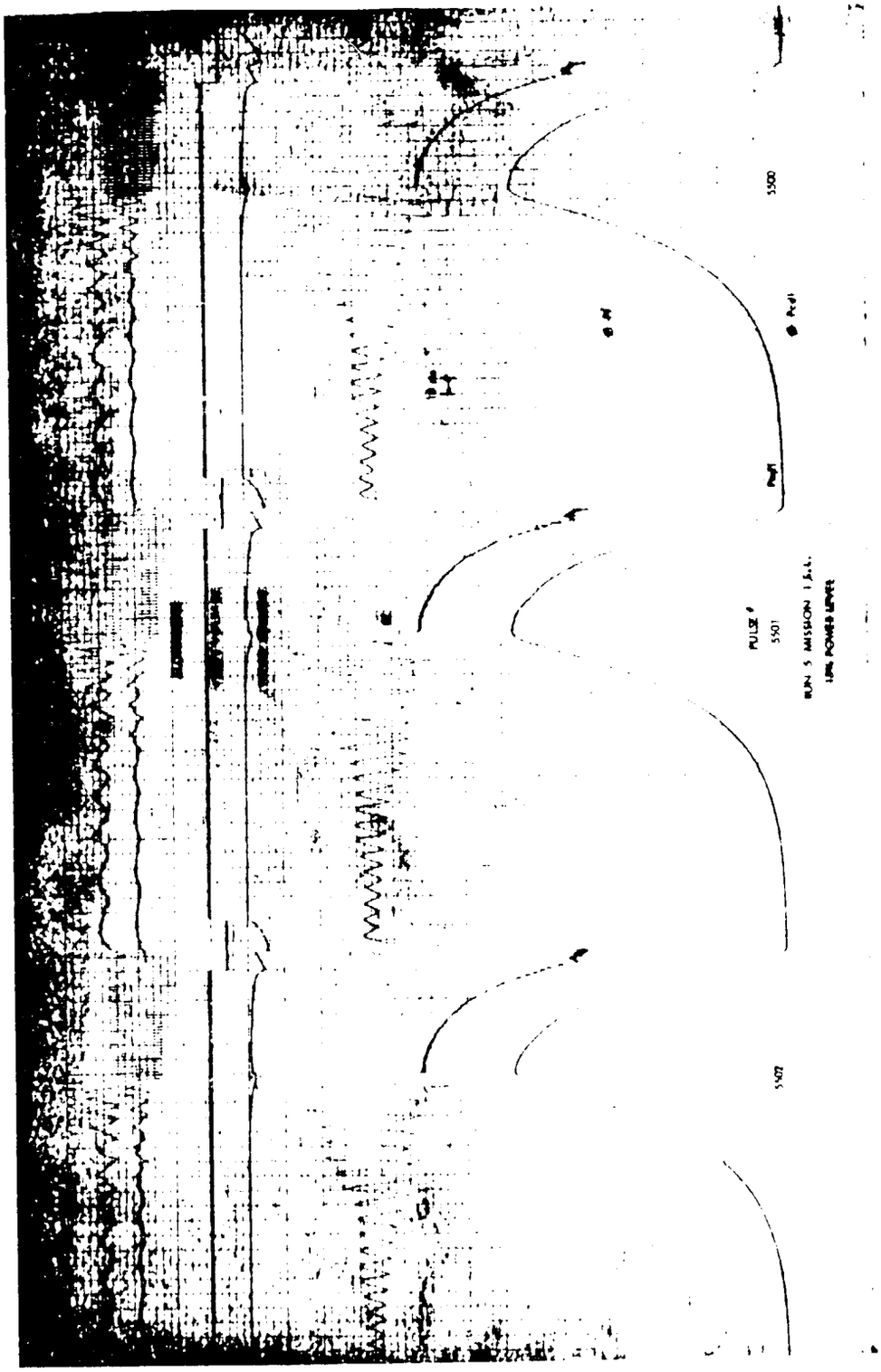

ORIGINAL PAGE IS
OF POOR QUALITY

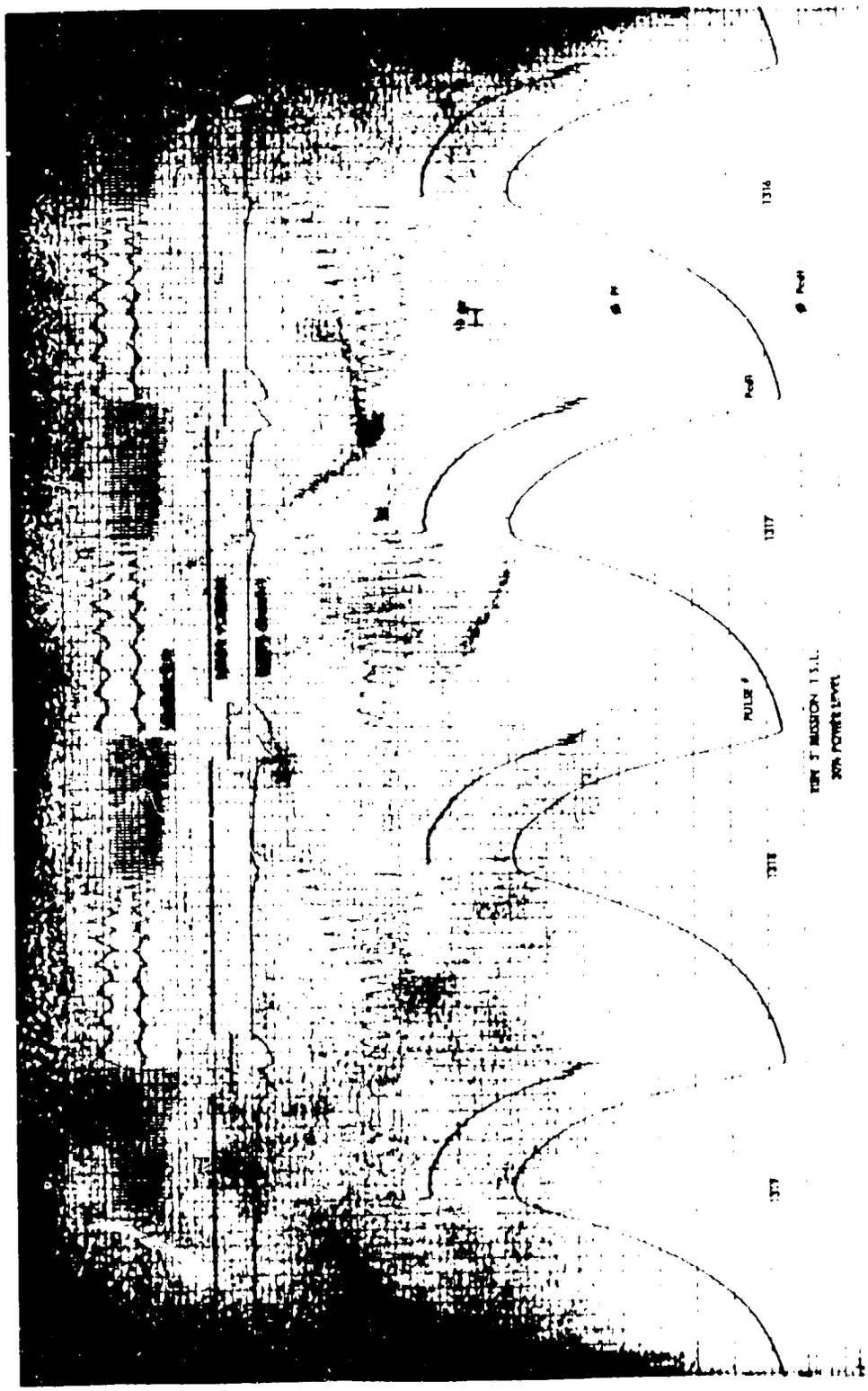

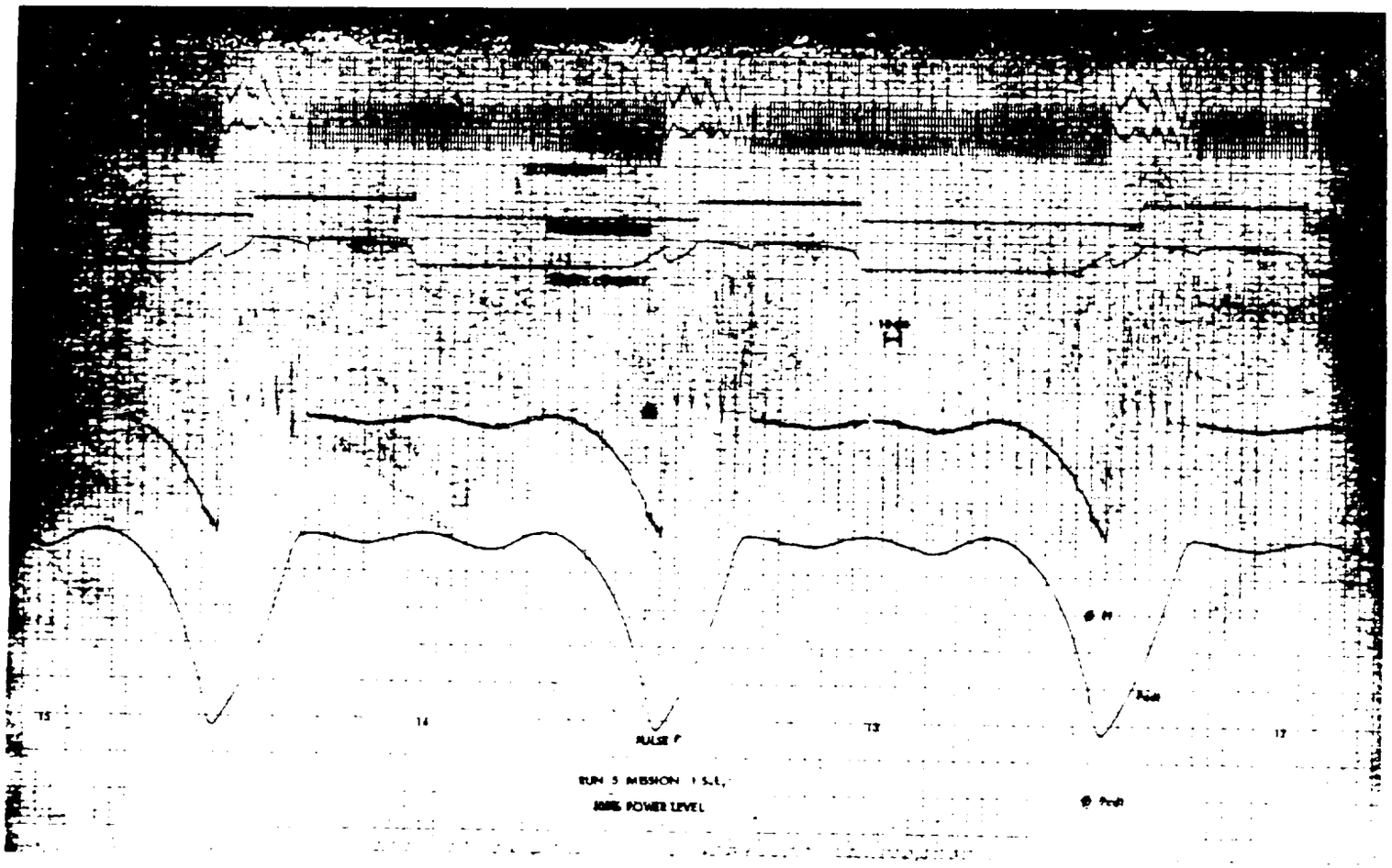
T5
T4
PULSE P
T3
T2
RUN 5 MISSION 1 S.E.
MRR POWER LEVEL

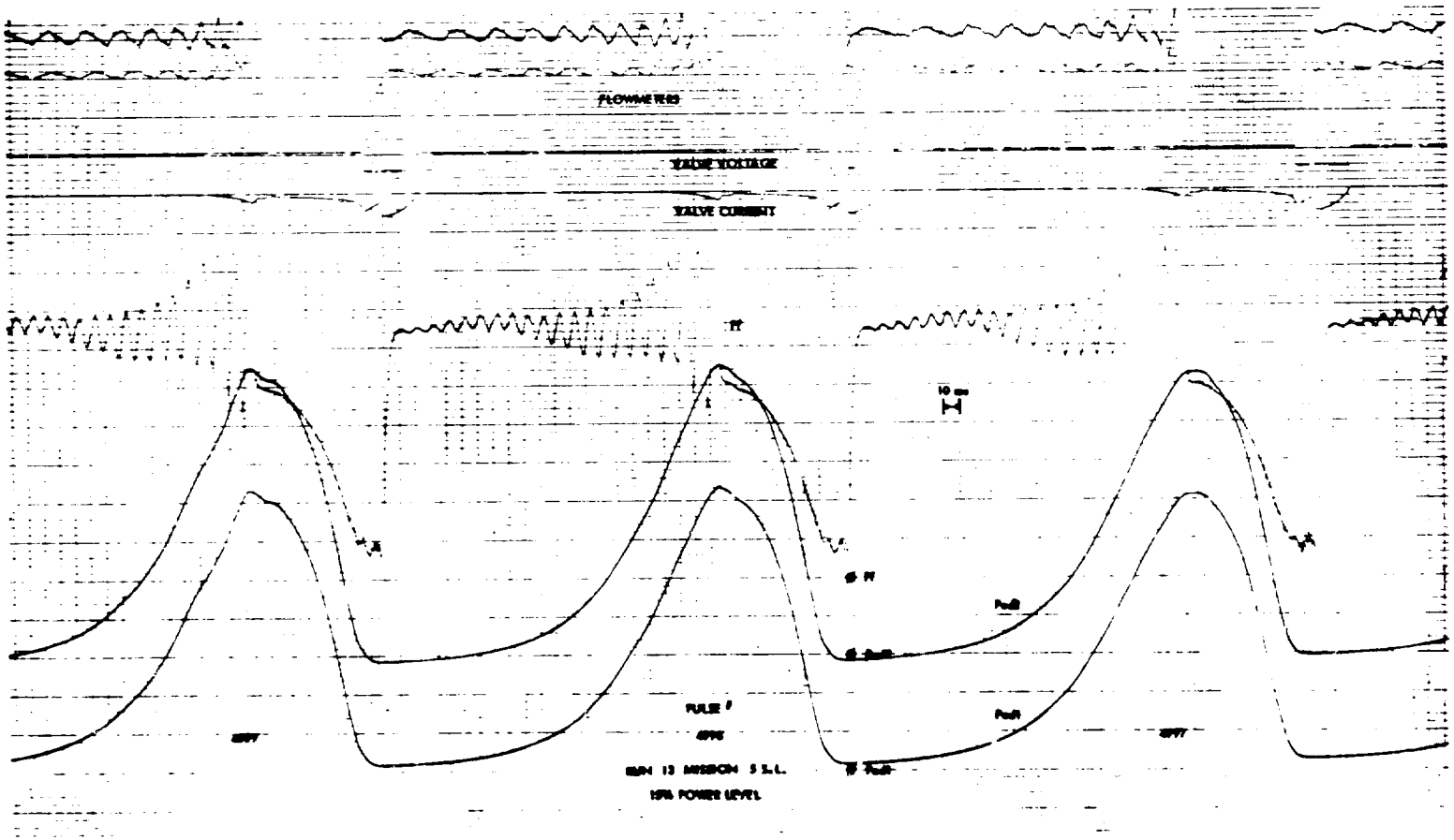
FLOWMETER
VALVE VOLTAGE
VALVE CURRENT
RUN 13 MISSION 5 S.L.
10% POWER LEVEL

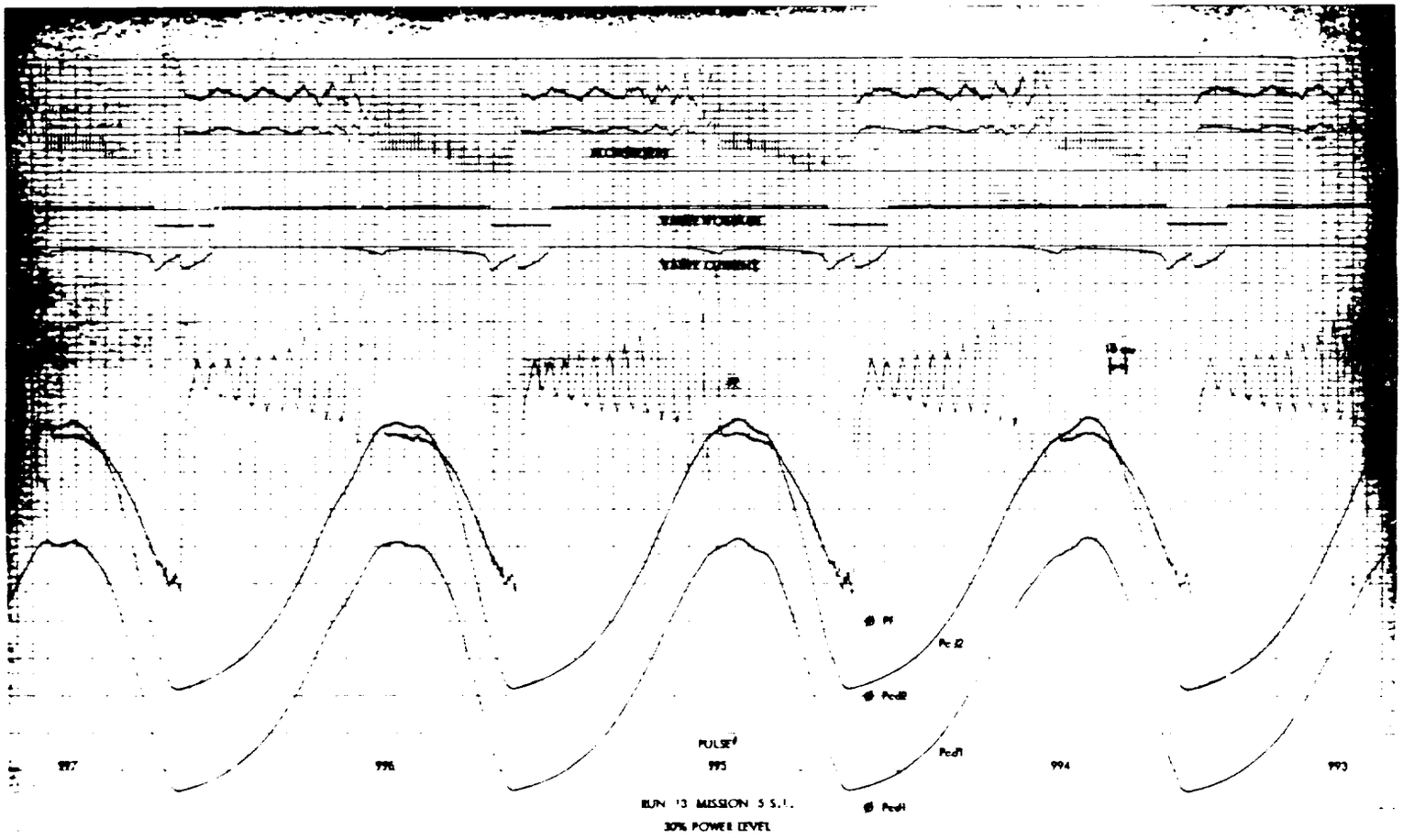
PULSE
997
996
995
994
993
RUN 13 MISSION 5 S.I.
30% POWER LEVEL

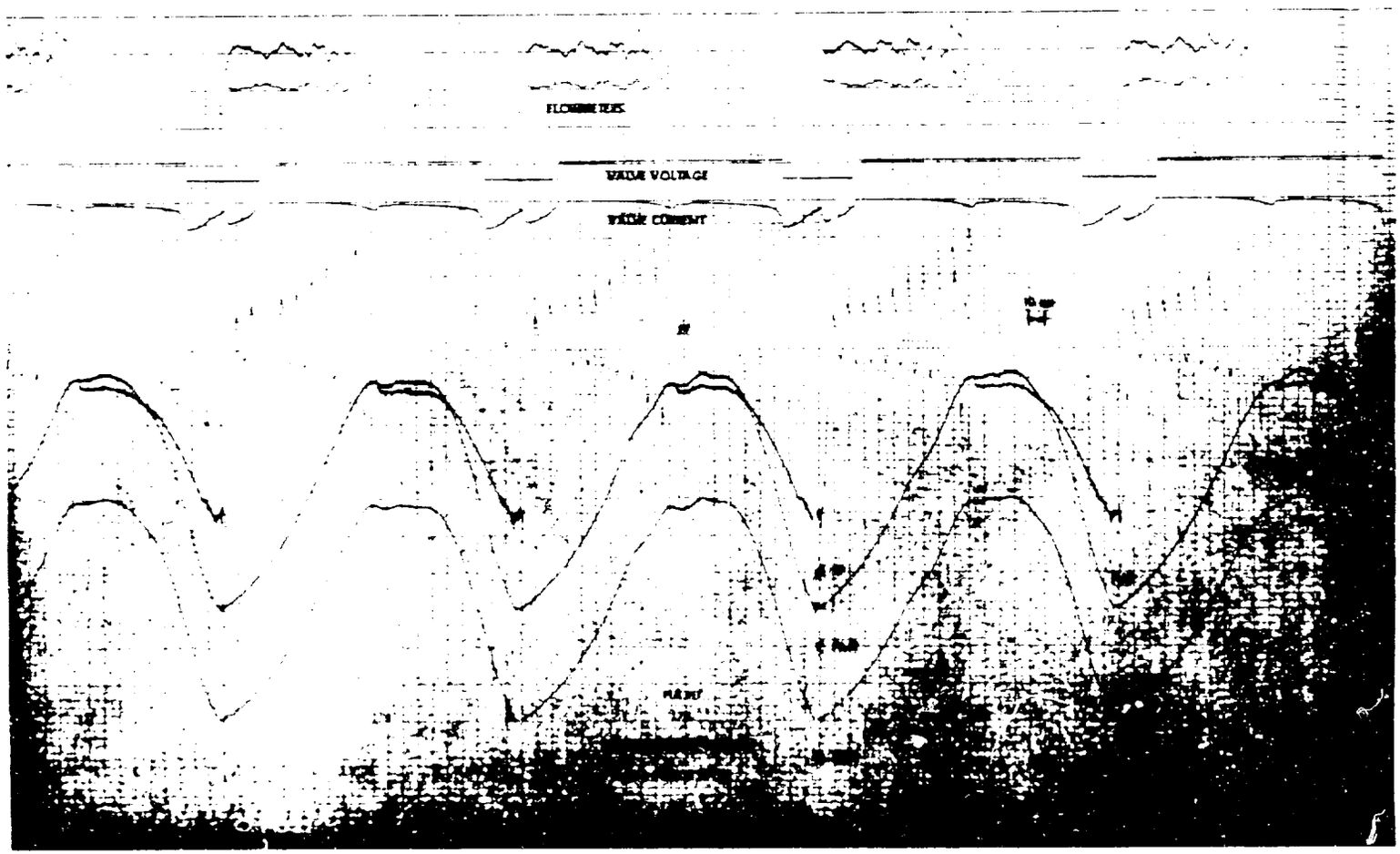
VALVE VOLTAGE
VALVE CURRENT

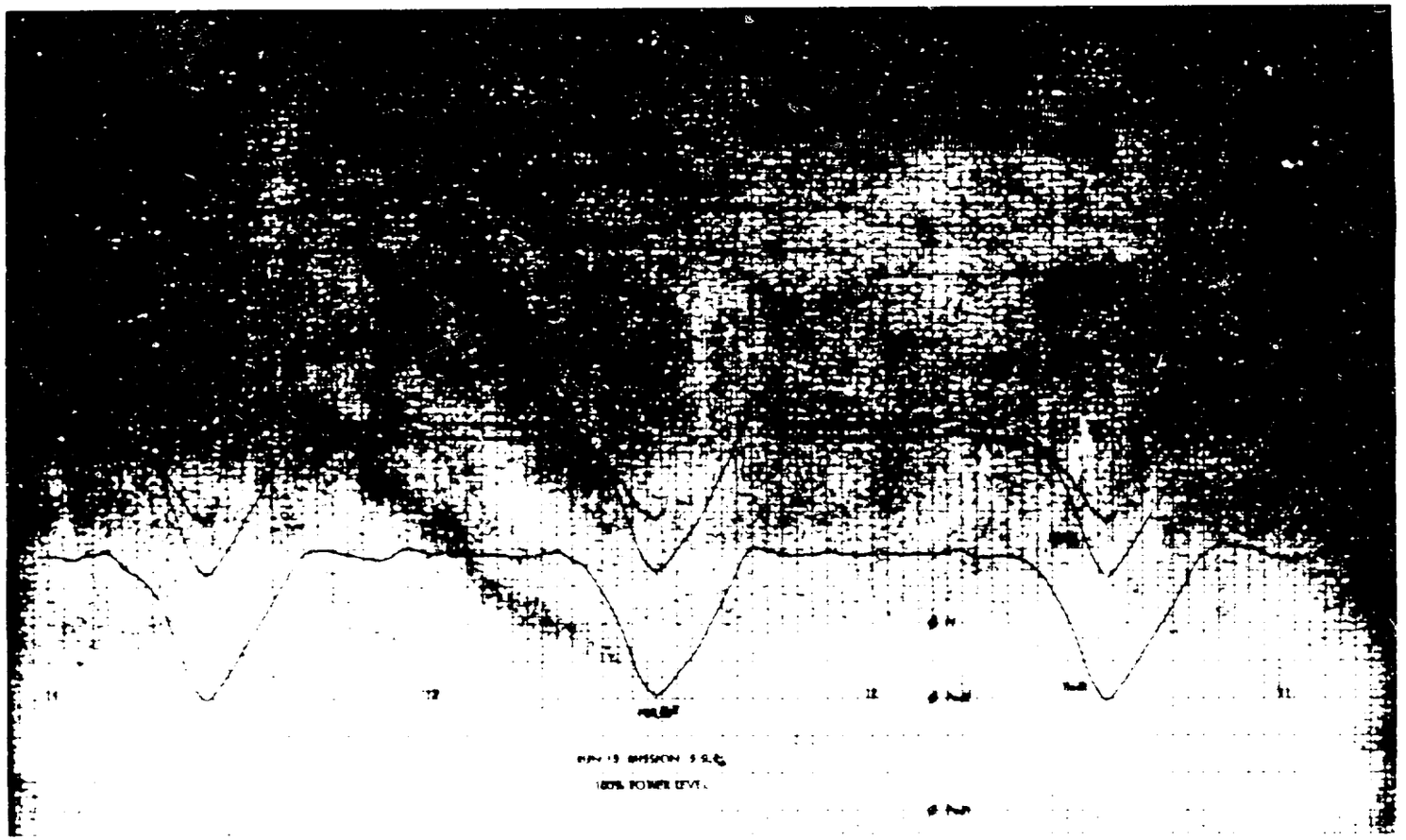

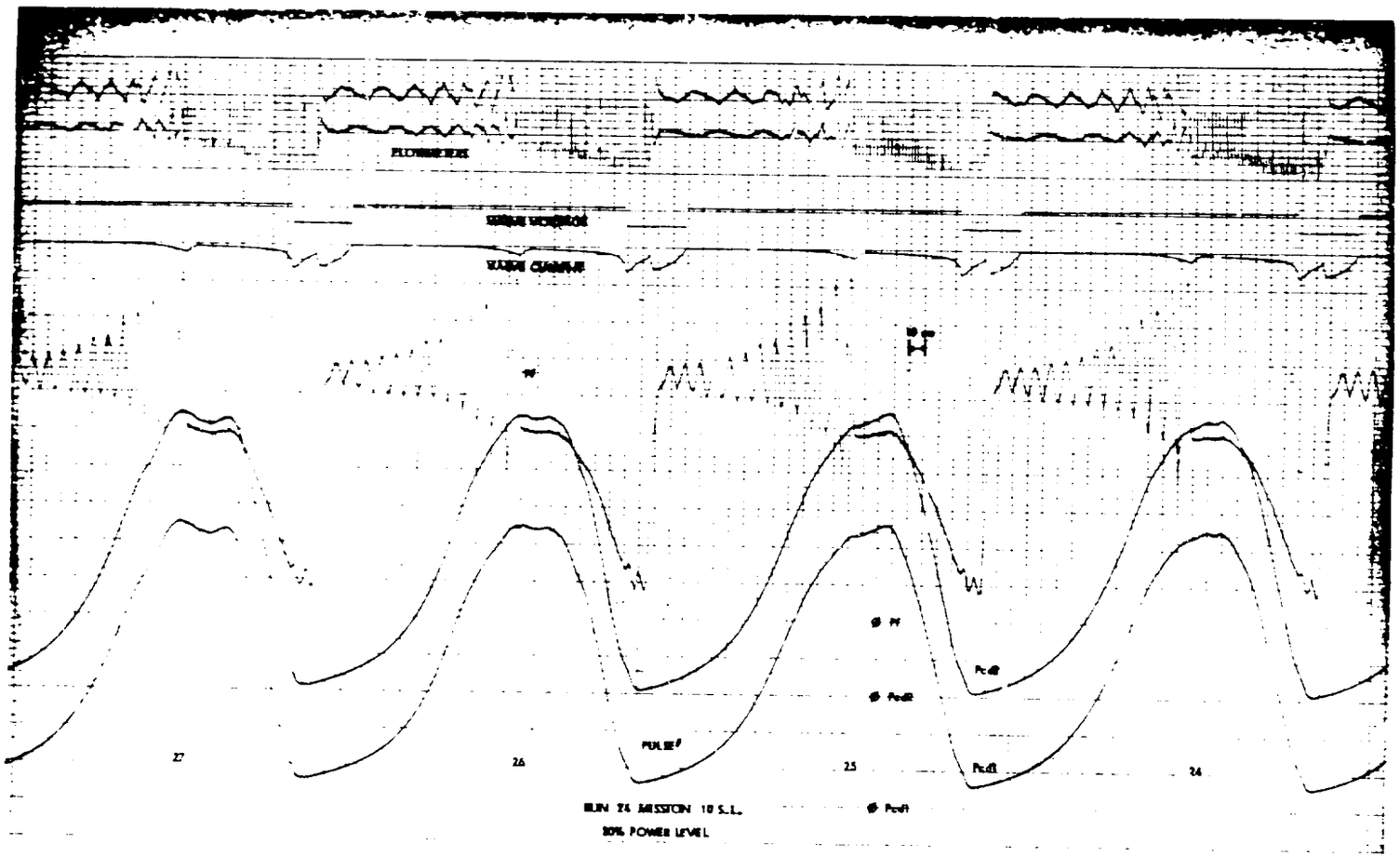
27
26
25
24
RUN 24 MISSION 10 S.L.
80% POWER LEVEL

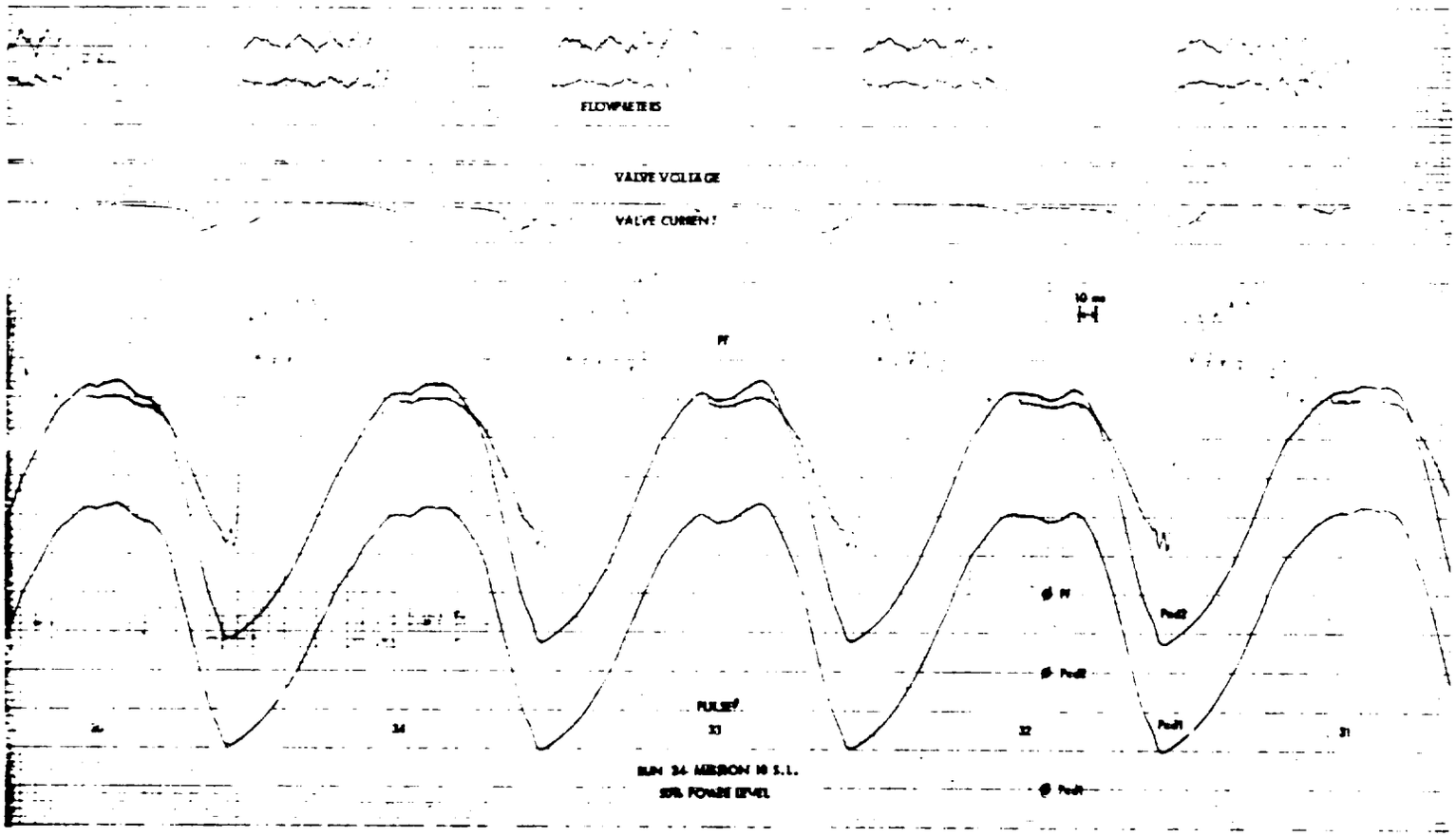
FLOWMETERS
VALVE VOLTAGE
VALVE CURRENT
PULSE
RUN 34 MISSION 10 S.L.
50% POWER LEVEL

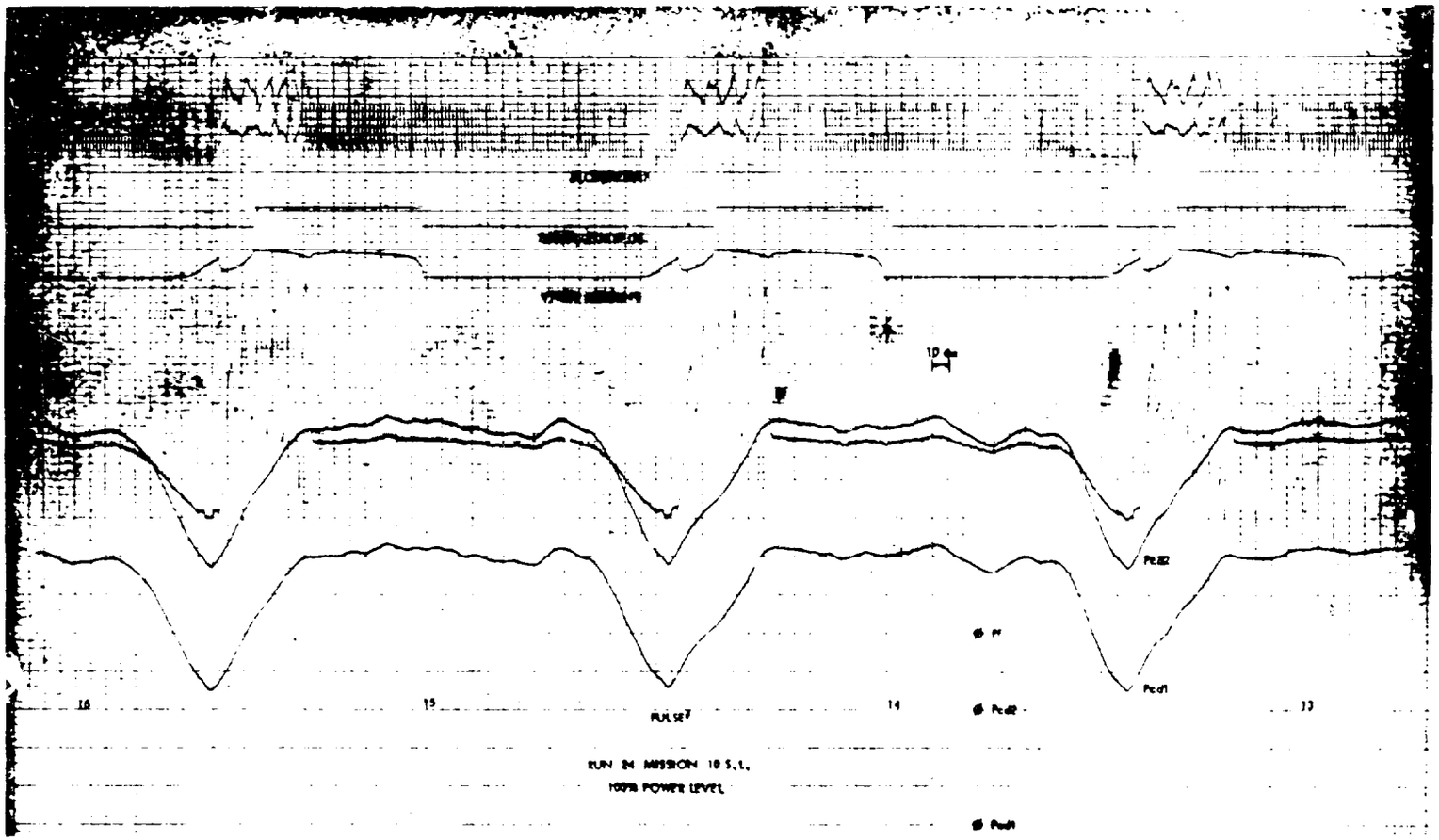
RUN 24 MISSION 10 S.L.
100% POWER LEVEL

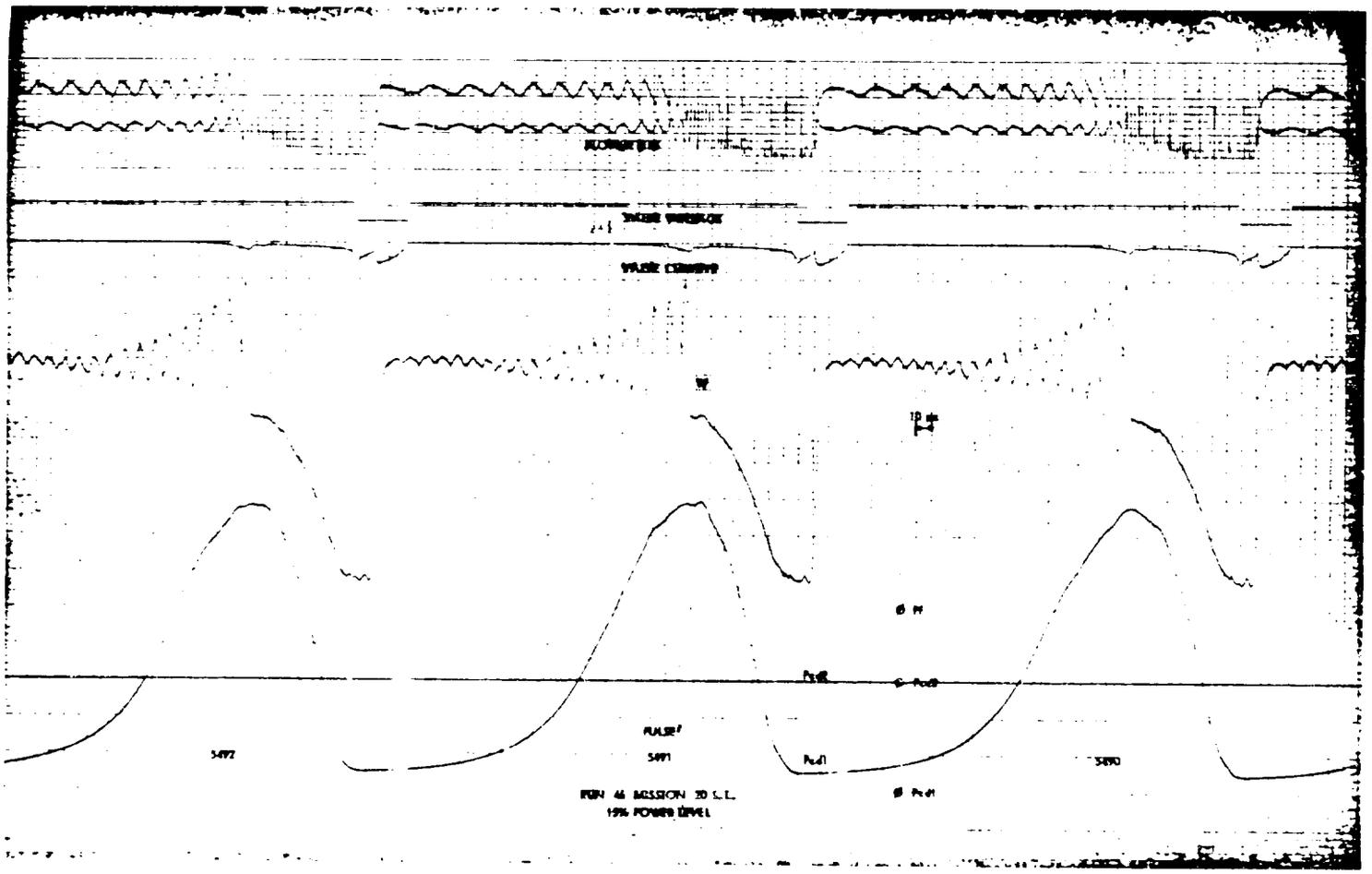
5492
5491
5490

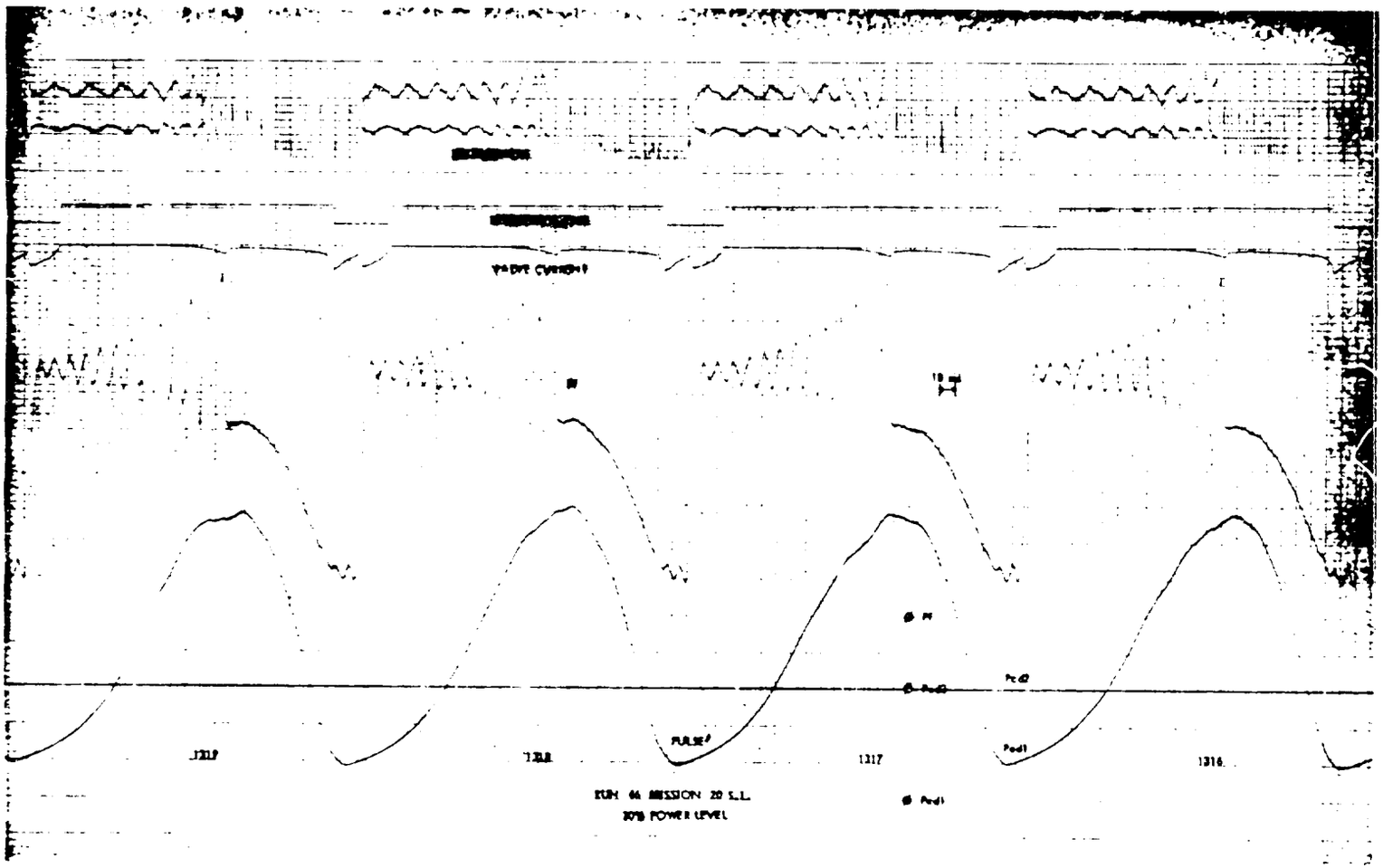
1319
1318
1317
1316

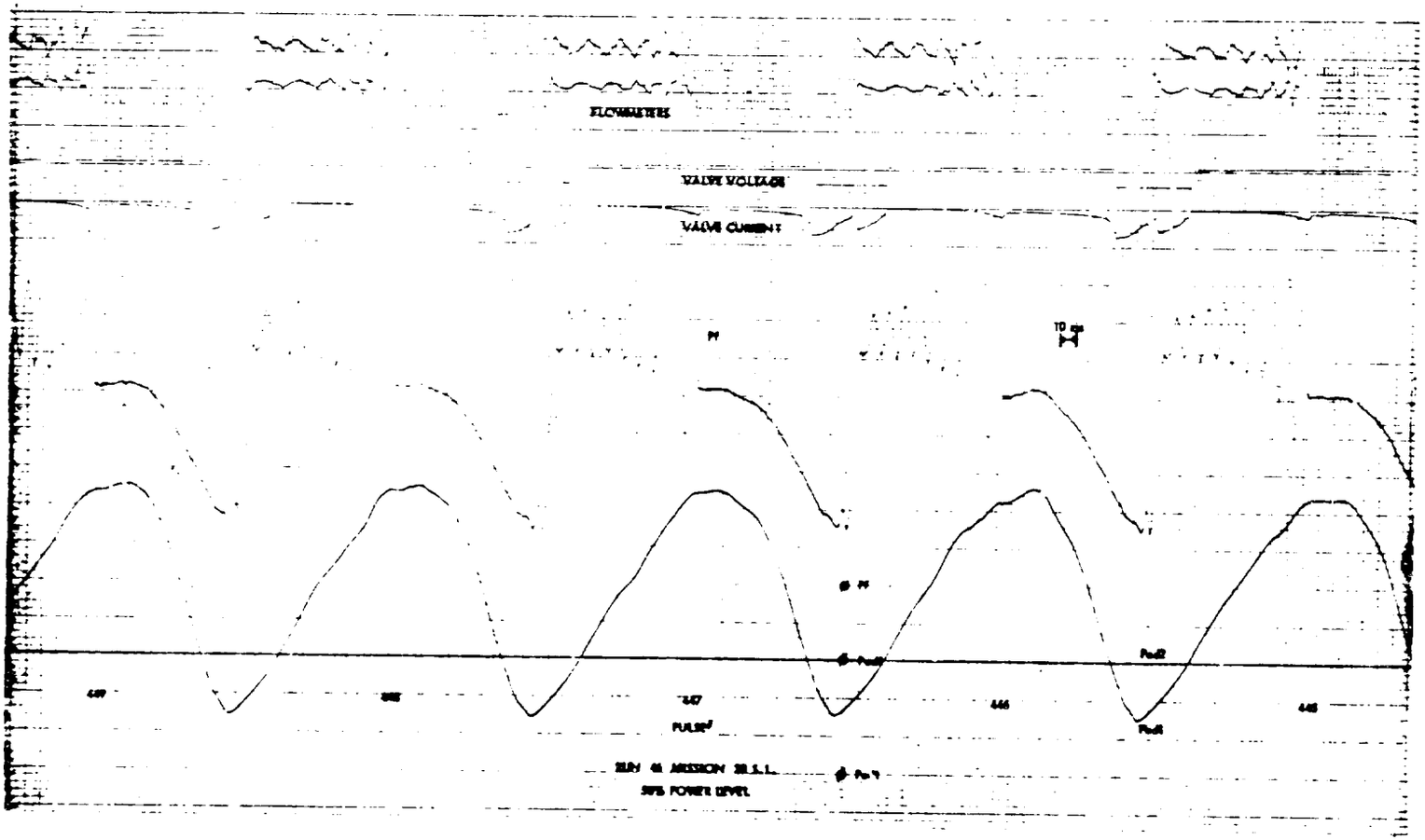
FLOWMETER
VALVE VOLTAGE
VALVE CURRENT
PULSE
SUN 46 MISSION 30 S.L.
50% POWER LEVEL

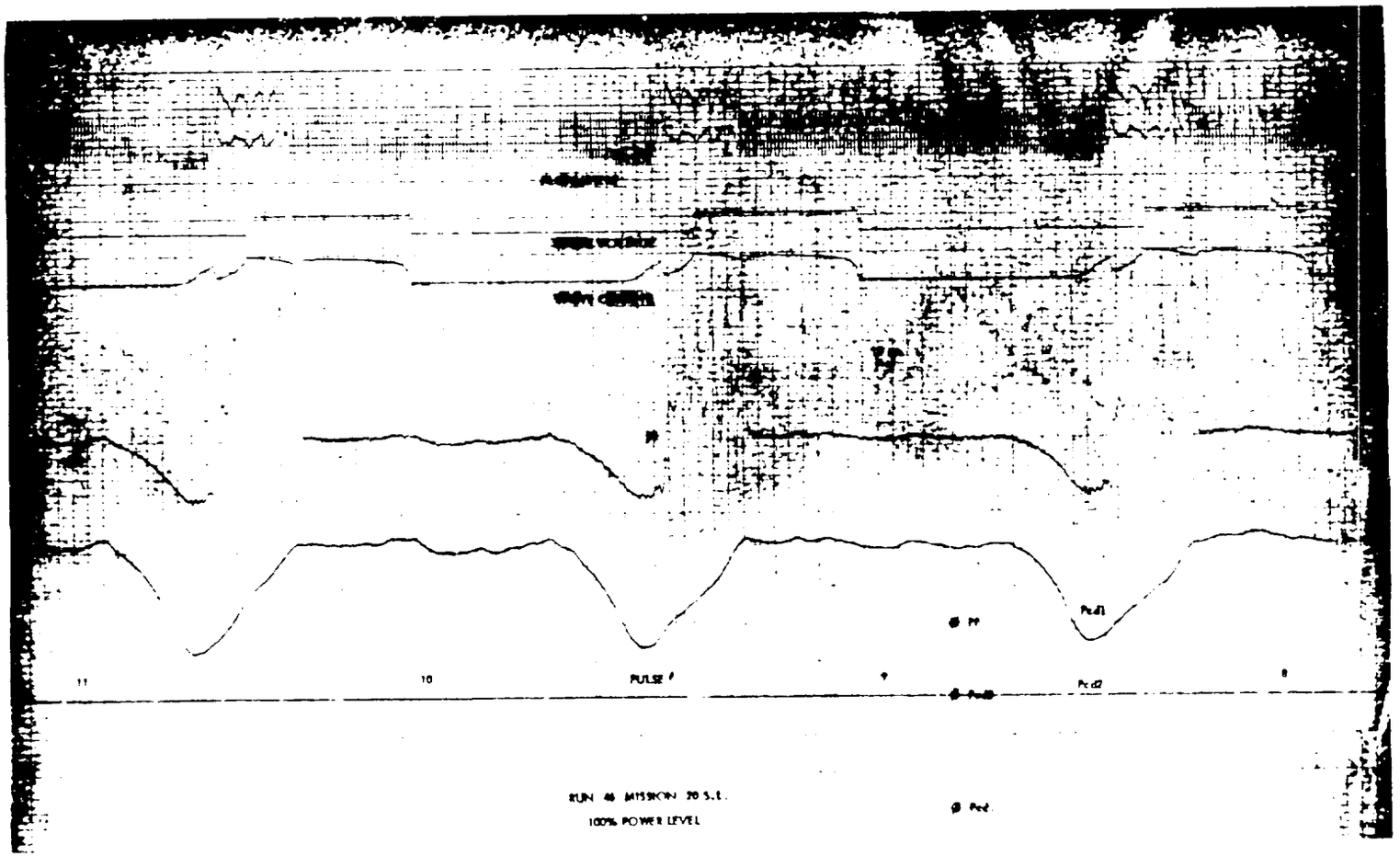

RUN 46 MISSION 20 S.L.
100% POWER LEVEL

REFERENCES

1-1 Emmons, D. L., Huxtable, D. D., and Blevins, D. R.: *Investigation of a Catalytic Gas Generator for the Space Shuttle APU*, AIAA Paper No. 74-1107, presented at AIAA/SAE 10th Propulsion Conference, October 1974

3-1 *Monopropellant Engine Investigation for Space Shuttle Reaction Control System*, Final Report, Volume 1, RRC 75-R-460, April 1975

4-1 *Test Plan – Performance and Life Test of a Catalytic Gas Generator for the Space Shuttle APU*, RRC 73-TP-0279, July 1973

4-2 *Test Plan for RRC Catalytic Gas Generator*, Document No. TTA-TP-2P684, Thermochemical Test Area, NASA Johnson Space Center, May 29, 1974